A REGIONAL STUDY OF THE DIAGENETIC AND GEOCHEMICAL CHARACTER OF THE PENNSYLVANIAN MORROW FORMATION, ANADARKO BASIN, OKLAHOMA

By

PATRICIA ELLEN GROVE WALKER

Bachelor of Science in Arts and Science

Oklahoma State University

Stillwater, Oklahoma

1979 1983

Submitted to the Faculty of the
Graduate College of the
Oklahoma State University
in partial fulfillment of
the requirements for
the Degree of
MASTER OF SCIENCE
MAY, 1986

A REGIONAL STUDY OF THE DIAGENETIC AND GEOCHEMICAL CHARACTER OF THE PENNSYLVANIAN MORROW FORMATION, ANADARKO BASIN, OKLAHOMA

Thesis Approved:

Thesis Adviser

Dean of the Graduate College

Preface

A diverse suite of diagenetic minerals has formed in the Morrow Formation since its deposition during the Pennsylvanian. Regional mapping of these minerals along with geochemical analyses allows for the interpretation of diagenetic and geochemical trends. The relationship of these trends to the development of the Morrow Formation as a reservoir can then be better understood and used as an aide in the prediction of hydrocarbon occurrences.

I wish to thank my thesis adviser, Dr. Zuhair Al-Shaieb for his support and guidance throughout this project. Appreciation is also expressed to Dr. Gary F. Stewart and Dr. Dennis Prezbindowski for their assistance and constructive remarks in this research.

I wish to express my appreciation to Masera Oil Company for the use of their thin section material, to Amoco Production Research for their assistance in obtaining isotope data, and to Phillips Petroleum Foundation for their financial support of this research.

Special thanks are given to my parents for their financial and moral support through so many years of higher education.

I also wish to thank all my friends in the geology department for their support, especially my office partners, Janet Cairns and Craig Throckmorton.

Finally, I would like to thank my husband, Lawrence, for his continued support, patience, and tolerance during the course of this study.

TABLE OF CONTENTS

LIST OF TABLES

LIST OF FIGURES

CHAPTER I

INTRODUCTION

The Anadarko basin represents one of North America's largest sedimentary basins occupying approximately 35,000 square miles in central and western Oklahoma, southwestern Kansas, and the Texas Panhandle. The basin is bounded to the east by the Nemaha Ridge, and to the south, abruptly by the ancient eroded Amarillo-Wichita mountain range. On the west and north it is flanked by vast, shallow shelf areas, such as the giant Hugoton-Panhandle gas field, and undergoes a northward transition to the Central Kansas Uplift (Figure 1). The basin contains approximately 40,000 ft. of sediments ranging from Cambrian to Permian in age (Figure 2). Hundreds of deep and intermediate depth fields have been discovered with production from both structural and stratigraphic traps.

Prior to 1941, most of the exploration in the Anadarko basin was confined to the shallower horizons. In May 1943, a well in Cimarron County, Oklahoma was completed as a gas well in the lower Morrow Keyes Sandstone of the Lower Pennsylvanian. This well focused considerable attention on the deeper horizons in the basin and led to the discovery of many new oil and gas fields. The major oil and natural

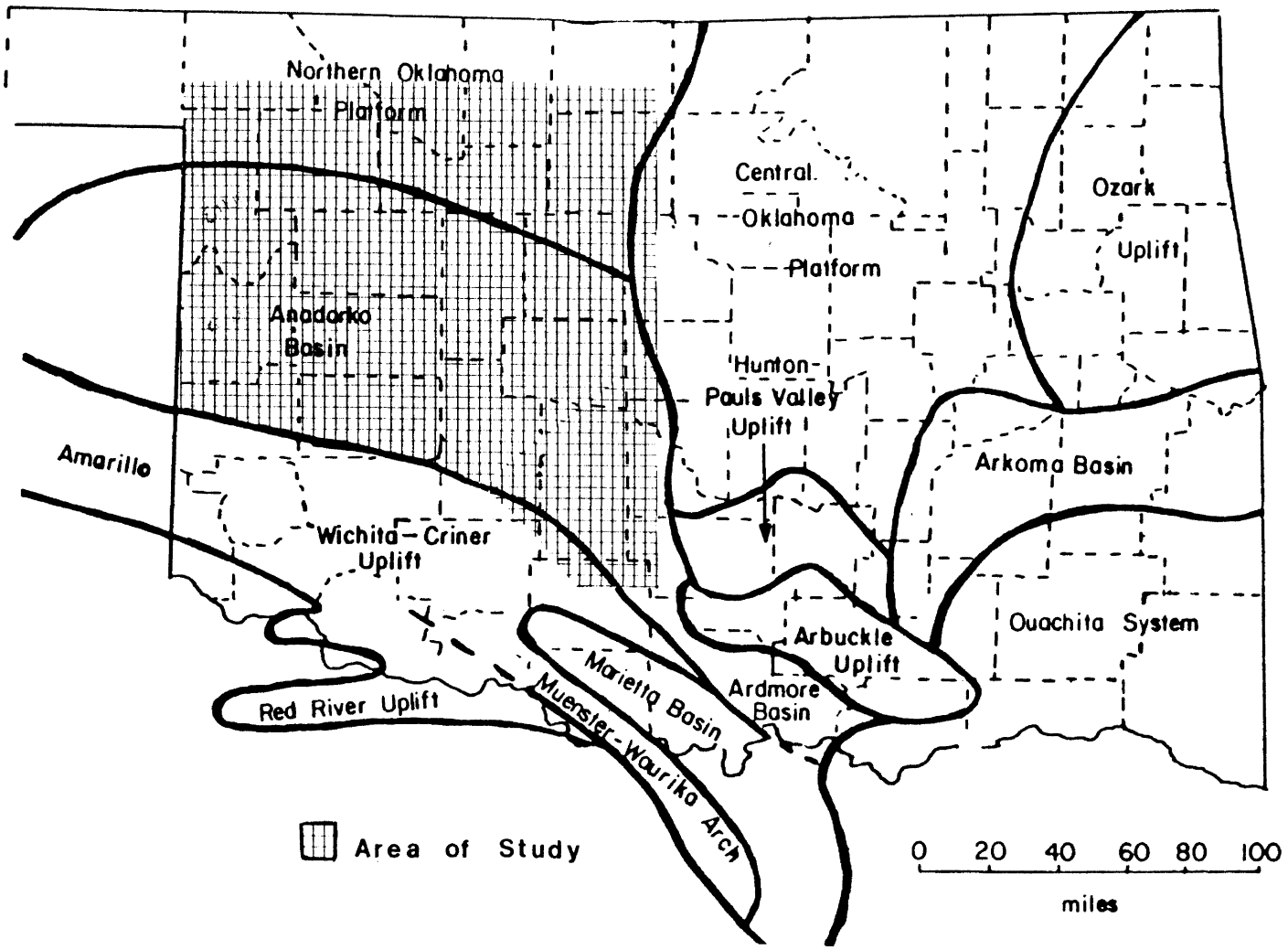

Figure 1. Major Geologic Provinces (Al-Shaieb, Shelton, and Others, 1977)

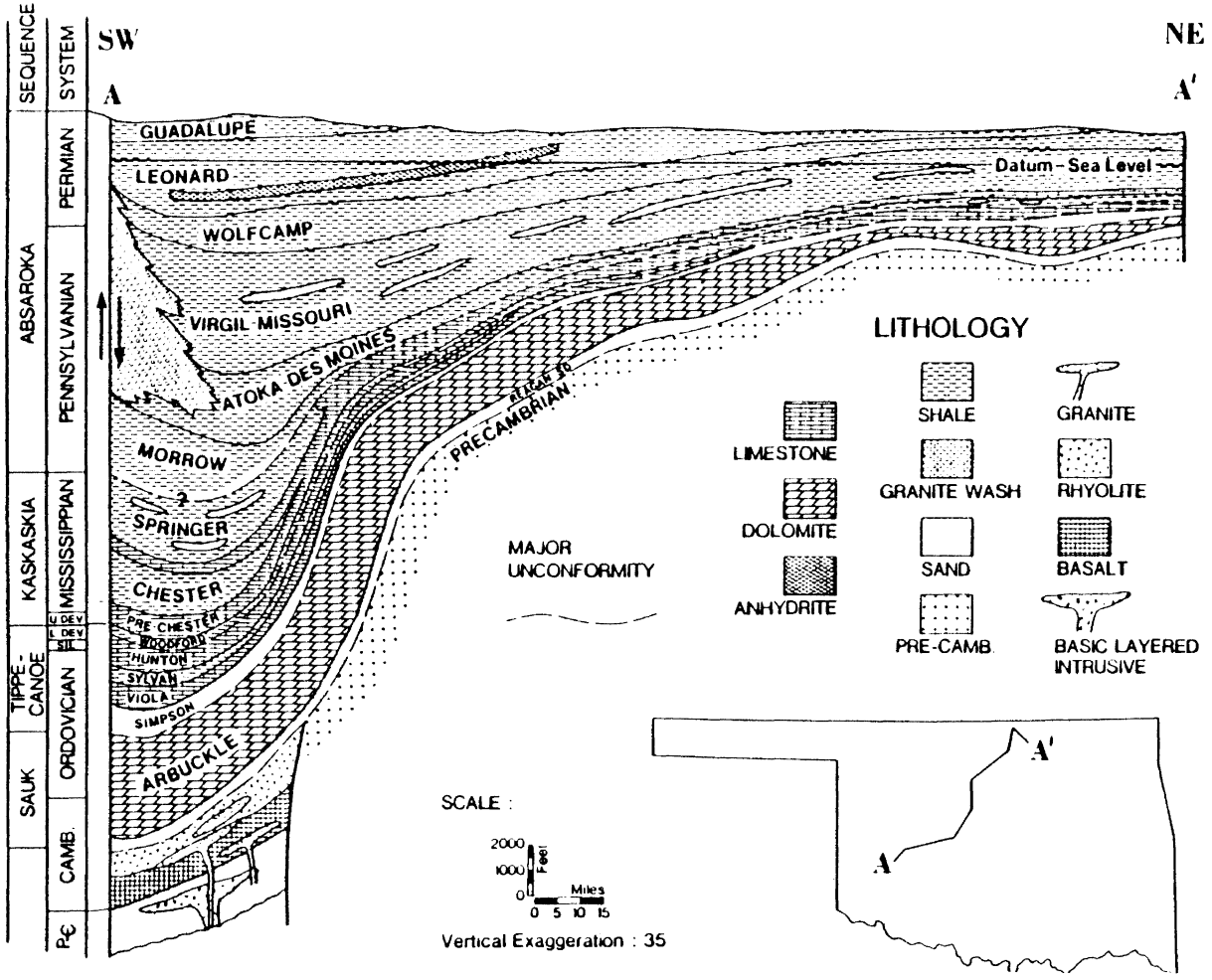

Figure 2. Idealized Stratigraphic Section Showing Variations in Thickness and Facies from the Shelf (Right Side) into the Anadarko Basin (Left Side) (Modified from Wickham, 1978)

gas producing trends occur along the shallow shelf areas of the basin with predominant gas production in the deep basin.

The Pennsylvanian Morrow sandstones are the major reservoir rocks in the Anadarko basin.

Previous Works

Regional studies of the Mid-Continent have been made by several investigators. Huffman (1959) outlined the major tectonic features of the Central Mid-Continent region. Adler (1971) discussed the major structural and stratigraphic features of the Mid-Continent and their relation to distribution and depositional history of the Morrow sandstones. Moore (1979) studied the tectonic events of the Pennsylvanian and the resulting regional paleoenvironmental patterns for the Mid-Continent. He was one of the first to recognize the development of the Anadarko basin as a sediment trap.

In relation to the Anadarko basin, Busch (1959) was one of the first to apply a geometry origin approach to classifying sandstone bodies. He used the Morrow sandstones of the Anadarko basin as an example by referring to them as beach sands and describing their en echelon appearance. Pate (1959) illustrated the occurrence of stratigraphic traps along the northern shelf of the Anadarko basin. Gibbons (1964) gave a stratigraphic and lithologic description of Pennsylvanian age sediments in

the northern Anadarko basin. Forgotson (1966) and Forgotson, Statler, and David (1967) characterized the structural framework, stratigraphy, and depositional history of the Morrow sandstones in the panhandle and northwestern regions of Oklahoma. Adler (1971) overviewed the production potentials for the Anadarko basin in relation to structural and stratigraphic features. Chenoweth (1979) produced several diagrams illustrating the distribution of oil and gas production in the Morrow sandstones. Galloway and Dutton (1979) related depositional environment to structural regime by characterizing the Morrow sandstones of the Anadarko basin as evolving in extremely shallow stable platforms. Evans (1979) reviewed the major stratigraphic and structural features specifically of the Anadarko basin. Hill and Clark (1980) related the stratigraphy and structural character of the basin to oil and gas generation.

Several studies in specific areas of the Anadarko basin have been conducted utilizing subsurface methods, petrography, and diagenesis. Abels (1959) conducted a subsurface lithofacies study in the northern Anadarko basin. His study allowed for an interpretation of depositional environment, source, and contribution of tectonics to the distribution of Morrow sandstones. Cullins (1959) and Barrett (1965) analyzed Pennsylvanian age sandstones in Texas, Beaver, and Ellis Counties, Oklahoma. Barby (1960) initiated a gas reserve study of Morrow sandstones in

Beaver County, Oklahoma. Adams (1964) studied the petrographic and diagenetic character of Lower Morrow sandstones in Ellis, Woodward, and Dewey Counties, Oklahoma. He recognized the importance of secondary porosity and showed an understanding of the diagenetic processes acting within the Morrow sandstones. An explanation of the conditions of deposition of Morrow sandstones in the Hough area was proposed by Arro (1965). Davis (1971),(1974) studied high pressure Morrow sandstones along the Watonga trend in Blaine and Canadian Counties, Oklahoma and gave examples of producing Morrow areas in Oklahoma and Texas. Mapping of the regional distribution of subsurface pressures within the Morrow in eastern Oklahoma was conducted by Breeze (1971). Benton (1972) and Curtis and Ostergard (1980) illustrated the geometry and stratigraphic behavior of producing Morrow sandstones in Texas County, Oklahoma. Khaiwka (1973) interpreted the depositional environment of Morrow sandstones based on stratigraphic, petrologic, and geometric criteria in Beaver, Harper, Ellis, and Woodward Counties, Oklahoma. A summary of the lower Morrow sandstone petroleum potential in southern Ellis County, Oklahoma was conducted by Bloustine (1975). Characterization of the Morrow Formation's depositional environment through detailed core examination along with conventional subsurface techniques was accomplished by Swanson (1979) and Kasino and Davies (1979). Swanson (1979) gave a detailed description of deltaic facies deposition of the

Upper Morrow sandstones. Kasino and Davies (1979) discussed Morrow sandstone depositional environments in Cimarron County, Oklahoma. Shelby (1980) discussed the distribution of Upper Morrow chert conglomerates in the southwestern Anadarko basin. Godard (1981) reviewed the depositional environment trends of Morrow sandstones in Major and Woodward Counties, Oklahoma. A study of the organic geochemistry of the uppermost Morrow shales in the Anadarko basin was conducted by Tsiris (1983). South (1983) reviewed the depositional environment and diagenetic character of the Morrow sandstones in the Canton Field area, Blaine County, Oklahoma. He also gave a detailed petrographic analysis of the sandstones and a brief thermal history.

Methods and Procedures

The objective of this study was to examine the mineralogical and chemical changes within the Morrow sandstones and to establish geochemical and diagenetic trends. These trends could then be regionally mapped and interpreted in order to better understand the development of the Morrow Formation as a reservoir and to aide in the prediction of hydrocarbon occurrences.

Mineral constituents were determined using analysis by standard petrographic microscopy of more than 500 thin sections. Values used in mapping were averages for the entire core and/or averages for specific depositional

environments. X-ray diffraction, scanning electron microscopy coupled with energy dispersive x-ray analysis (SEM/EDXA), and cathodoluminescence were used to analyze selected samples.

Isotope data were obtained through Amoco Production Company Research Center. Samples containing greater than 5% carbonate cement based on thin section analysis were selected for isotope analysis from each core within the study area. These samples were ground to a fine sand and the bulk powder was subject to x-ray diffraction analysis to determine carbonate mineralogy and approximate carbonate content. Samples containing carbonate were reacted with anhydrous H_3PO_4 at a constant 50^{o} C to release CO_2. This gas was then analyzed isotopically according to standard techniques (McCrea, 1950). Comparison of six duplicate analyses carried throughout the entire chemical preparation process yielded a standard deviation of approximately + 0.2 per mill.

Vitrinite reflectance measurements were made for more than sixty samples of the Morrow shales (Tsiris, 1983).

CO_2 data were obtained from the Bureau of Mines publications.

Values used for mapping are included as data tables in Appendix C. Well locations are indexed on the maps and a list of well index numbers and well name abbreviations are included in Appendix A.

A factor analysis program was run on all available

data to analyze the interrelationships. The results of these analyses are included in Appendix D.

Data compiled were used to evaluate the diagenetic, thermal, and isotopic character of the Morrow sandstones.

CHAPTER II

GEOLOGICAL SETTING

Stratigraphy

The Morrow Formation is the basal transgressive predominantly clastic unit of the Pennsylvanian System. The name "Morrow" is a commonly accepted rock-stratigraphic term for the sequence of rocks in the study area. The top of the Morrow is defined as the base of the Atoka "Thirteen Finger" Limestone, while the base of the Morrow is commonly picked as the top of the Mississippian unconformity (Abels, 1959).

A cross section of the basin demonstrates the wedge character of the Morrow with thick accumulations near the Wichita Uplift and progressive thinning onto the shelf to the north-northeast (Figure 2). The Morrow rocks thin at the base by onlap and at the top by erosion. The lower Morrow beds exhibit transgressive overlapping away from the basin axis. The sediments assigned to the Morrowan series are dominantly shales with discontinuous and erratic sandstones and limestones. Distribution of coarse terrigenous clastics within the predominantly fine clastic Morrow Formation indicates one source of sand west-northwest of

the Oklahoma and Texas panhandles and another source to the north-northeast (Forgotson, 1969). The Upper Morrow chert conglomerate shows a predominant source from the southwest (Shelby, 1980).

The Morrow Formation is commonly divided into upper and lower units based on lithology and depositional environment. Oil and gas production from the Morrow sandstones is primarily stratigraphically controlled and usually not related to structural features.

Structural Setting and Tectonics

The Anadarko basin is an elongate, west-northwest trending basin whose cross-sectional asymmetry is due to a complex of fault zones on its southern margin which separates it from the Wichita Uplift. Structural displacement between uplift and basement exceeds 30,000 ft. The basinal axis extends northwest-southeast and becomes progressively shallower to the north and east. Regionally, the Morrow rocks strike northwest and dip to the southwest (Abels, 1959).

The Pennsylvanian Upper Morrow sandstones occur around the -13,600 ft. level.

The Anadarko basin is one of several north-northwest trending basins and uplifts from the Ouachita foldbelt in southern Oklahoma to the Texas panhandle. Other basins include the Marietta, and Ardmore. Positive structural features include the Wichita-Criner Uplift, the Muenster-

Waurika Arch and the Arbuckle Uplift including the Tishomingo Uplift (Figure 1).

Initially, this area of southern Oklahoma was described by Schatski (1946) as an example of an aulacogen Burke and Dewey(1973) explained the origin of aulacogens using the concept of hot spots and plate tectonics. By Early Pennsylvanian, local basins were well developed and the Anadarko basin with 10,000 ft. of Morrow and Atokan sediments was very evident. Pennsylvanian age deformation within the aulacogen was dominated by displacements along major high angle fault zones. During the Mississippian and early Pennsylvanian ages, the Anadarko basin began to subside at a fast rate. According to Donovan et al. (1983), subsidence rate curves for the Anadarko basin show rapid rates of sedimentation in Cambro-Ordovician times, followed by relatively slow sedimentation rates in Silurian, Devonian, and early Mississippian times. Extremely rapid rates of sedimentation for the late Mississippian to Pennsylvanian age coincide with tectonic development in the Anadarko basin area during this time. As time progressed, flooding of the craton occurred, followed by the slowing of subsidence, regression of the sea and filling of the basin from east to west (Adler,1971).

Depositional Framework

Much of the Morrow section in the Anadarko basin formed during overall transgressive conditions; however,

the sandstone bodies generally reflect temporary regressive stages.

Two primary depositional models are recognized for the Morrowan clastics. Generally, Lower Morrow sandstones are characterized by features formed by marine processes. These sandstones show a northwest-southeast trend. Busch (1959) has interpreted these sandstones as beach deposits that parallel the ancient shorelines. These sandstones could also be the result of reworked deltaic deposits by longshore currents and redeposited as offshore bars (Simon, 1979). Diagnostic sedimentary structures observed in the cores indicating shallow marine deposition consist of burrows, ripple bedding, interstratification, penecontemporaneous deformation, and some horizontal bedding. These deposits can contain fine to coarse sand with contacts being both sharp and gradational. Diagnostic constituents include glauconite and fossil fragments (Figure 3). Primary shallow marine depositional facies in the Morrow can be classified as tidal ridge/shoal deposits, offshore bars, tidal flat, and transgressive deposits (Figure 4).

The Upper Morrow sandstones are generally characterized by deltaic processes with sources from the north-northeast and from the west-northwest. The Upper Morrow chert conglomerate, which is a fan delta deposit, indicates a source direction from the southwest. Morrow deltas are believed to be small and tide-dominated.

Diagnostic sedimentary structures observed in the

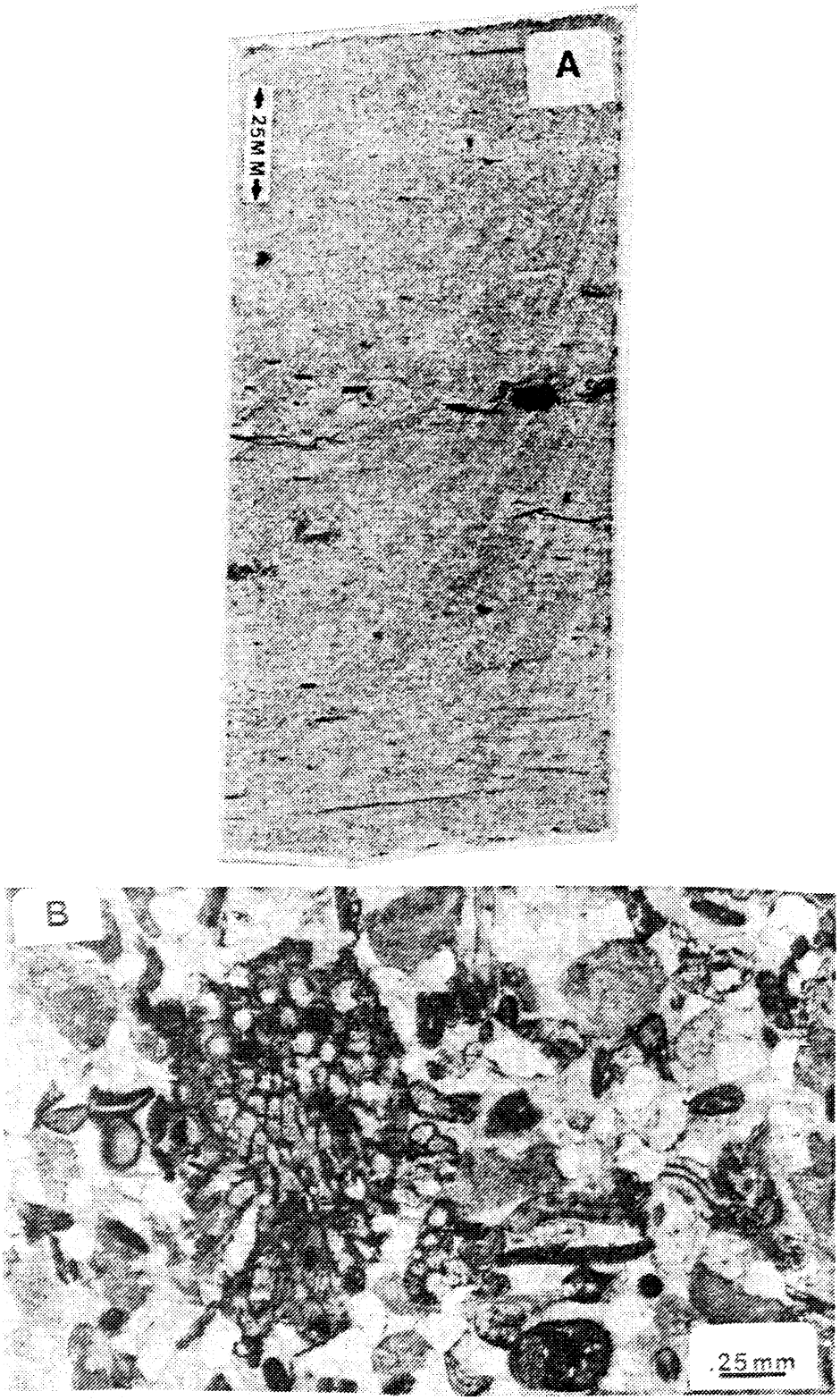

Figure 3. Lithologic Characteristics of Crossbedded Shallow Marine Sandstone (A) With Abundant Pelmatozoan Fragments and Other Fossils (B)

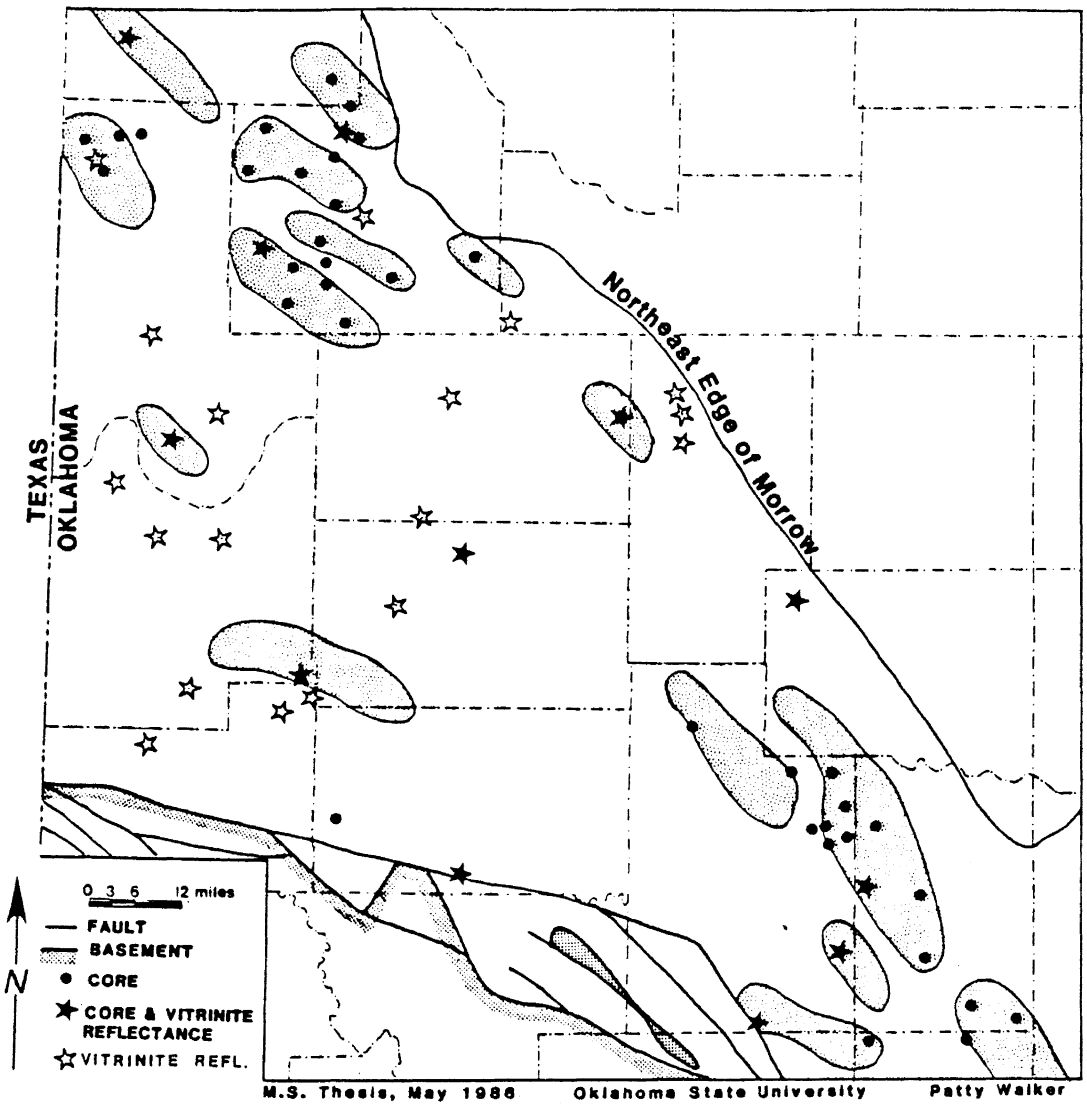

Figure 4. Known Distribution of Shallow Marine Sandstones (Modified from Busch, 1959; and Others)

cores that indicate deltaic deposition consist of cross-bedding, penecontemporaneous deformation, and minor bioturbation. These deposits generally contain fine sand and demonstrate sharp basal contacts (Figure 5). The sands fine upward with a corresponding increase in amount of clay. Diagnostic constituents include interclasts of clay and siderite, carbonaceous material, and occasional glauconite. Some deltaic sandstones are characterized by channel base conglomerate. Primary deltaic depositional facies observed in the Morrow sandstones include delta fringe deposits, distributary channels, interdistributary bays, and levee/splay deposits (Figure 6).

Khaiwka (1968) proposes two depositional types for the Morrow sandstones. Morrow deltas, which were small, were the depocenters for the shore sands deposited along the northeast shelf of the Anadarko basin. He has also suggested that levels of energy are expressed by textural differences within the sediments.

According to Simon (1979), there are different environments for the lower and upper Morrow sandstones. The Lower Morrow sandstones represent a marginal marine-transgressive system. These sandstones can be further subdivided into high and low energy environments.

Regressive fluvial/deltaic depositional systems existed during deposition of Upper Morrow sandstones (Simon,1979; Swanson,1979; Shelby,1980). Shelby (1980) also shows the presence of a chert conglomerate in the south-

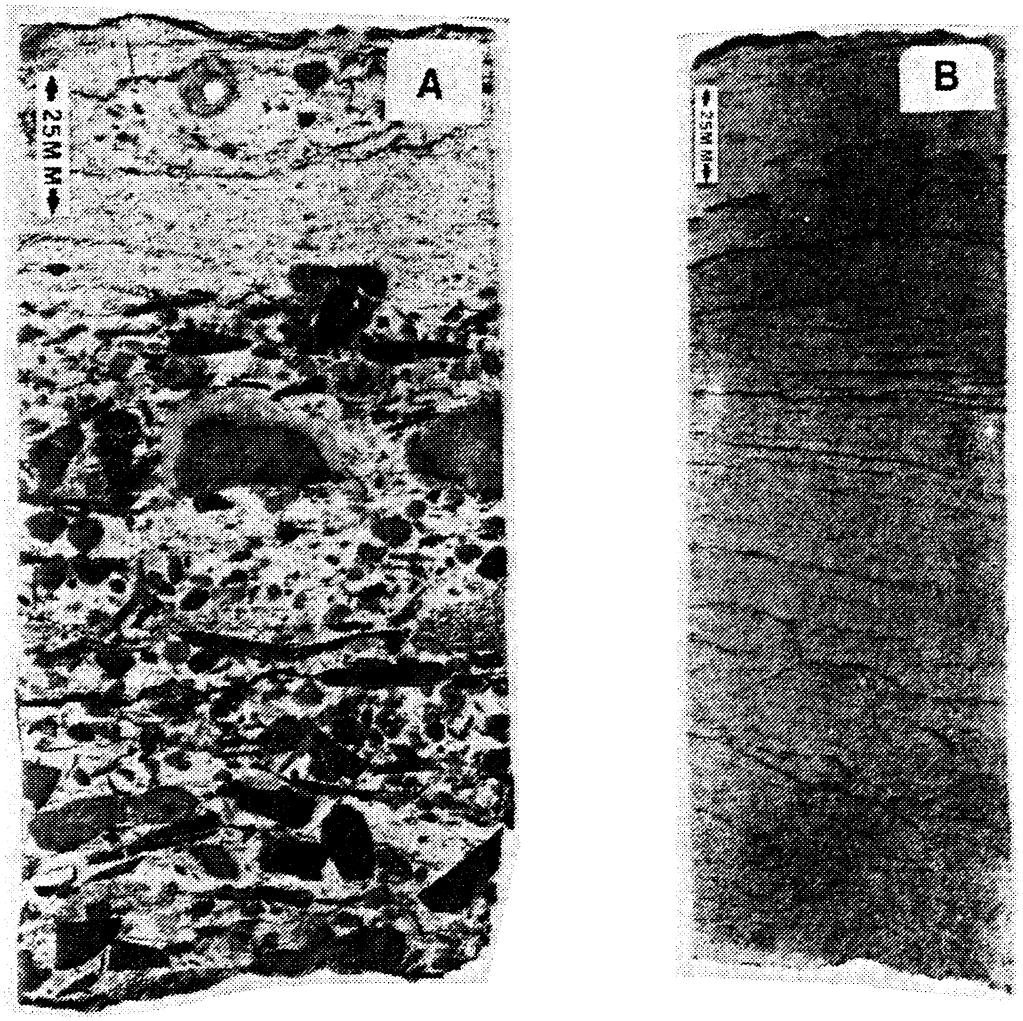

Figure 5. Lithological Characteristics of Deltaic Facies;
(A) Conglomerate at the Base of the Distributary Channel Fill Sandstones Pebbles are Composed of Collophane, Chert and Siderite.
(B) A Typical Crossbedded Distributary Channel Fill Sandstone

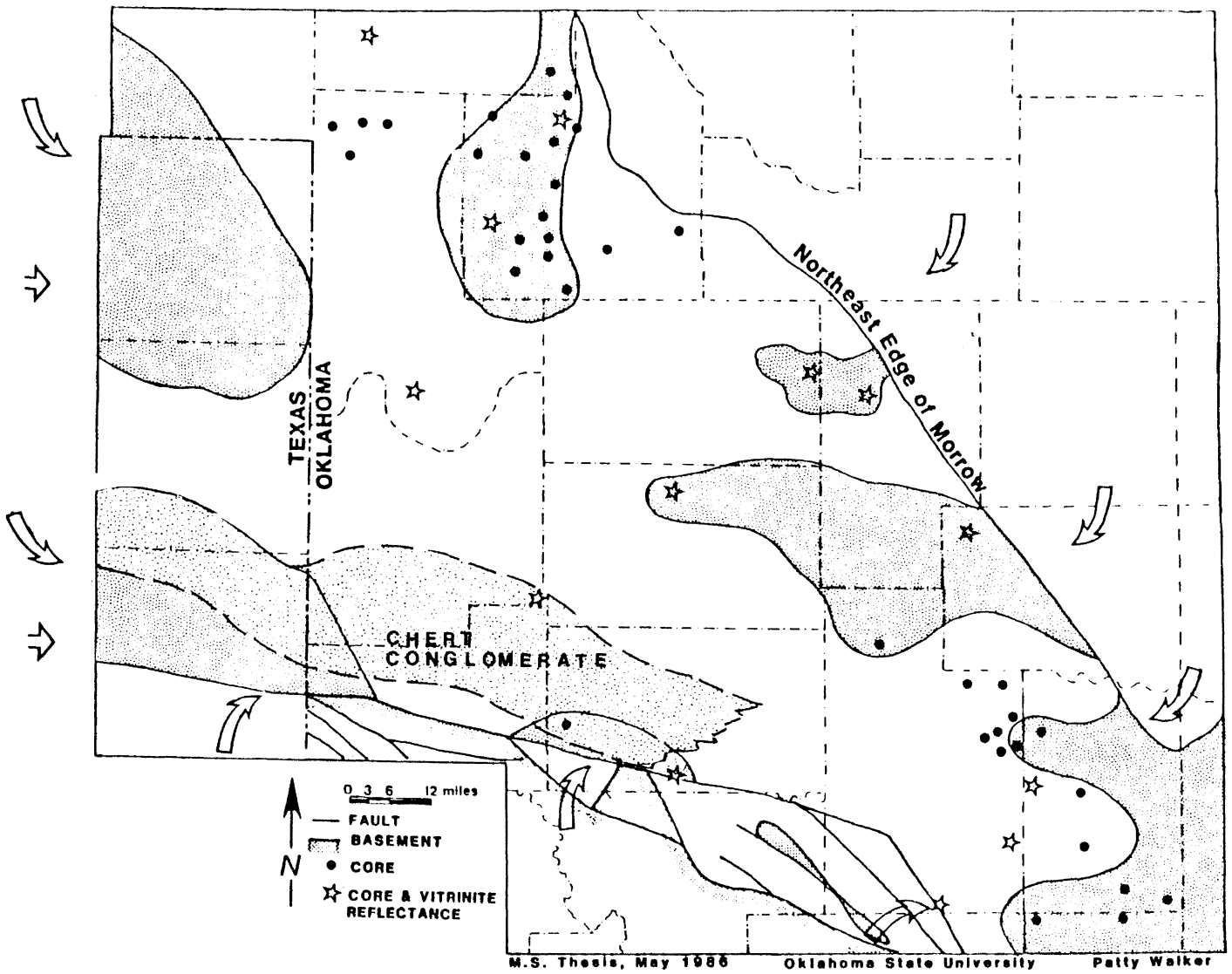

Figure 6. Known Distribution of Deltaic Sandstones (Modified from Evans, 1979; Forgotson, 1979; and Others)

western Anadarko basin. This Upper Morrow unit was deposited in a fan delta system prograding eastward across the shallow marine basin adjacent to the Amarillo-Wichita mountain front.

CHAPTER III

SANDSTONE PETROLOGY

Morrow sandstones contain a diverse suite of both detrital constituents and diagenetic products. Seven lithologic types are recognized on the basis of the major detrital components that characterize the Morrow sandstones (South,1983) (Figure 7). The major detrital constituents are quartz grains, skeletal fragments, detrital clay matrix, and rock fragments.

Lithologic Types

Within the Morrow sandstones of the study area, five lithologic types were noted. These lithologies are based on constituent averages for each core. A ternary diagram plot and well name abbreviations for the cores are included in Appendix C. The five lithologies are as follows:

1) Quartz arenite
2) Bioturbated quartz wacke sandstone/clayey sandstone
3) Quartz dominated skeletal litharenite
4) Arenaceous skeletal grainstones
5) Lithic pebble skeletal conglomerate

The quartz arenite sandstones are generally fine grained and well sorted. Quartz grains are rounded to

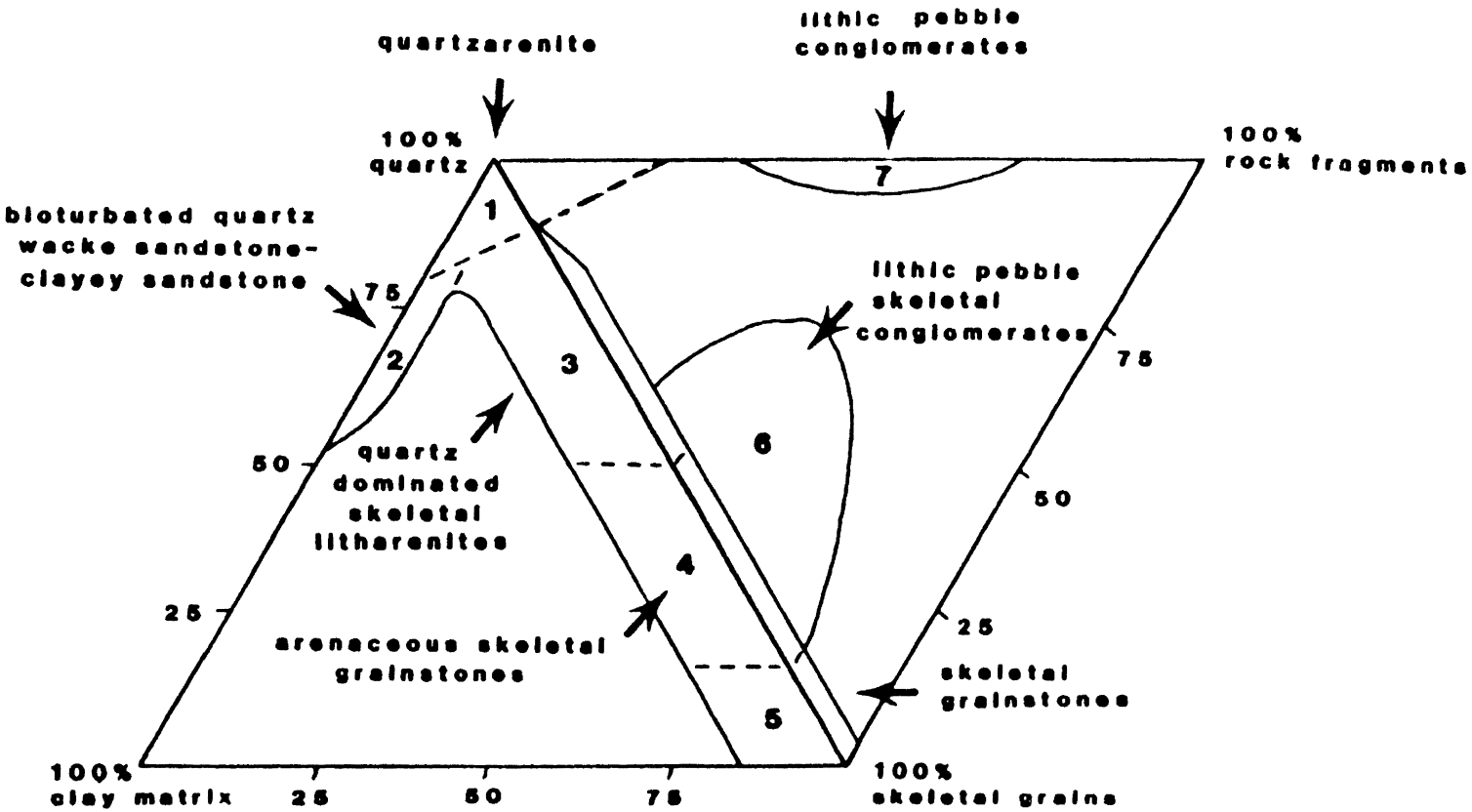

Figure 7. Various Lithologies of the Morrow Sandstones

subrounded. These sandstones can vary from supermature to immature based on clay matrix percentages. Examples are the Apache Atwell No.1 core which has a supermature sandstone and the Humble Richardson No.1 core which has an immature sandstone.

Bioturbated quartz wacke sandstones are generally poorly sorted and immature. They have a lower quartz content than the quartz arenites and exhibit a very fine grain size. Clay matrix is mixed and occurs in larger quantities. Examples of this lithology are sandstones within the Gulf Laverne State No.1 and the Gulf Ida No.1 cores.

Quartz dominated skeletal litharenites are similar to the quartz arenites but contain a higher fossil percentage. Examples are from the Humphrey-Packard Venable-Verden No.1 and the Arkla Exploration Carter No.1 cores.

Arenaceous skeletal grainstones are poorly sorted, submature to immature. Grainstones are medium pebble to medium sand in size. An example of this lithology is contained in the Shell Coulter No.1 core.

Lithic pebble skeletal conglomerates contain a diverse mineralogy. These rocks often grade into arenaceous skeletal grainstones. Examples are contained in the Shell Coulter No.1 and the Shell White No.1 cores.

There is a distinct petrologic difference between Morrow sandstones in the study area and those in the Oklahoma panhandle area of the basin. Morrow sandstones in

the extreme northwest part of the Anadarko basin are more feldspathic and can be classified as subarkosic. These rocks are generally subangular to subrounded and have poor to moderate sorting (Jobe, 1984). In general, Morrow sandstones in the Oklahoma and Texas panhandles contain up to 10 to 12% more feldspar than Morrow sandstones in the study area. Morrow sandstones in the Oklahoma panhandle are sourced from the Keyes Dome area and have undergone far less recycling than sandstones in the study area (Evans, 1979).

Another distinct petrologic type is the Upper Morrow chert conglomerate in the southwestern part of the basin. These conglomerates contain various colors of chert in a fine to coarse, poorly sorted quartz sand, chert, and feldspar matrix. Chert grains are rounded to subangular ranging in size from coarse to pebble. Morrow chert conglomerates were sourced from the southwest (Shelby, 1980).

Detrital Constituents

Quartz

Monocrystalline quartz is the dominant framework grain averaging 40 to 80 percent. Texturally, quartz grains vary from fine to medium grained; grains are subrounded to rounded. Advanced to medium stage syntaxial quartz overgrowths are common (Figure 8). Where the quartz occurs with carbonate, corrosion of the grain boundaries and overgrowths is common. Extinction of the grains varies from

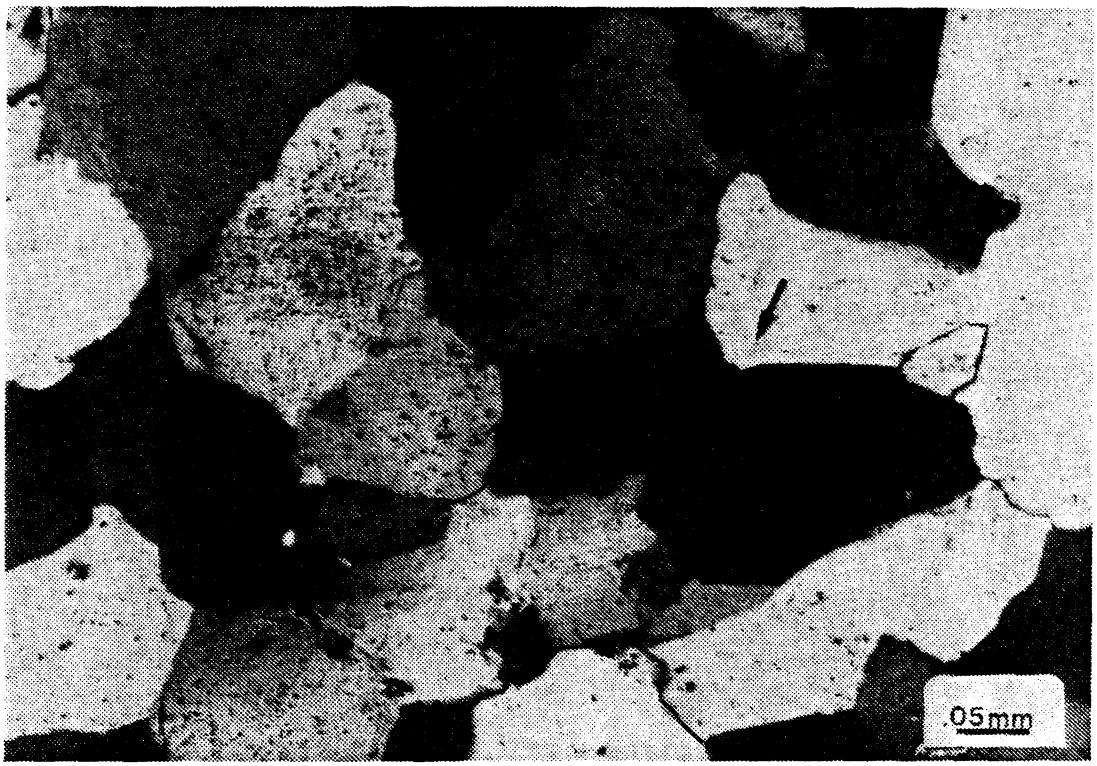

Figure 8. Quartz, as the Major Constituent, is Composed Mainly of Single Crystals, Some With Overgrowths (Arrows); Cross Polarized

straight to undulose with some grains exhibiting "boehm lamella". Some grains have inclusions and small vacuoles. Polycrystalline quartz, as composite grains, is rare and generally occurs in minor amounts.

Skeletal Fragments

A variety of fossil fragments occur within the Morrow sandstones; percentages range from a trace to amounts typical of a calcarenite sandstone. Fossil types include echinoderm plates and stems, brachiopod shells and spines, bryozoans, trilobites, ostracods, forams, gastropods, and algae. These fragments range in size from medium pebble to medium sand (Figure 9).

Rock fragments

Several types of rock fragments occur within the Morrow sandstones and are rounded to subrounded, pebble to granule size clasts with a variable sphericity.

Siderite and skeletal grainstone pebbles make up the carbonate rock fragments (Figure 10A). The siderite clasts are reddish-brown, finely crystalline with iron stained rims. These clasts occasionally contain corroded silt size quartz, chert, and skeletal grains. The skeletal clasts are tan to light gray and contain fine-grained fossil fragments within a sparry calcite cement.

Collophane clasts are common and are characterized by a reddish-brown color in plane-polarized light, with an

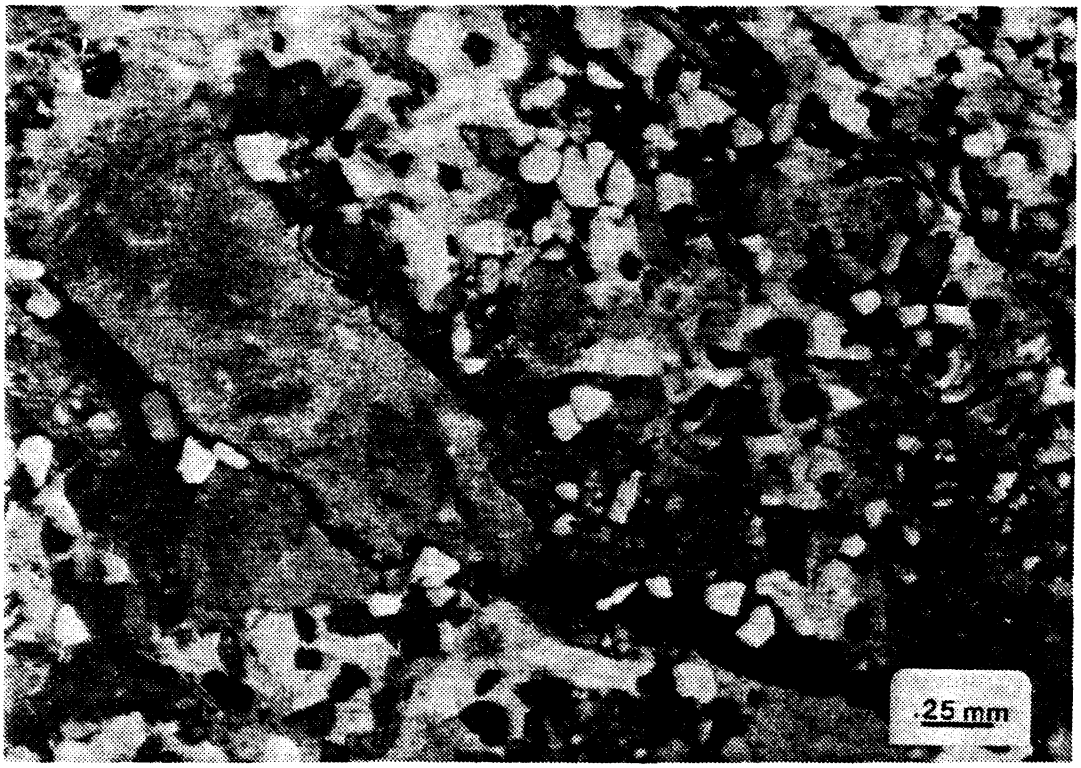

Figure 9. Photomicrograph of a Variety of Fossil Fragments in Sandstone; Cross Polarized

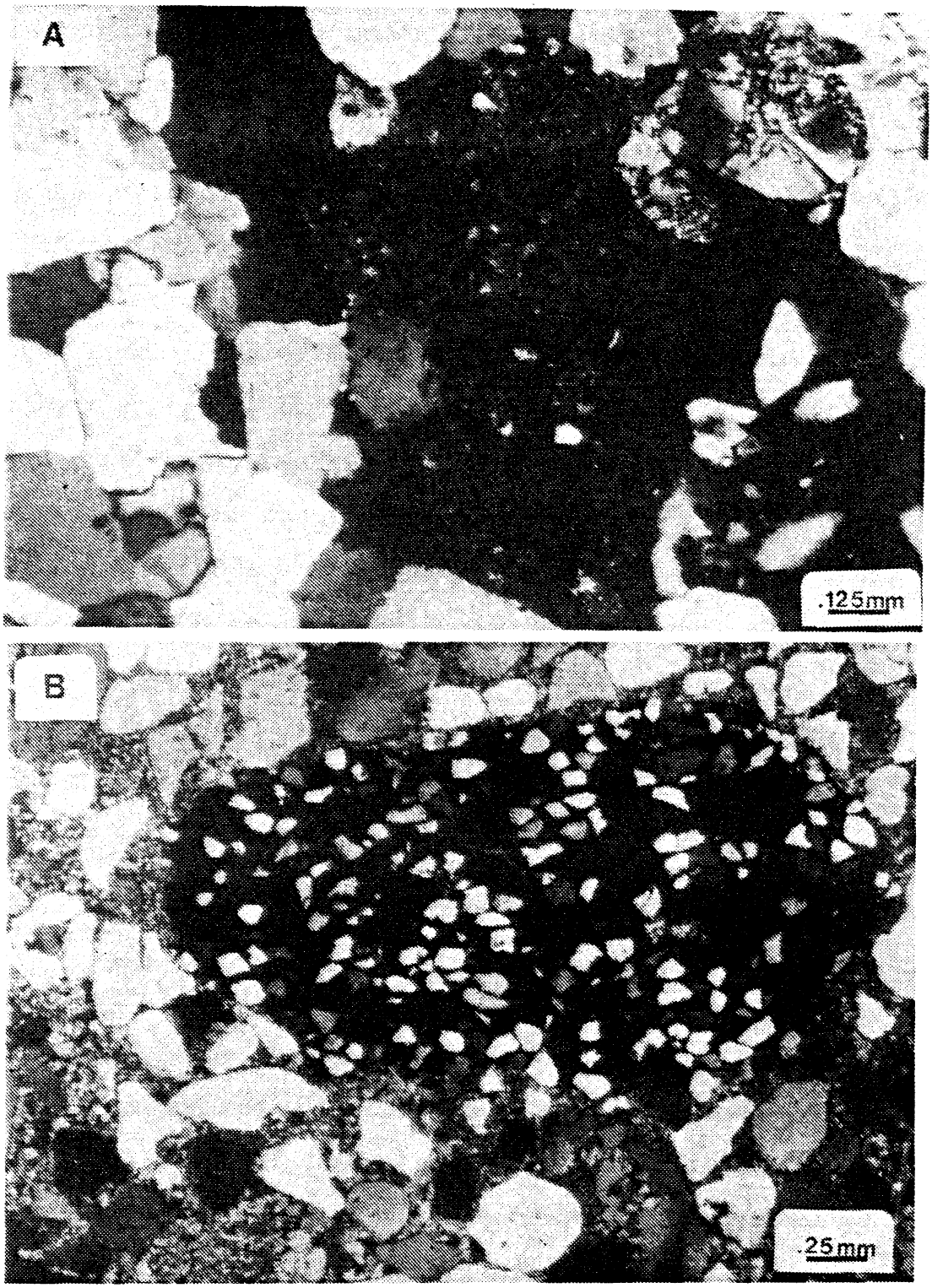

Figure 10. (A) Photomicrograph of Rock Fragment Composed of Finely Crystalline Siderite; Cross Polarized
(B) Photomicrograph of Collophane Cemented Rock Fragment; Cross Polarized

isotropic appearance under crossed polarized light. These collophane clasts can include fossil fragments, silt size quartz, chert, coated grains with quartz nuclei, carbonate grains, and occasionally apatite crystals and pyrite cubes (Figure 10B).

Siliciclastics in the form of mud/shale clasts are less common than carbonate and collophane clasts. These clasts appear as silty claystones, intraformational shales, and fossiliferous shales. The silty claystones are tan to dark brown with occasional replacement by micrite. The intraformational shale clasts appear dark brown to black and show ductile deformation along the edges. These clasts are associated with silty shale laminae.

Carbonized wood fragments are a minor rock type within the Morrow sandstones. These fragments range in size from pebble to sand and are opaque.

Clay Matrix

Detrital clay matrix and glauconite occur in a majority of the rocks. Clay matrix is composed of illite and is associated with bioturbation and flowage. Re-crystallization of this matrix to chlorite is common. The matrix appears greenish-brown to brown. The greenish tint reflects chlorite clay and/or deformed glauconite. The brown tint is due to mixed-layer clay and/or altered glauconite.

Glauconite

Glauconite occurs as a penecontemporaneous deposit and is characterized by a bright green color and spherical to ovoid shaped grains (Figure 11). Some of the grains show concentration along bedding. A common feature of the glauconite grains is their deformation to form pseudomatrix (Figure 12A,B). The deformed glauconite may then be altered to brown glauconite which becomes difficult to distinguish from clay matrix. X-ray diffraction and EDXA analyses show Morrow sandstone glauconite to be of an illitic composition (Figure 13 A,B). The green glauconite is high in iron and magnesium and the brown glauconite is high in aluminum and potassium and shows a loss of iron. The presence of glauconite is usually indicative of a shallow marine environment.

Other constituents seen in minor amounts include mica, zircon, staurolite, framboidal pyrite, rutile, leucoxene, and occasionally plagioclase. These constituents are usually fine grained.

Diagenetic Constituents

Silica

Authigenic silica is present in several varieties in the Morrow sandstones. Syntaxial quartz overgrowths are very common. Dust rims which separate overgrowths from detrital cores occur very commonly but where they do not,

Figure 11. Photomicrograph of Glauconite, Occurring as Rounded Green Grains; Plane Polarized.

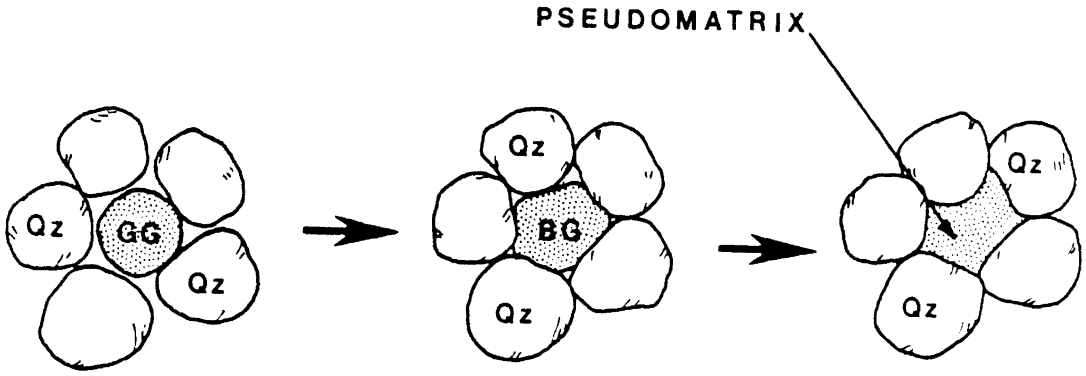

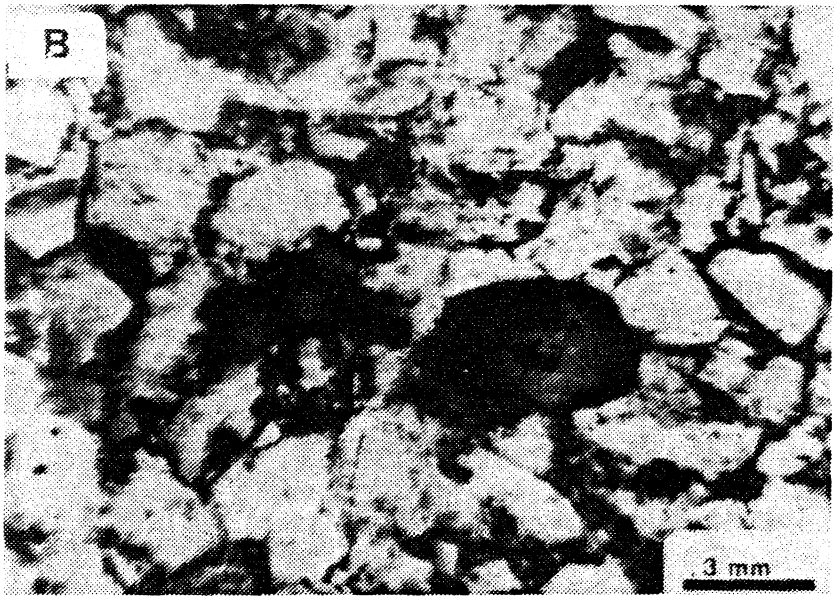

Figure 12. Ductile Deformation of a Glauconite Pellet During Compaction to Form Pseudomatrix (A & B); Arrow Points to Brown Rim of Green Glauconite Pellet

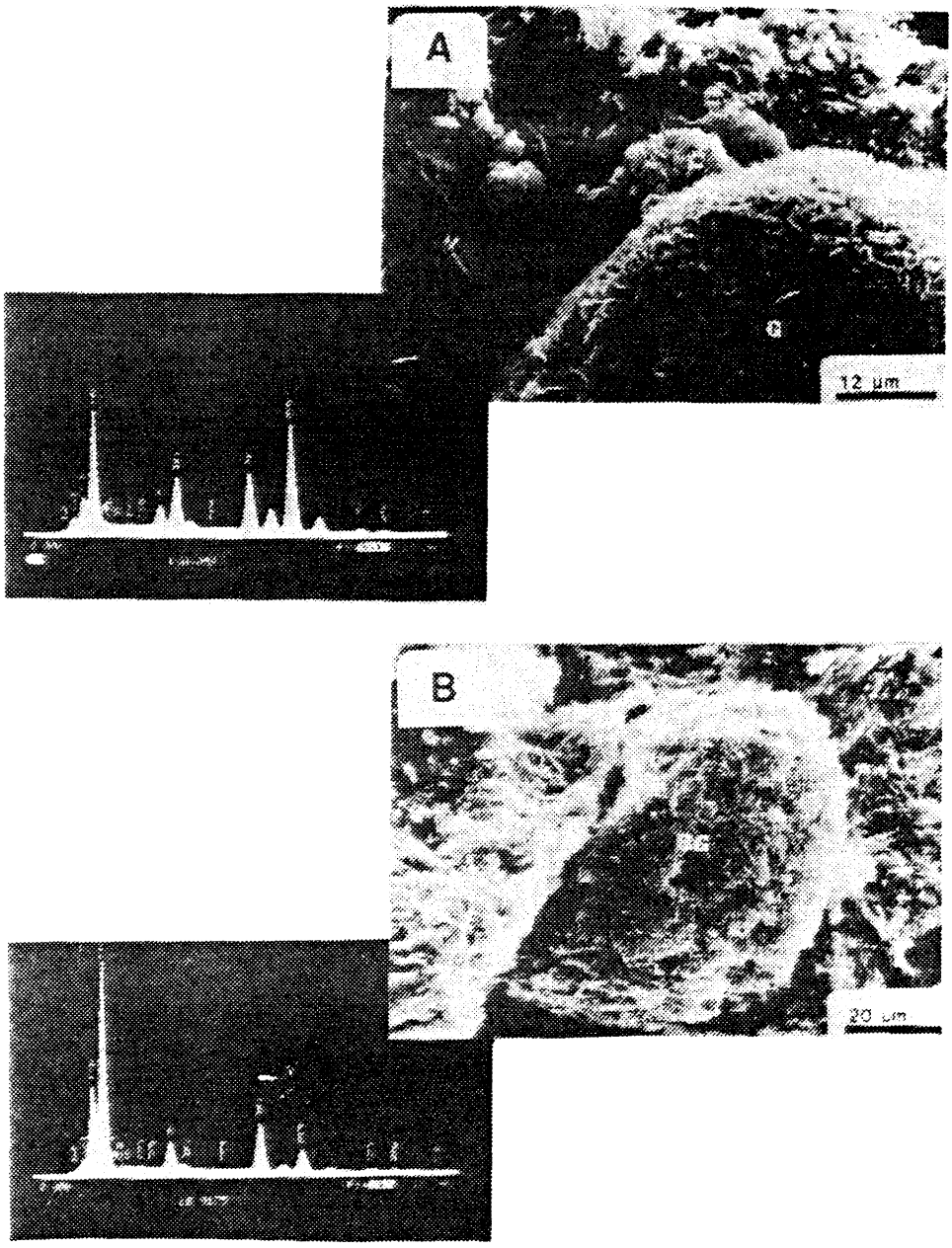

Figure 13. (A) SEM Photomicrograph of Green Glauconite (G) Pellet in Sandstone. Energy Dispersive X-Ray Analysis (EDXA) Showing a Typical Iron Peak
(B) SEM Photomicrograph of Brown Glauconite Pellet (BG) Formed from Alteration of Green Glauconite. EDXA of Pellet Showing Iron Content Depletion and Enrichment in Potassium and Aluminum

the overgrowth is not readily distinguishable. However, these overgrowths can be distinguished by cathodo-luminesence or by their euhedral outlines. Chalcedony, microquartz, drusy megaquartz, and meniscus silica cement occur as pore-filling cements and as replacement features (Figure 14).

Carbonates

Authigenic carbonates occur in several forms. Poikilotopic and mosaic calcite are common in the quartz dominated sandstones but occur less commonly in the skeletal grainstones. Poikilotopic calcite is characterized by large single crystal cements that enclose several quartz grains (Figure 15). Mosaic calcite occurs as large patches of equant crystals that often appear to displace quartz crystals. Sparry calcite, ferroan calcite, dolomite, siderite, and ankerite also occur in the Morrow sandstones.

Sparry calcite occurs as a void filler in inter-granular pockets and intra-skeletal voids.

Dolomite and siderite were observed as isolated euhedral rhombs, grain linings, and as replacement of detrital skeletal grains, glauconite, and chert. Dolomite and siderite were also observed as void filling cements and matrix aggregates. Siderite has a characteristic "wheat-grain" crystal habit and is reddish-brown under plane polarized light (Figure 16).

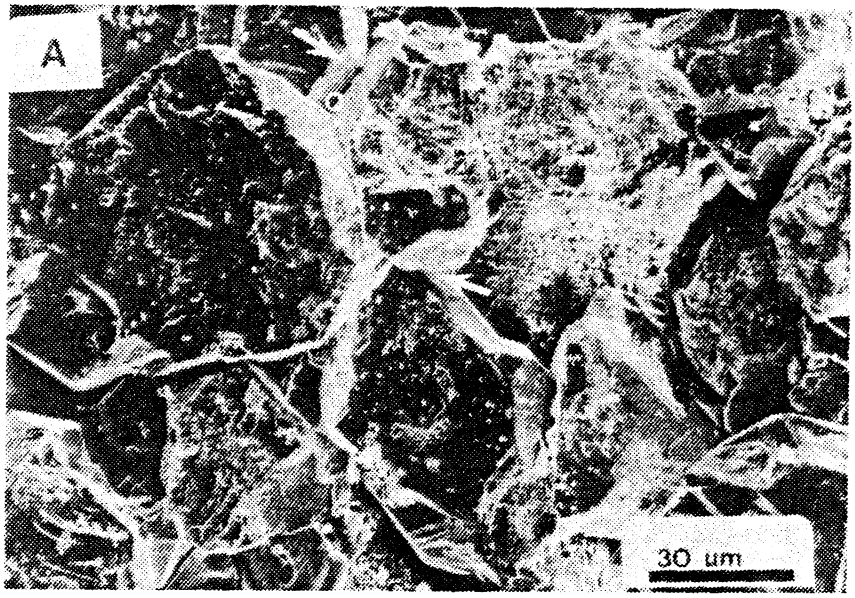

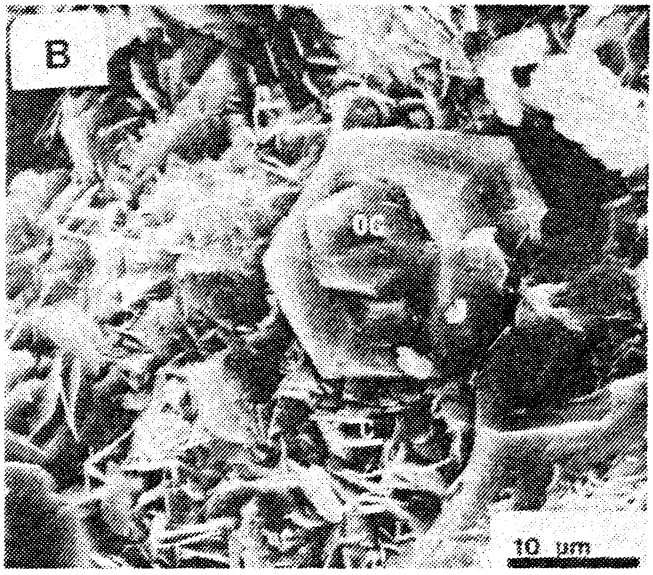

Figure 14. (A) SEM Photomicrograph of Silica Cement as an Early Syntaxial Overgrowth (Arrow)
(B) SEM Photomicrograph Showing Two Distinct Zones of Quartz Overgrowth

Figure 15. Poikilotopic Calcite Cement. Arrow Indicates Corroded Boundaries of Quartz Crystals; Cross Polarized.

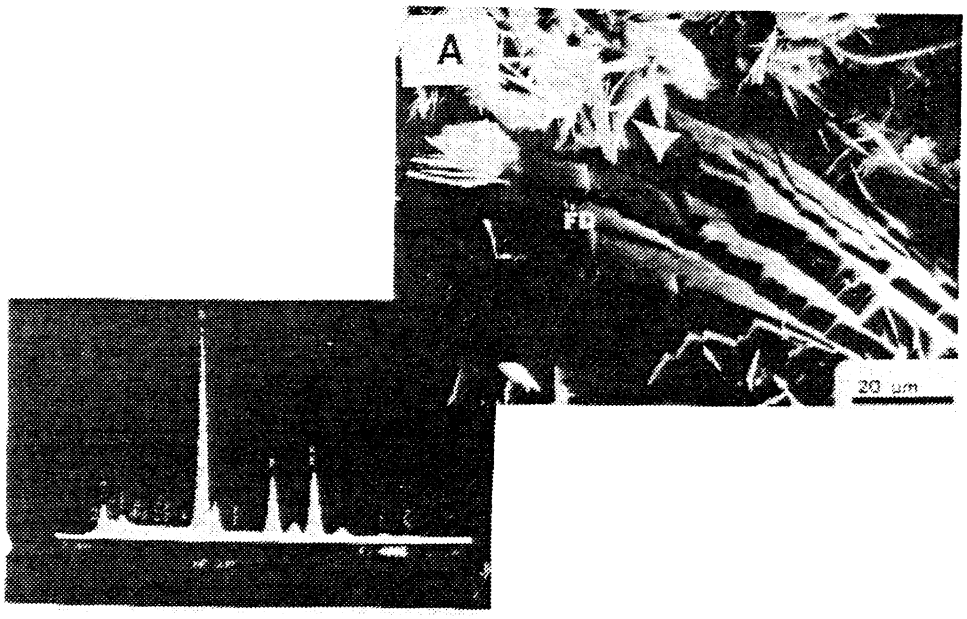

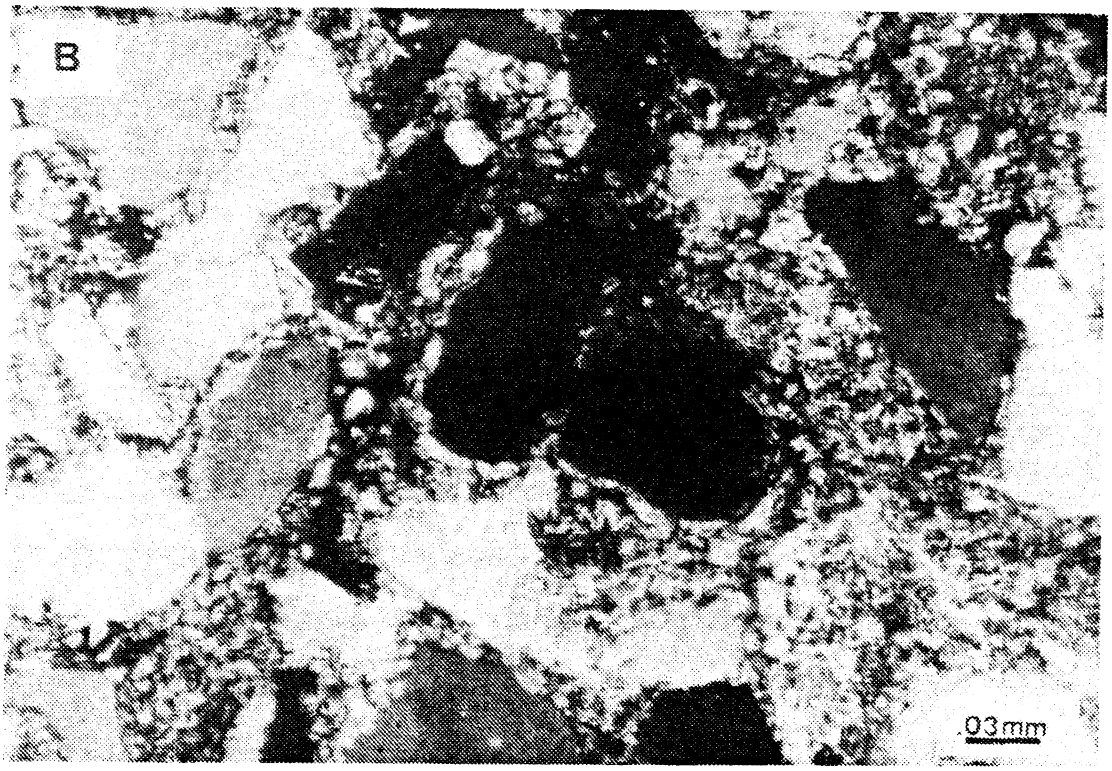

Figure 16. (A) SEM Photomicrograph of Ferroan Dolomite (FD) and Chlorite (Arrow); Both Formed from Alteration of Glauconite. EDXA Indicates that Dolomite is Iron Rich
(B) Photomicrograph of Wheat-Grain Texture Siderite and Partially Dissolved Glauconite; Plane Polarized

The distribution of authigenic carbonate cement in the Anadarko basin for the Morrow Formation is shown in Figure 17. The areas enriched in carbonate cement show the same approximate NW-SE trend as the shallow marine sandstone bodies of Figure 4.

Pyrite

Authigenic pyrite occurs as patchy cement, replacement of detrital constituents, along stylolites, and as framboidal aggregates. The most common grains replaced by pyrite are skeletal grains and collophane fragments.

Authigenic clays are by far one of the most abundant constituents and occur as kaolinite, chlorite, illite, and illite-smectite mixed layer clay.

Kaolinite

Kaolinite occurs as a pore-filling authigenic clay that forms discrete booklets or vermicular morphologies (Figure 18). Kaolinite is more abundant in the northern study area than in the southern.

The distribution of areas enriched in authigenic kaolinite in the Anadarko basin for the Morrow Formation is shown in Figure 19. The northwest-southeast trend of kaolinite zone coincides with the Watonga Production Trend. With the onset of thermal maturation, organic acids and their decarboxylation products (mainly CO_2 gas) are released into the formation waters which are conducive to

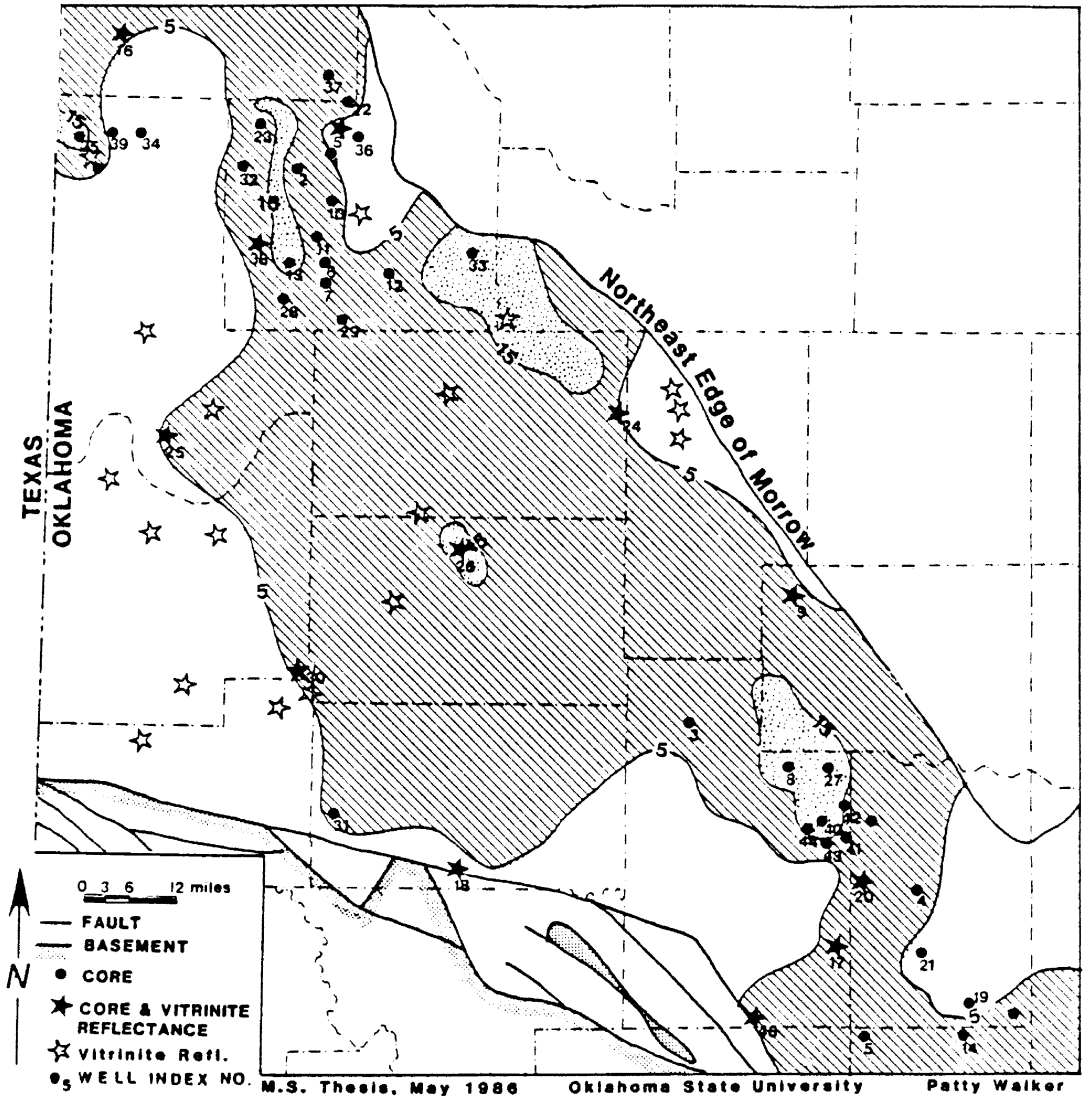

Figure 17. Distribution of Authigenic Carbonate Cement (Greater than 5% and 15%)

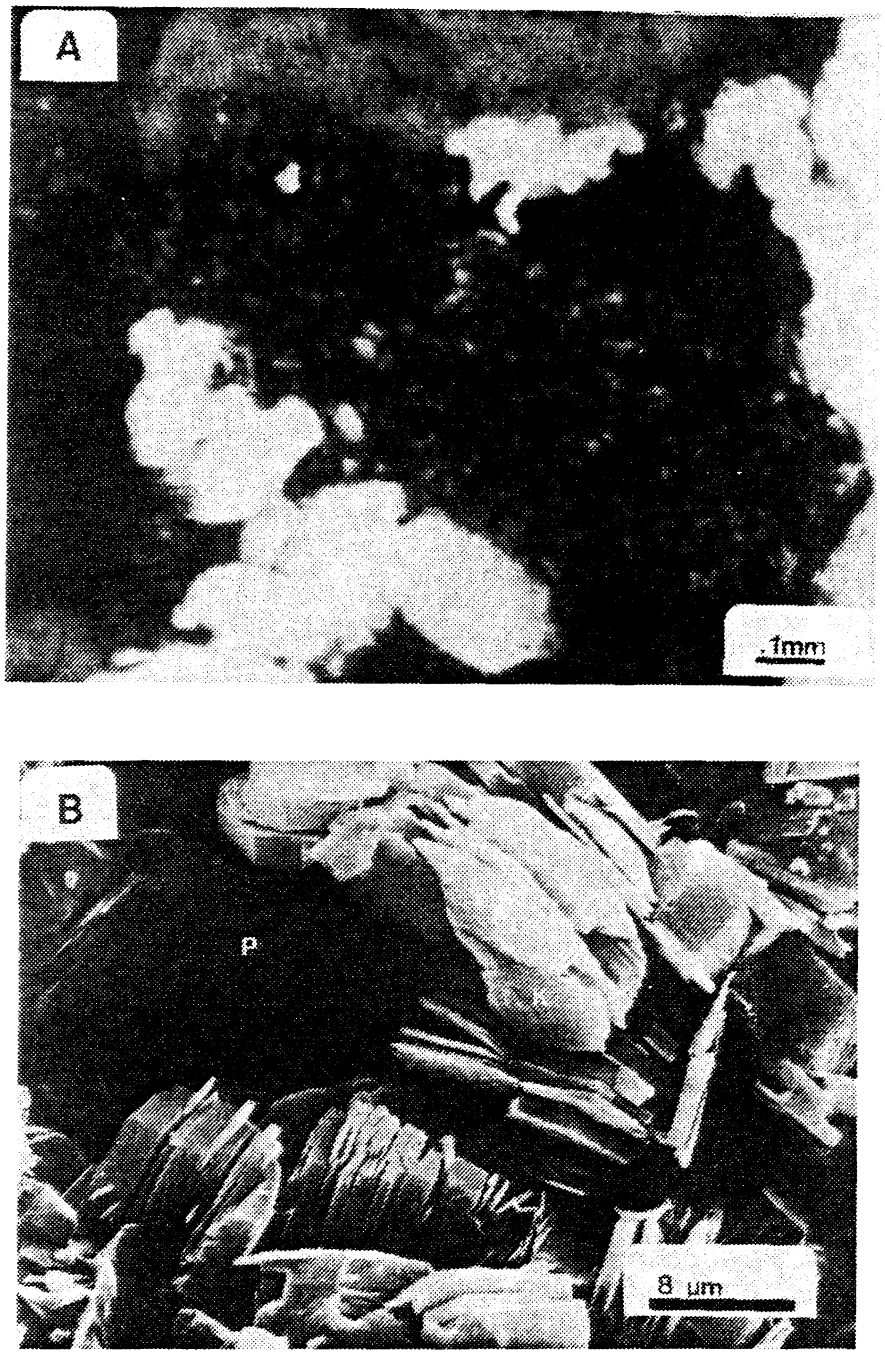

Figure 18. (A) Photomicrograph of Pore Filling Kaolinite; Plane Polarized
(B) SEM Photomicrograph of Kaolinite Exhibiting Vermicular Morphology

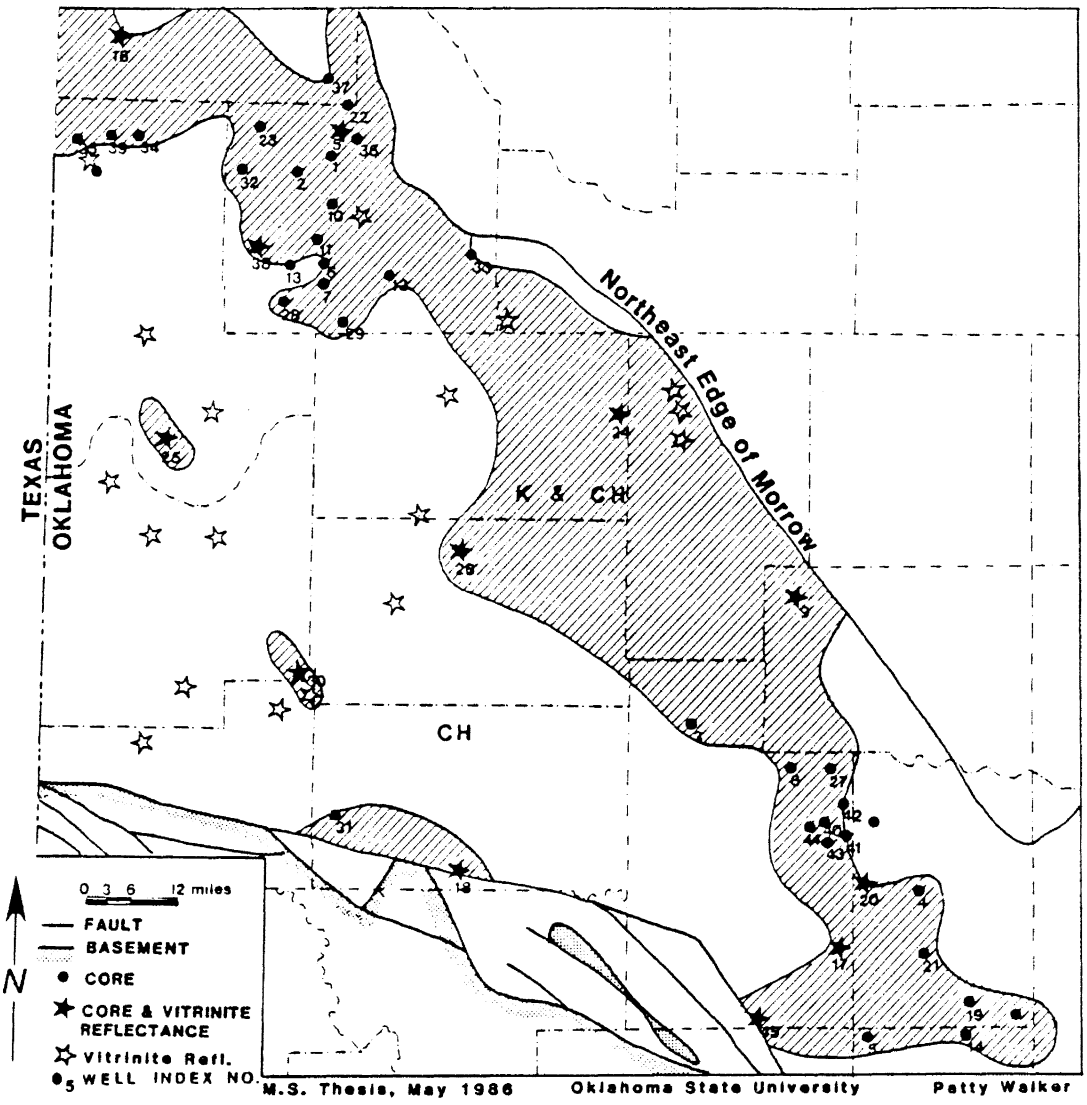

Figure 19. Distribution of Authigenic Kaolinite Rich Zone.(CH & K) Kaolinite Rich Zone; (CH) Predominantly Chlorite

the formation of kaolinite. Kaolinite also appears to become less abundant with depth, where it is replaced by chlorite.

Chlorite

Chlorite is the most common authigenic clay in the Morrow sandstones. It occurs as pore filling, pore lining, replacement of glauconite, and replacement of matrix (Figure 20).

Authigenic chlorite occurs in various morphologies such as edge-to-face, cluster, and rosette type arrangement. Microanalysis by EDXA shows chlorite to be iron rich. Chlorite is present in the majority of the thin sections examined. It appears to be more abundant in the sandstones than interbedded shales and exhibits an increase in abundance with depth.

Illite

Illite-smectite mixed layer clay is the major component of glauconite and recrystallized matrix. Pure illite occurs as pore-lining and pore-filling. Illite occurs sporadically within the Morrow Formation in the basin (Figure 21). Brown glauconite which is the product of alteration of green glauconite is composed of illite (Figure 22).

Carbonaceous material is a minor constituent and is most common in shaly sandstones or along stylolites.

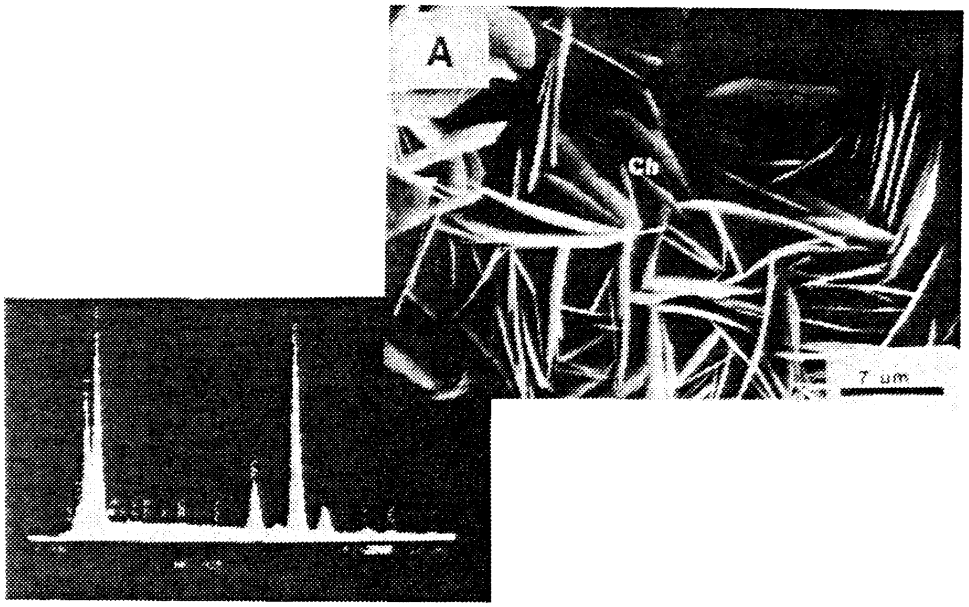

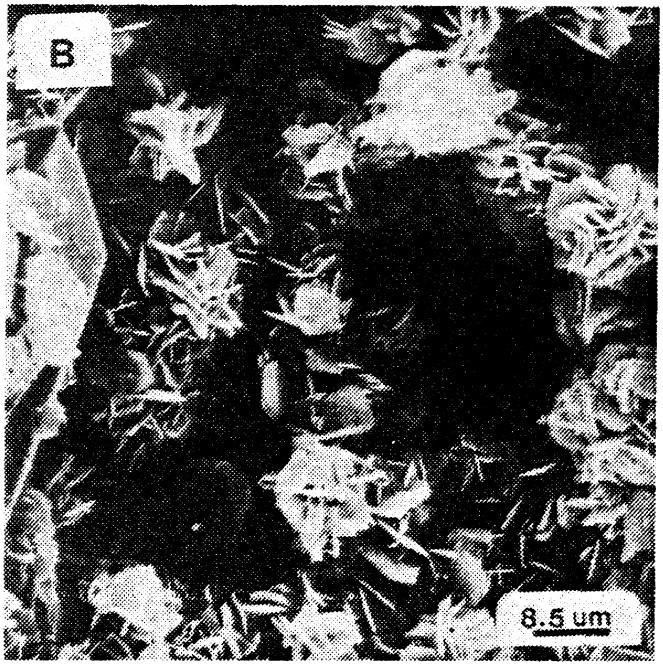

Figure 20. (A) SEM Photomicrograph of Iron-Rich Chlorite (CH) With Edge-To-Face Morphology. EDXA Indicates Chlorite is Iron Rich
(B) SEM Photomicrograph of Chlorite Exhibiting Edge-To-Face and Cluster Morphologies

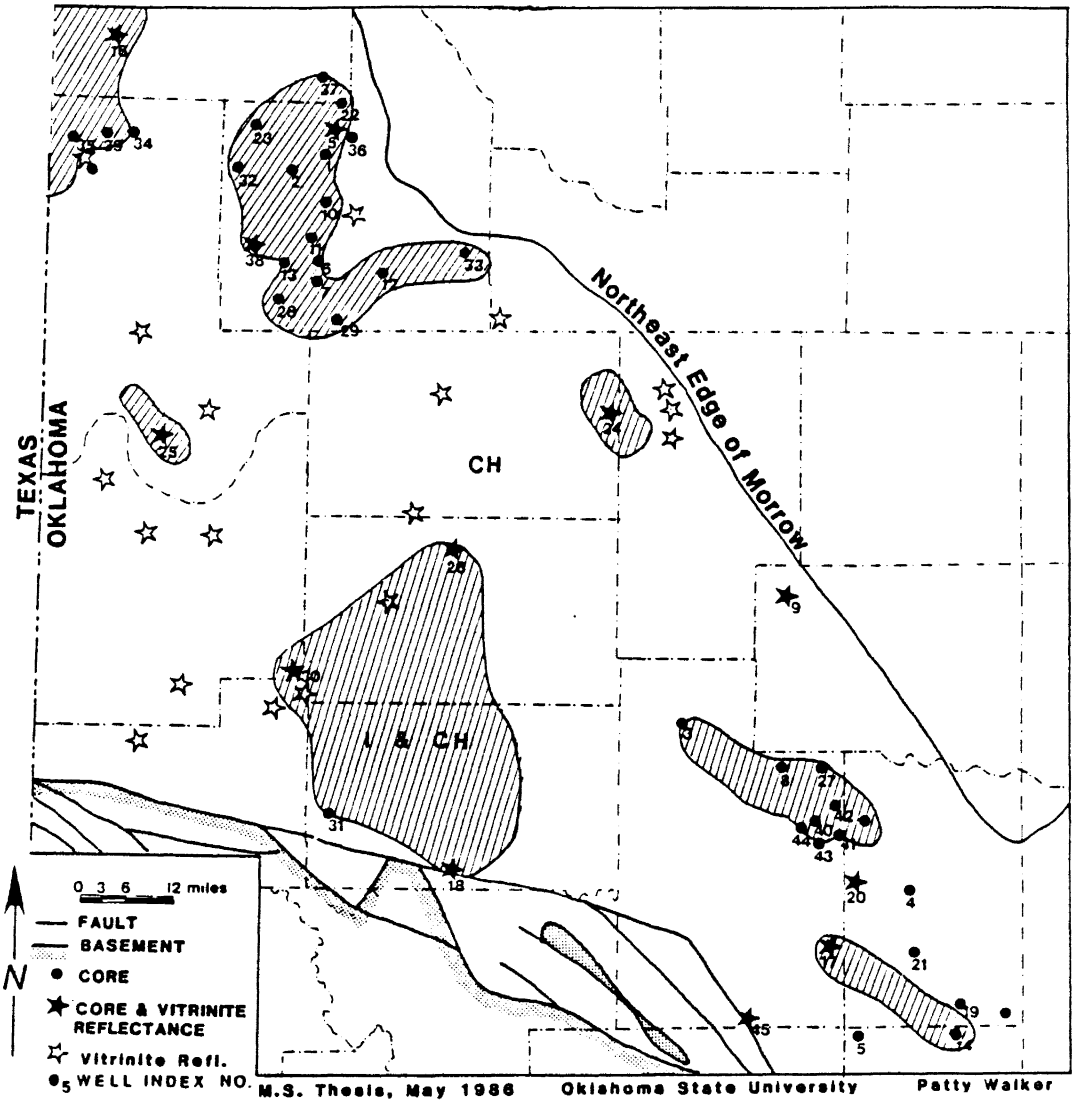

Figure 21. Distribution of Authigenic Illite Rich Zones. (I & CH) Illite Rich Zones; (CH) Predominantly Chlorite

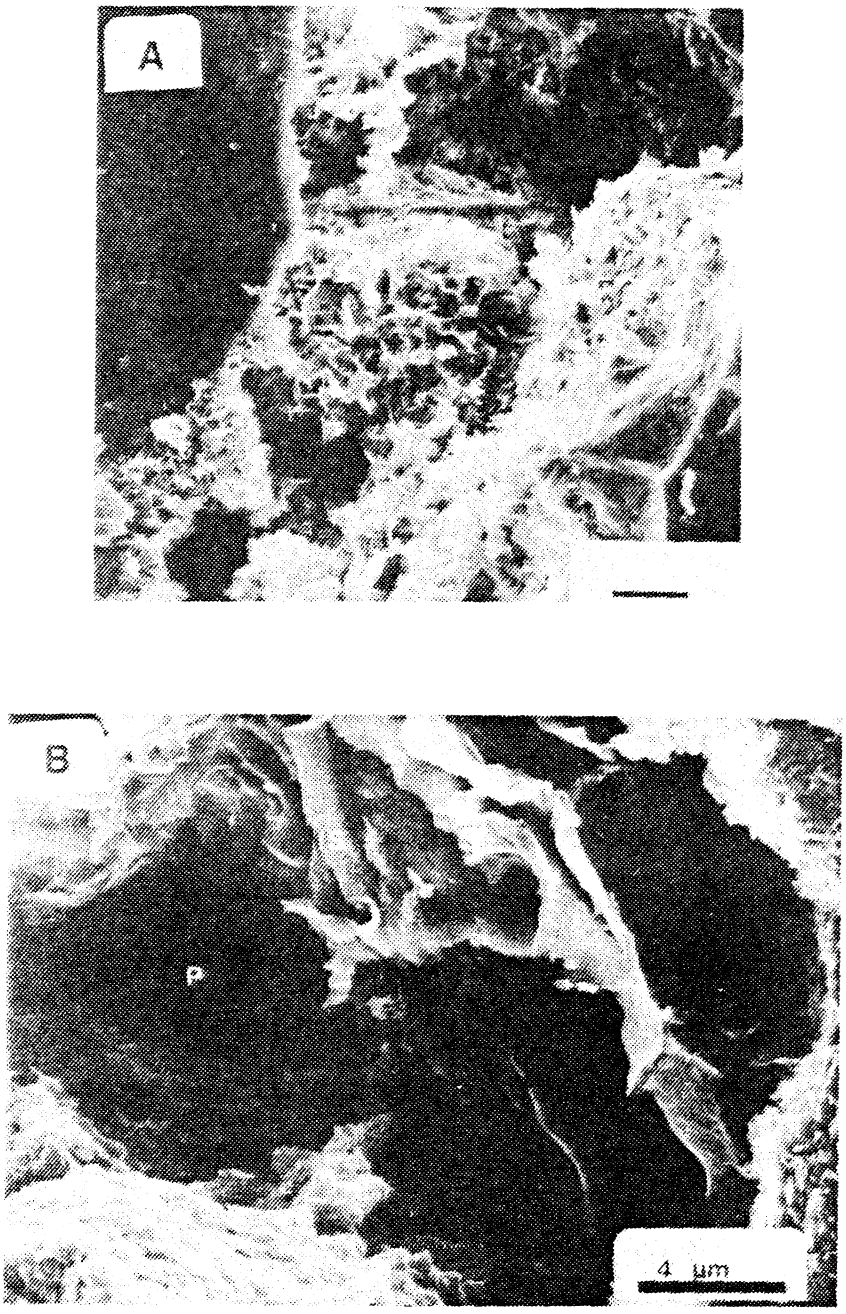

Figure 22. (A) SEM Photomicrograph of Lath Like Grain Coating Authigenic Illite
(B) SEM Photomicrograph of Illite-Smectite Mixed Layer Clay

CHAPTER IV

DIAGENESIS

Diagenesis played an important role in both the development of secondary porosity and reduction of reservoir quality in the Morrow Sandstone. Figure 23 summarizes the diagenetic history of Morrow sandstones.

Silica

Early silica is formed as syntaxial quartz overgrowths. Advanced and intermediate stages of overgrowth were observed. Advanced quartz overgrowths completely encase the original grain forming sinuous contacts and obliterating the intergranular pore space. Dust rims composed of clay and/or hematite may separate the overgrowth from the detrital grain; however, dust rims are not always observed in the Morrow. Cathodoluminesence was useful in differentiating the detrital quartz from quartz overgrowth and also in determining the extent of silica diagenesis. Advanced stages of quartz overgrowths are present in the relatively clean quartz arenite sands. Hower (1976) suggested that the alteration of adjacent shales could be a possible source of silica for the overgrowths.

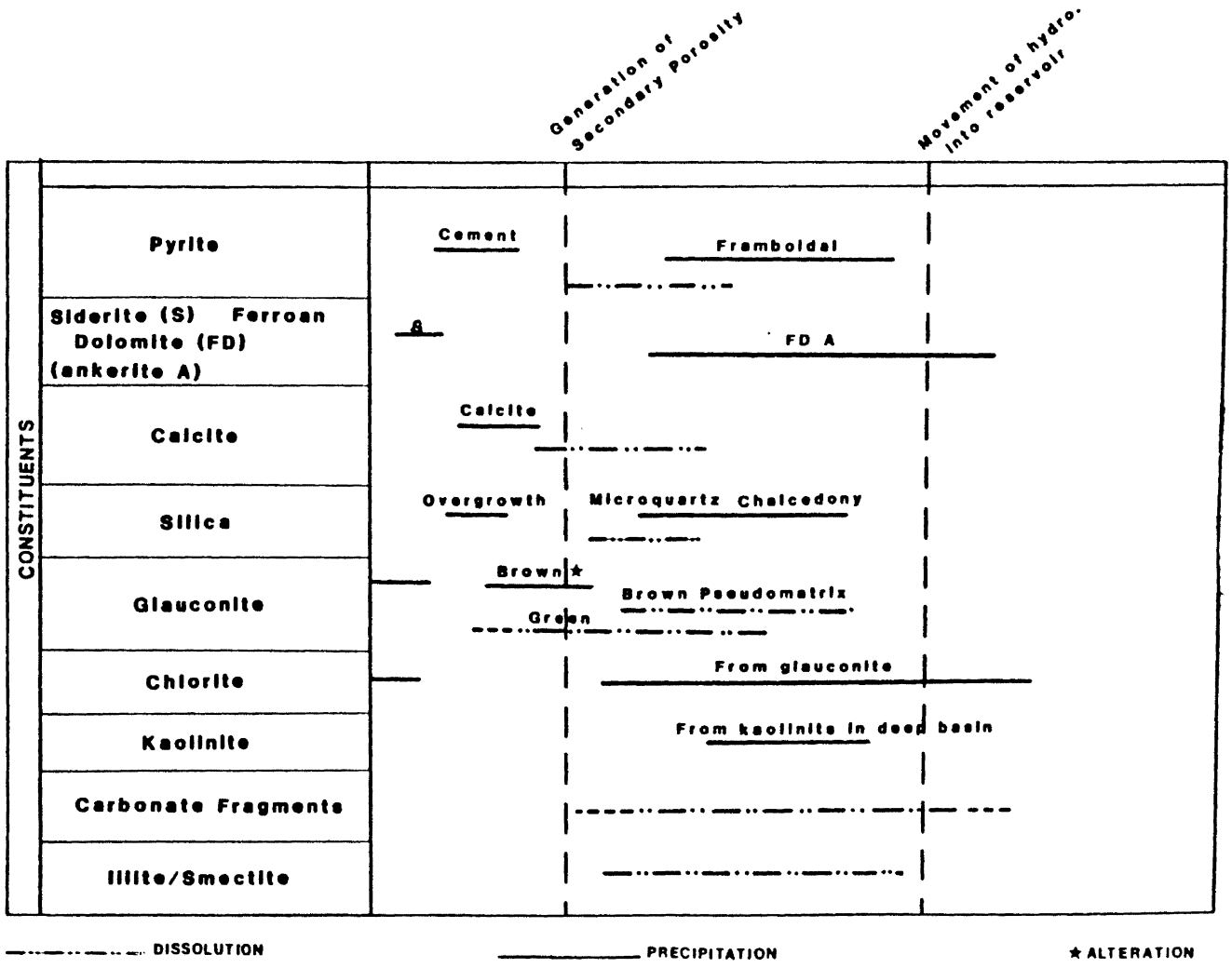

Figure 23. Diagenetic History of Morrow Sandstones

Late silica diagenesis is characterized by the presence of microquartz and chalcedony. Al-Shaieb and Shelton (1981) suggest that alteration of clay matrix and glauconite releases silica that may induce the precipitation of these cements. Corrosion of quartz boundaries by carbonate and matrix is common. Pressure-solution was observed and is identifiable by sutured contacts at grain boundaries.

Carbonate

Early carbonate cementation consists of mosaic calcite which has replaced/displaced quartz grains and poikilotopic pore-filling cements. Carbonate exhibits a corrosive relationship with adjacent quartz grains.

Siderite exhibits a "wheat grain" texture and is believed to have derived its iron from the alteration of glauconite to illite. Crystals form rims between detrital grains and overgrowths indicating an early stage of carbonate cementation before quartz overgrowths. Siderite is a common early diagenetic product. Late siderite occurs in minor amounts.

Late ferroan dolomite (ankerite) occurs as a replacement of early calcite cement and as pore filling euhedral rhombs. Ferroan dolomite also occurs as an alteration of glauconite. Replacement of calcite by ankerite utilizes iron and magnesium released during the breakdown of glauconite to illite. Boles and Franks

(1979) proposed a temperature of approximately 120° C for the formation of ankerite.

Pressure-solution of skeletal grains could be a source of carbon for carbonate cement within the Morrow sandstones. The decarboxylation of organic acids could also be another source of carbon for carbonate cement.

Clays

Chlorite, kaolinite, and mixed layer illite-smectite are the major authigenic clays.

Chlorite occurs in minor amounts as an early constituent of dust rims but is primarily a late diagenetic cement.

Kaolinite is a late diagenetic mineral filling secondary pore spaces. Kaolinite occurs only in minor amounts within the Morrow in the deeper parts of the basin where it is readily replaced by chlorite.

Illite-smectite occurs as replacement of glauconite and recrystallized matrix. It is conceivable that clay matrix recrystallization occurred both before and after clay matrix dissolution and secondary porosity generation. Ductile deformation of clay matrix is an early diagenetic feature in response to compaction during burial.

Glauconite

Glauconite is very abundant in the Morrow sandstones and has undergone several diagenetic changes. Glauconite

diagenesis has also had a drastic effect on the reservoir quality of the Morrow sandstones. Dissolution of glauconite is a spectacular feature of the Morrow Formation and will be discussed under porosity evolution. The alteration of green glauconite to brown glauconite may be either partial or complete. Generally, this alteration is exhibited in sandstones that have also undergone ductile deformation. Some of the brown glauconite also shows dissolution features.

Flowage of glauconite into pore spaces to form pseudo-matrix is very common. Deformation of brown glauconite is much more prominent than that of green glauconite. Both the green and brown glauconite show various degrees of alteration to chlorite.

Pyrite

Early pyrite occurs as a cementing agent of detrital grains after quartz overgrowths. In some areas, pyrite cement exhibits a poikilotopic texture, with quartz grains appearing to "float" in pyrite cement. Pyrite also occurs as a replacement of wood and fossil fragments and is observed infilling stylolites. Late-stage pyrite forms as spheroidal-like aggregates that are pore filling. Scanning electron microscopy (SEM) examination reveals its framboidal morphology (Figure 24).

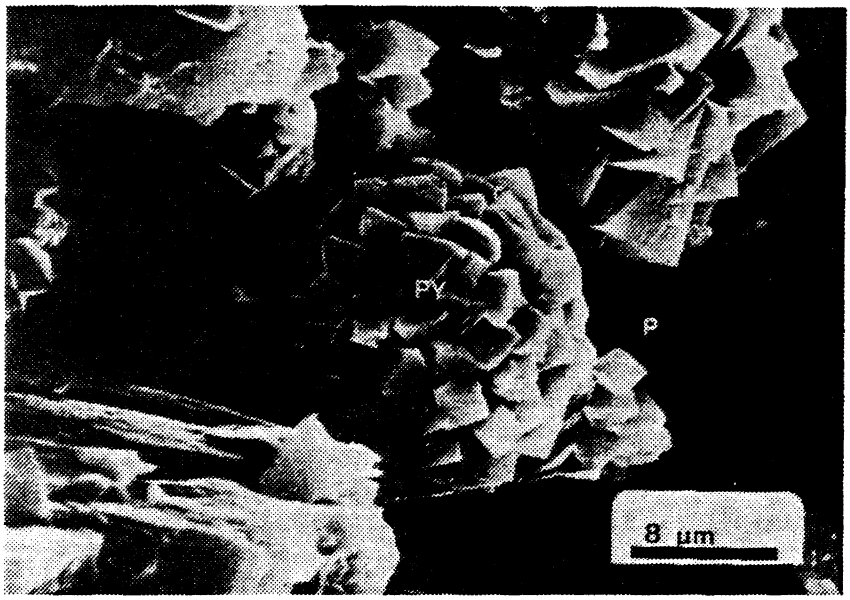

Figure 24. SEM Photomicrograph of Pyrite With Framboidal Morphology

CHAPTER V

POROSITY

Primary intergranular porosity in the Morrow sandstones was virtually destroyed during early diagenesis as a result of silica precipitation, occulusion of pore space by clays, and the production of pseudomatrix from glauconite and clay clast deformation. Subsequently, secondary porosity is the predominant type observed in the Morrow sandstones. Secondary porosity, of course, occurs as a result of diagenetic processes. Schmidt and McDonald (1979) propose a genetic classification of secondary porosity which reflects these processes. The predominant types of secondary porosity observed in the Morrow include dissolution of glauconite, fossil fragments, matrix, and to a lesser extent silica and pyrite.

Secondary porosity values range from 2 to 25% with maximum pore development in the quartz dominated sandstones.

Porosity Types

Dissolution of glauconite is evidenced by the ovoid nature of the pore spaces. Approximately 34% of the thin sections examined contained glauconite, making it a pre-

dominant source for secondary porosity (Figure 25).

Matrix dissolution is a common feature of the Morrow sandstones. The resultant porosity is referred to as enlarged intergranular porosity. Leaching of pseudomatrix (deformed glauconite and/or detrital silty matrix) produces enlarged intergranular pores. Remnants of clay matrix are present rimming pore spaces and as isolated patches "floating" in pore spaces where dissolution has occurred (Figure 26).

Dissolution of fossil fragments has also resulted in the formation of moldic pores. Fossils were noted in 37% of the thin sections making this type of dissolution another significant source of secondary porosity (Figure 27). In addition, minor amounts of secondary porosity can be attributed to the dissolution of silica (microquartz and chert) and pyrite; especially pyrite associated with stylolites.

Kasino and Davies (1979) suggested that secondary porosity in the Morrow sandstones was primarily the result of dissolution of carbonate cements. However, evidence from this study indicates very little carbonate cement dissolution.

Mechanism of Secondary Porosity Development

Secondary porosity evolution in sandstone has been the focus of many investigations of the past decade, with several mechanisms having been proposed for formation of

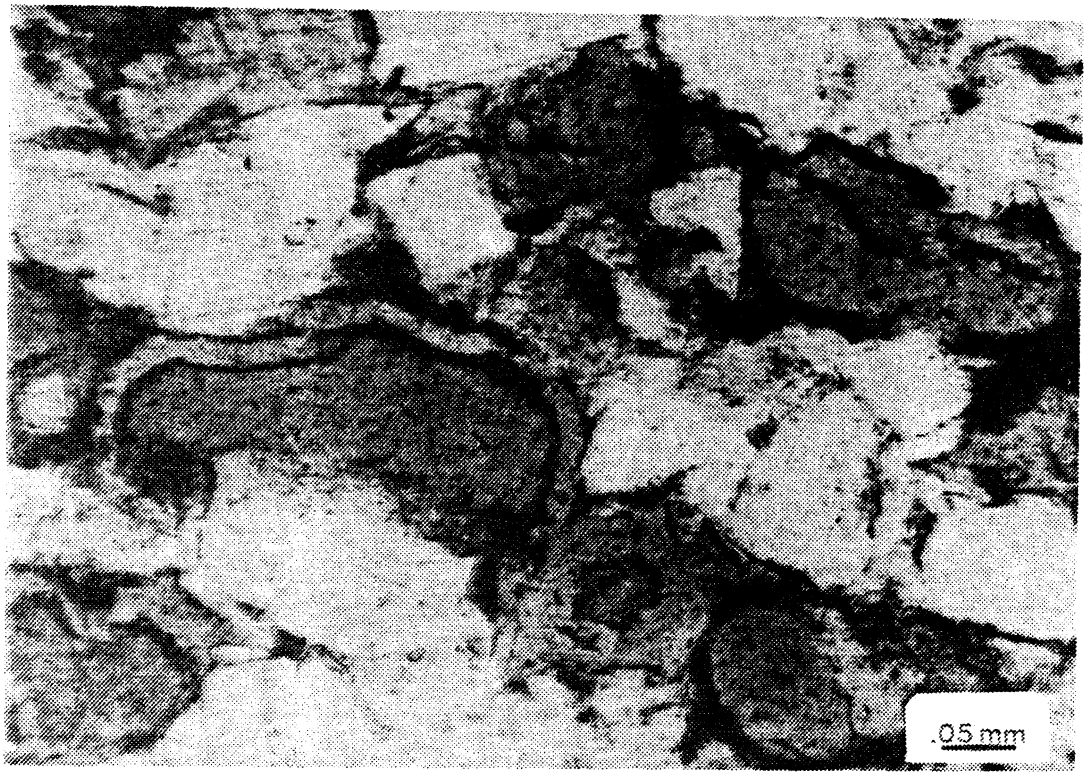

Figure 25. Photomicrograph of Dissolution of Green Glauconite to Form Secondary Porosity; Plane Polarized

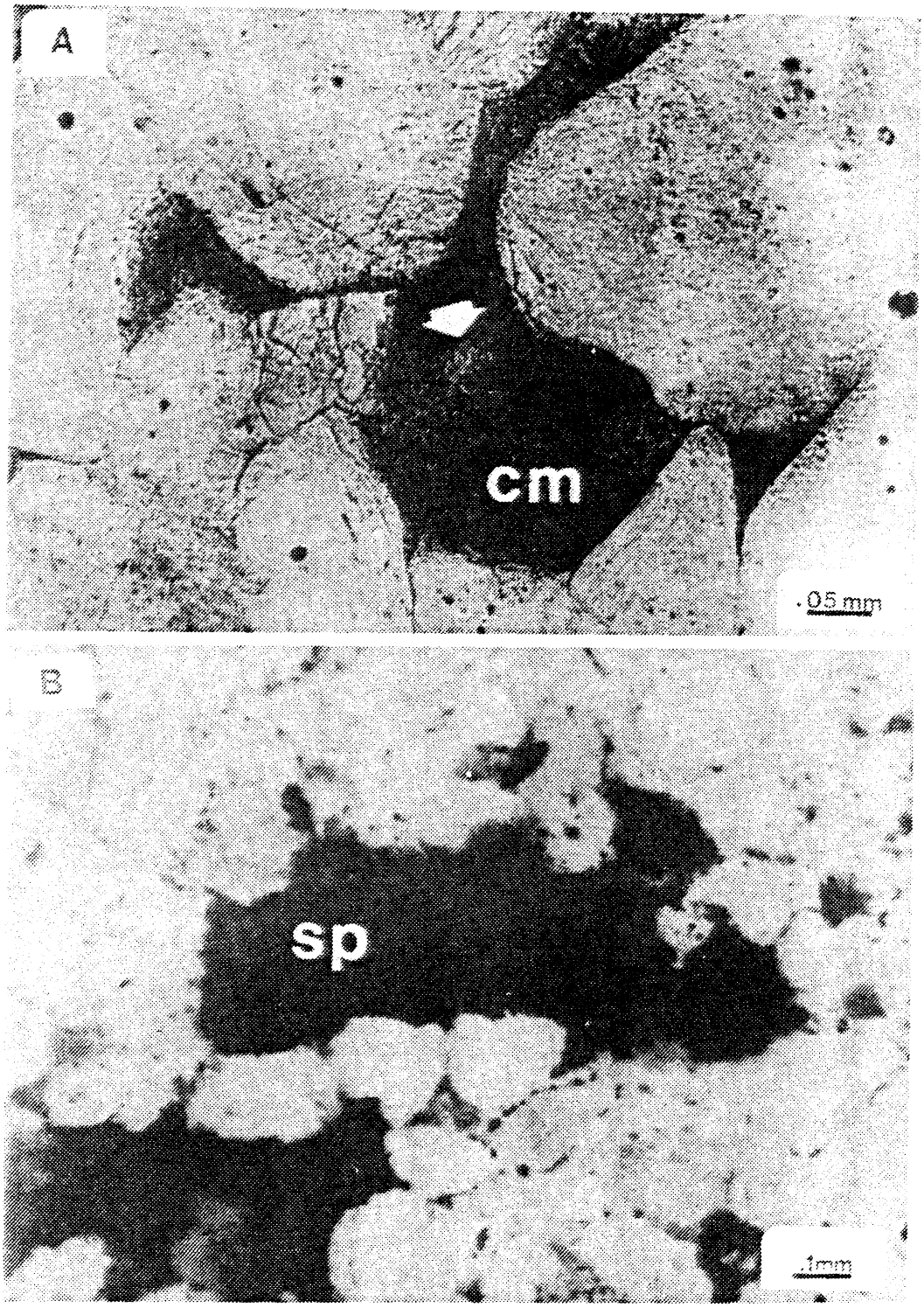

Figure 26. (A) Photomicrograph of Partial Dissolution of Detrital Clay Matrix (CM); Plane Polarized
(B) Photomicrograph of Partial to Complete Dissolution of Detrital Silty Matrix (SM) to Form Enlarged Intergranular Porosity (SP); Plane Polarized

Figure 27. Photomicrograph of Dissolution of Fossil Fragments to Form Moldic Porosity (MP); Plane Polarized

secondary porosity. Schmidt and McDonald (1979), Al-Shaieb and Shelton (1981), Loucks et al. (1984), Franks and Forester (1984), and Larese et al. (1983) emphasize the role of CO_2 in leaching of sandstone constituents, both detrital and authigenic. The CO_2 is a product of decarboxylation of organic acids generated in shales during thermal maturation. However, Surdam et al. (1984) suggested that organic acids generated during the maturation of kerogen and the complexing of aluminum and other ions are the dominant processes in development of secondary porosity. Bjorlykke (1983) and Markert and Al-Shaieb (1984) demonstrated that meteoric and ground water leaching of rock constituents may be an important mechanism in secondary porosity development in certain sandstones.

Two important parameters needed to be examined very thoroughly in order to construct a comprehensive model for the development of secondary porosity within the Morrow Formation in the Anadarko basin. They are the nature of the leaching fluids and the lithologies and texture of sandstones.

Nature of the leaching fluids

Secondary porosity development or enhancement of initial porosity is accomplished by reaction of the leaching fluids with the metastable rock constituents. The most significant property of these fluids is the availability of H^+ ions for reaction. These hydrogen ions

may be supplied by :

1. Organic acids (Surdam et al., 1984; Carothers and Kharaka, 1978)

2. Carbonic acid as the result of decarboxylation of organic acids according to the following reaction:

$$C_nH_{2n+1}\text{-}COOH \longrightarrow C_nH_{2n+2} + CO_2 \qquad 5\text{-}1$$

if n=1 then products are $CH_4 + CO_2$

3. H_2S associated with hydrocarbons which are formed by decomposition of mercaptans and other sulfur bearing organic material at relatively higher temperatures (greater than 200 °C) (Andreev, 1968).

$$C_{10}H_{21}HS \longrightarrow C_{10}H_{20} + H_2S \qquad 5\text{-}2$$

The following discussion will be focused on the contribution of each above source to the leaching fluids. No data on organic acid concentration have been reported from the brines in the Morrow Formation. However, it is reasonable to assume organic acids may have formed during thermal maturation of the Morrow shales as the Anadarko basin subsided in post-Morrowan time.

The composition of natural gas in the Anadarko basin has been published periodically by the U. S. Bureau of Mines. Data concerning the abundance of CO_2 in the natural gas from the Morrow Formation were obtained between 1917 to 1980 (Moore, 1981). Figure 28 shows the relationship between the mole% CO_2 and depth. The content of CO_2 in natural gas tends to increase with depth. In addition, the

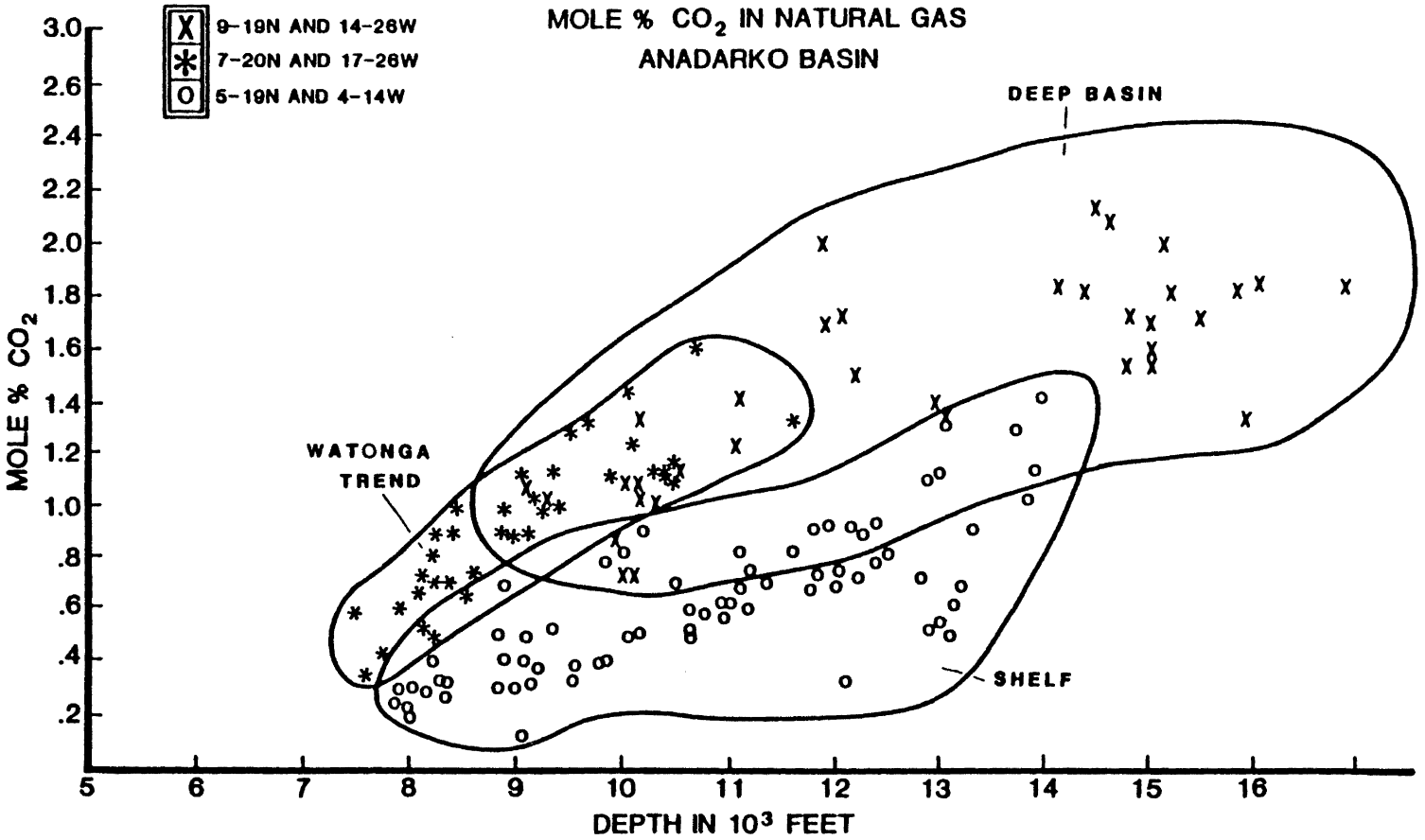

Figure 28. Variation of CO_2 Content of Natural Gas With Depth

data are distributed in three major clusters, representing the Watonga trend, shelf area, and the deep basin, respectively. A contour map of the CO_2 values for the Morrow Formation in the basin is shown in Figure 29. It is very interesting to note the similarity between the map and configuration of the basin. Figure 30 shows the relationship between the vitrinite reflectance values obtained from the Morrow shales, and the CO_2 data from natural gas in associated sandstone reservoirs. The increasing values of vitrinite reflectance with increasing concentration of CO_2 suggest a genetic relationship between the CO_2 gas and Morrow shale. It is worthwhile to note that, according to Hunt (1979), the deltaic facies with terrestrial source rocks are major producers of CO_2 gas. Spread of the values from a linear trend in the deep part of the basin may suggest an additional source of CO_2 in the deep basin, which possibly reflects degassing of the Ordovician Arbuckle limestone Formations. Takenouchi and Kennedy (1965) show that the solubility of CO_2 is dependent on the pressure, temperature, and the salinity of water. Based on bottom-hole pressure measurements, two major pressure regimes are present in the Anadarko Basin: normal-pressured zone, with gradients of < .7 psi/ft, and overpressured zone with > .7 psi/ft (Davis, 1974). According to Davis, the overpressured zone in the Morrow is approximately south of T19N and includes areas of the deep basin. Figure 31 modified after Takenouchi and Kennedy

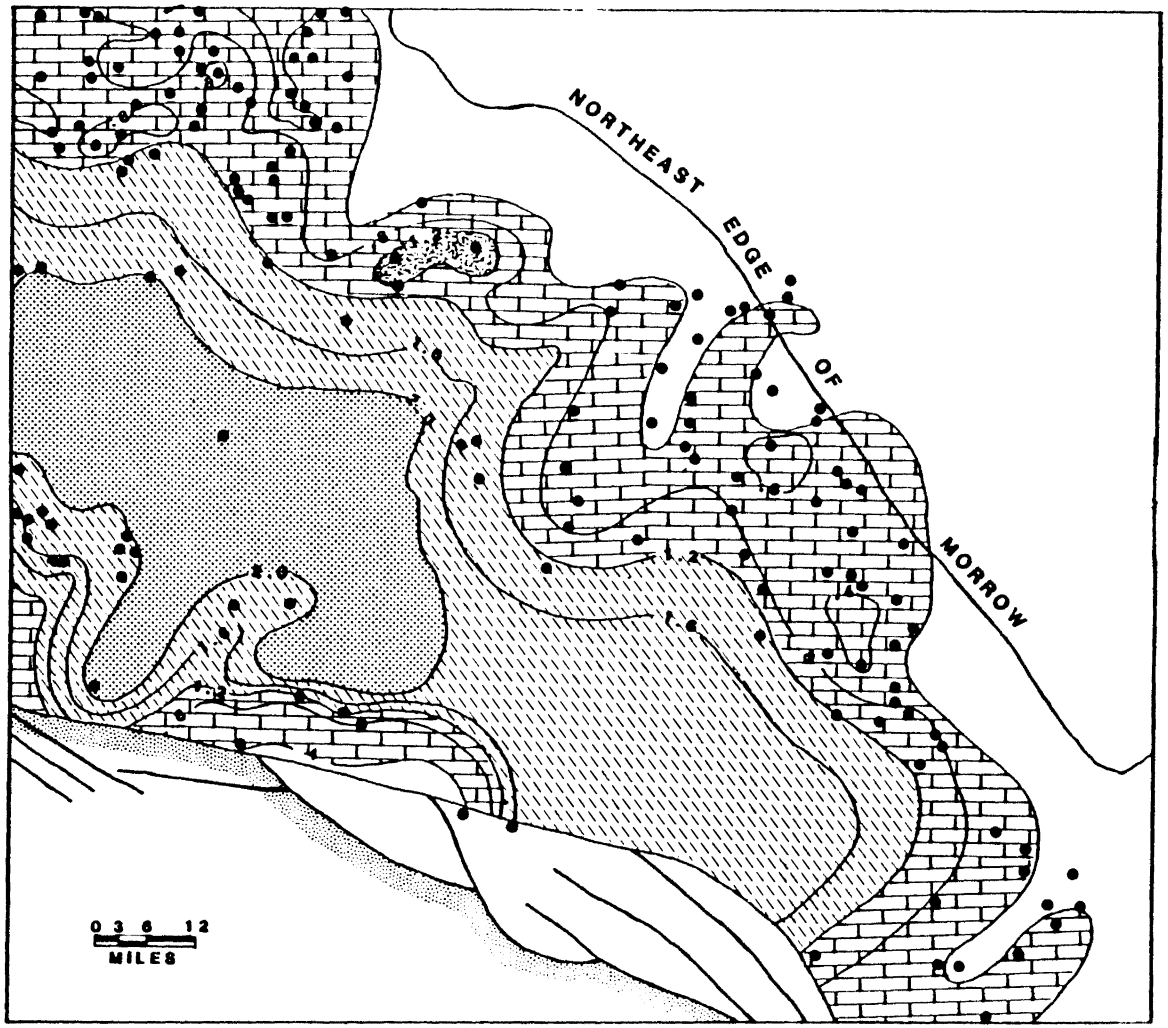

Figure 29. Distribution of CO_2 Content of Natural Gas in the Basin (Contour Interval is Equal to 0.4 Volume % in Natural Gas)

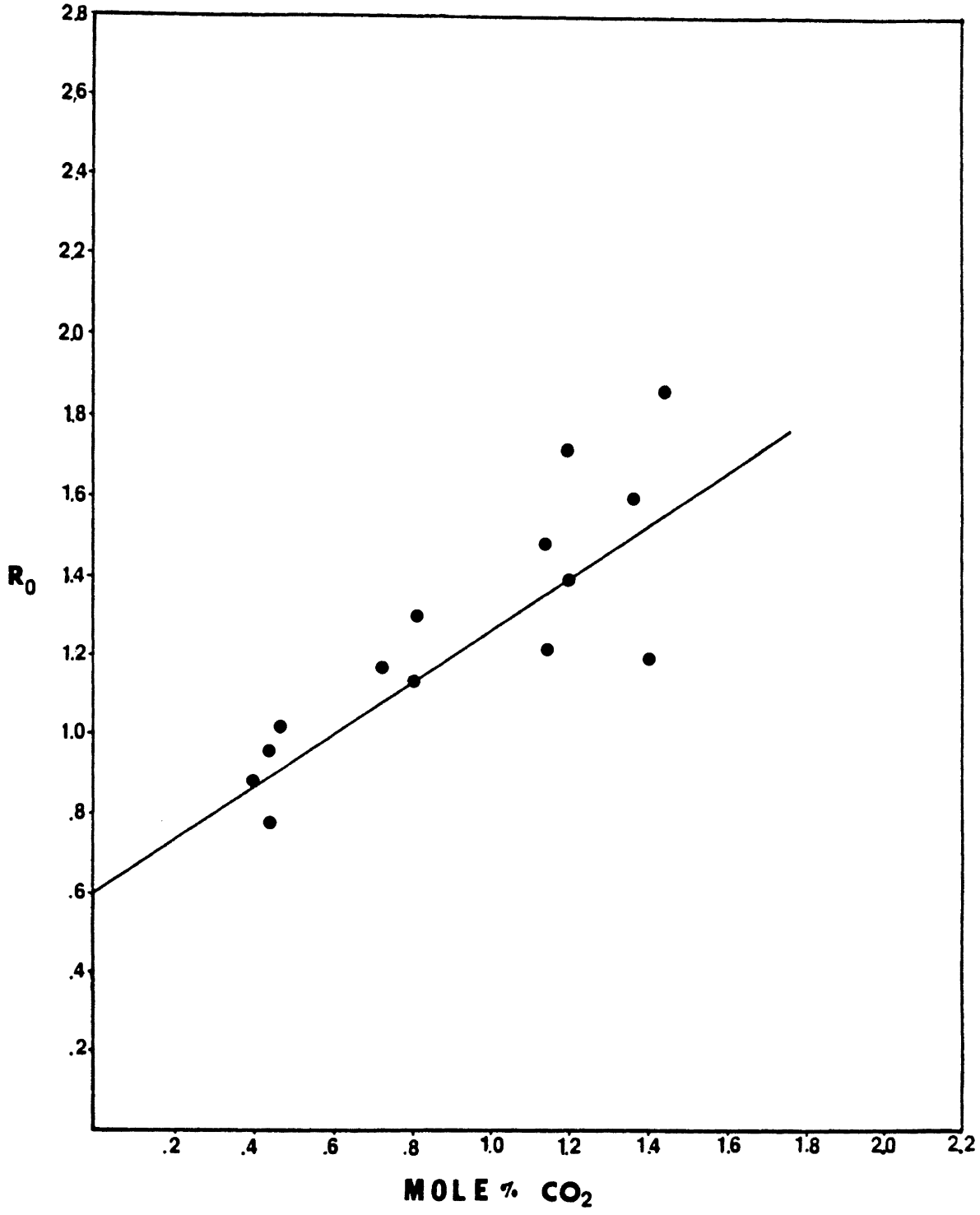

Figure 30. Relationship Between CO^2 Content of Natural Gas and the Vitrinite Reflectance of Associated Shales

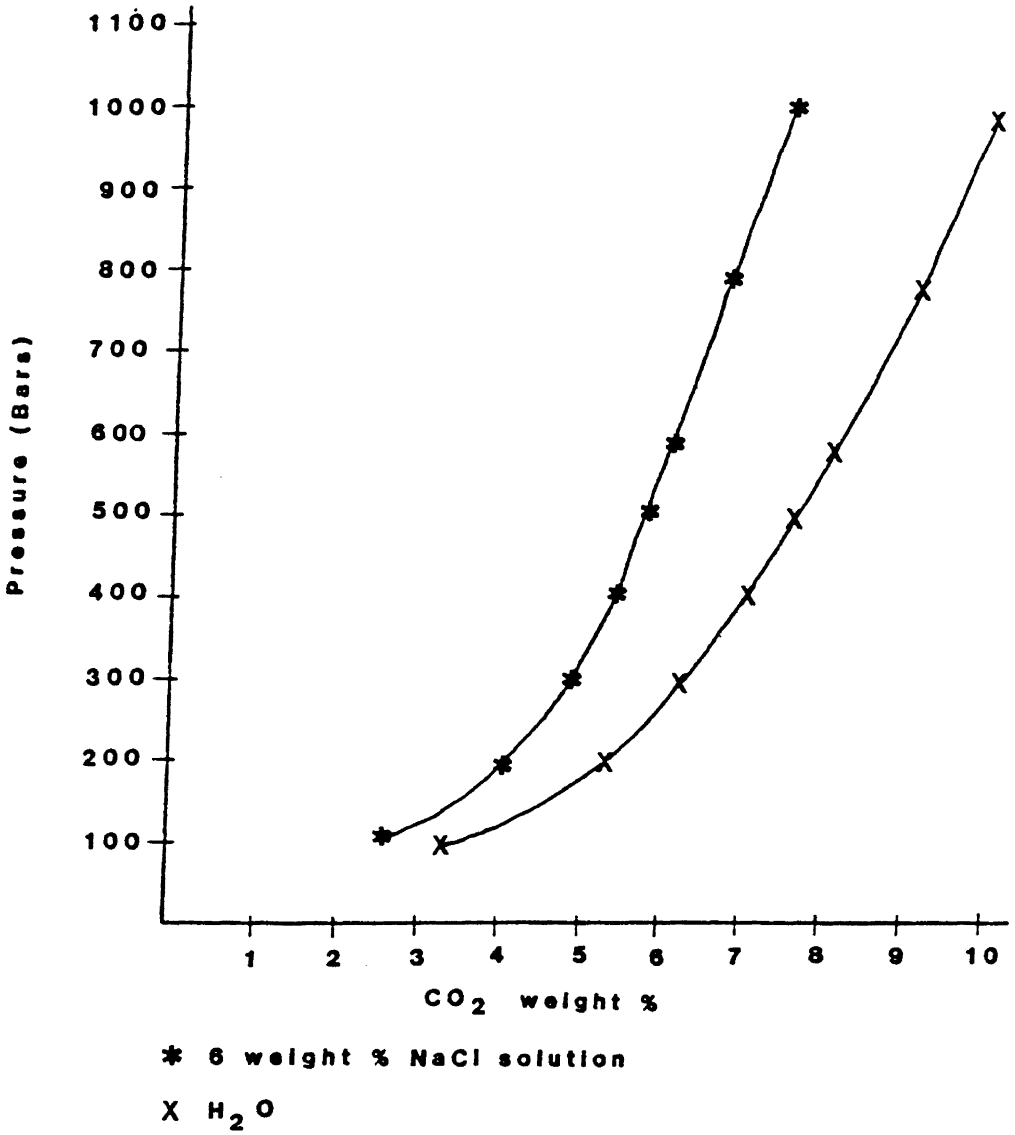

Figure 31. Solubility of CO^2 in Fresh and Saline Waters at 150°C (After Takenouchi and Kennedy, 1965)

(1965), shows the relationship of CO_2 solubility at 150° C to pressures for fresh and saline water. Since the Morrow Formation water is basically a brine, it is reasonable to assume that the solubility of CO_2 at Morrow Formation pressures may range from 3 to 5 weight % for the normally pressured zones and up to 10 weight % for the overpressured.

Hill and Clark (1981) show an increase in H_2S content of natural gas in the Morrow with basin depth. The dissolved H_2S gas in formation water at higher temperatures may produce slightly acidic fluids.

To summarize, in a subsiding basin such as the Anadarko basin, the contribution of H^+ ions to the leaching fluids were derived from several sources. These are organic acids (?), carbonic acids, and dissolved H_2S in formation water. Since the production of H^+ ion sources is not restricted to a single maturation stage during the subsidence history of the basin, a multi-stage model is proposed for secondary porosity development in the Morrow sandstones in the Anadarko basin. These are:

Stage I - dominated by organic acids and carbonic acid.

Stage II - mainly carbonic acid

Stage III - carbonic acid and dissolved H_2S in formation water.

The maximum development of porosity is directly related to the amount of H^+ ion produced during each stage.

Organic acids in complexing the Al^{3+} ions as proposed by Surdam et al. (1984) may be an important mechanism in preventing authigenic clay minerals from precipitating in pore spaces. The general decrease in secondary porosity with depth is explained by the precipitation of authigenic minerals in particular chlorite and to a lesser extent kaolinite and dolomite in pore spaces. The authigenic clays may have formed when aluminum organic complexes became unstable with increasing temperature.

Lithologies and texture of sandstone

Petrographic evidence suggests that enhancement of porosity is mainly due to removal of silicate components from the fabric such as detrital matrix, glauconite, etc. The Morrow sandstones exhibit various types of lithologies (Figure 7) which represent a variety of facies. The partial dissolution of these lithologies when they come in contact with H^{+} ion bearing fluids will be affected by:

a. The relative amount of the metastable constituents in the rock.

b. Textural parameters, particulary the initial porosity.

In the distributary channels of deltaic facies, rocks with initial porosity and metastable argillaceous constituents averaging 10-18% will develop significant secondary porosity. On the other hand, delta fringe and interdistributary facies with lower initial porosity and

more than 20% argillaceous constituents will not produce any significant effective porosity. In addition, very clean sandstone with minor amounts of argillaceous constituents are completely cemented with silica, producing a rather poor reservoir. Similary, the partial and complete dissolution of fossil fragments and glauconite is very important in enhancement of porosity in shallow-marine facies. Quartzarenite sandstones with a minimal amount of fossil or glauconite grains tend to be completely cemented with either silica or carbonate. Figure 32 shows the relationship between porosity and depth. The distinct scattering of the data points and general decrease of porosity with depth are the two striking phenomena. The scattering of the data may be related to the heterogenity of the lithologies and the textures of the Morrow sandstones. It could be reasonably assumed that lithologies of similar composition and texture would develop similar porosity patterns when exposed to the H^+ ion bearing fluids. The decrease of porosity with depth suggests the ability of leaching fluids to dissolve metastable constituents is decreasing with depth or the amount of succeptible components is decreasing. This may be due to the decrease of free H^+ ions. The degree of scattering of data is better understood if we consider the lithology of each data point. Figure 32 shows that lithologies with similar composition tend to permit construction of specific porosity-depth curves. These

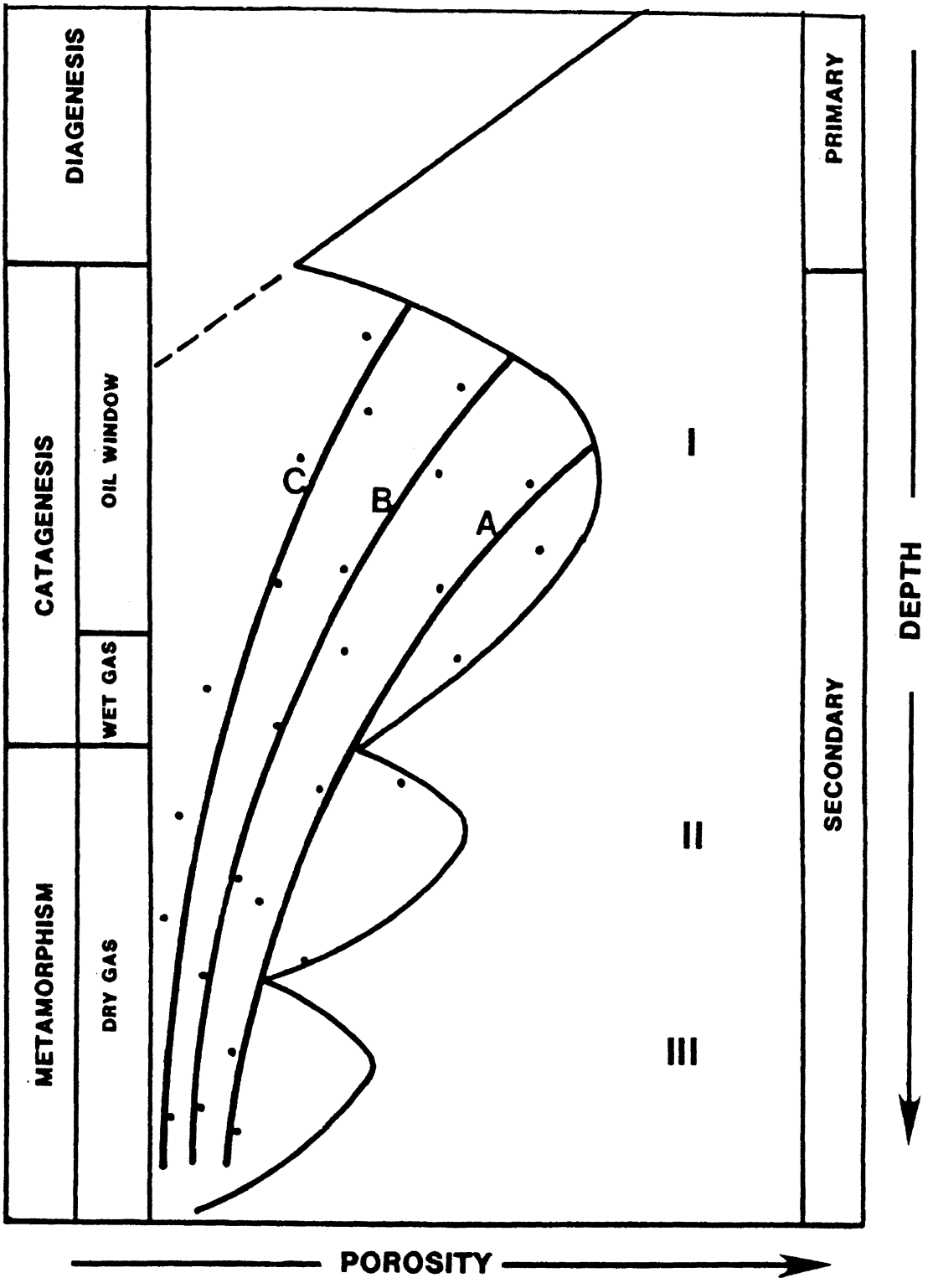

Figure 32. Relationship Between Porosity and Depth of the Various Facies of the Morrow Sandstones. A, B, and C are Isolithic Porosity Lines. I, II, and III are Multi-Stages of Secondary Porosity Development

curves are called isolithic porosity lines (IPL).

CHAPTER VI

THERMAL HISTORY

Introduction

It has been established in recent years that both time and temperature are important factors in the maturation of organic matter in source rock (Waples, 1980). Organic components dispersed in sedimentary rocks are commonly used as thermal maturation indicators. Several methods are available for determining the thermal maturation of rocks. These include kerogen color, organic geochemistry, vitrinite reflectance, and others.

Vitrinite reflectance was chosen for this study because it is a useful indicator of temperature histories in sedimentary units containing organic material. This method is less subjective than the others. It is a numerical system with values that can be measured and calibrated (Tissot and Welte, 1984; Waples, 1980).

Vitrinite reflectance values are essentially the amount of light reflected from coaly material (vitrinite) proportional to the degree of maturity of the organic matter. Since this maturity is not reversible, the values record the maximum thermal imprint a sedimentary unit has

undergone.

For the Anadarko basin area, depth of burial is also an important factor due to its direct relationship with temperature.

Morrow shales were chosen from 14 cores in the study area and analyzed for vitrinite reflectance values. Vitrinite reflectance values from 16 other Morrow cores in the study area were provided by Mr. V. Tsiaris. Table V (Appendix C) provides a list of the reflectance values. Core locations are indicated by a star on the following maps.

Vitrinite Reflectance and Geothermal Gradient

An isoreflectance map (Figure 33) prepared from the mean vitrinite reflectance values demonstrates a general trend of maturity of the Morrow Formation in the Anadarko basin.

Vitrinite reflectance values of the Morrow Formation range from 0.62-0.95% Ro in the shallower northeastern part of the basin to 3.34% Ro in the deep basin. Shallower parts of the basin correspond to milder organic diagenesis and catagenesis, whereas the deeper basin reflects more severe organic metamorphism. Figure 34 shows a good correlation between % Ro and depth. An increase in depth produces a corresponding increase in % Ro.

Staplin (1969) has stated that for reflectances of greater then 2.5% Ro, paleotemperatures are said to have

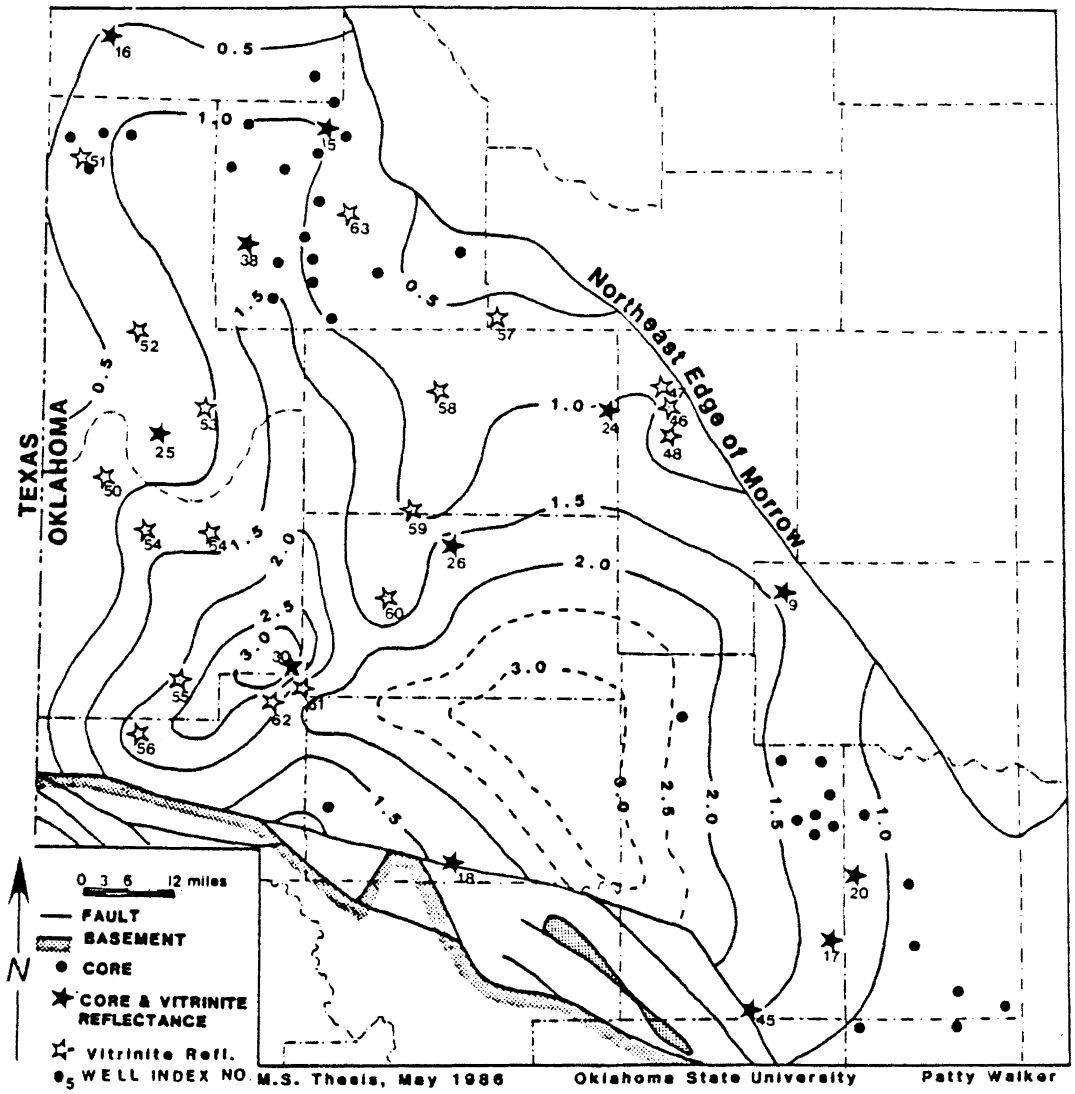

Figure 33. Distribution of % Vitrinite Reflectance (Contour Interval is Equal to 0.5% Ro)

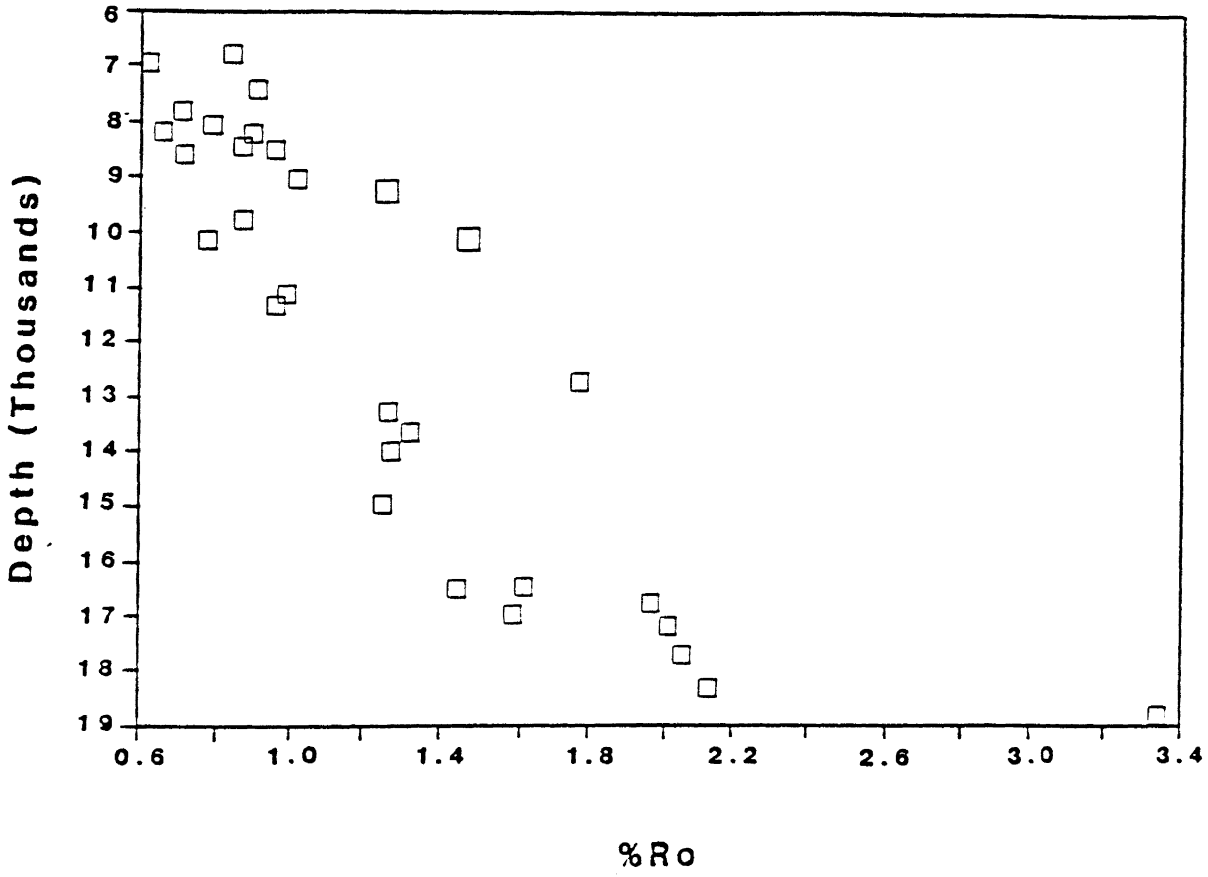

Figure 34. Graph of %Ro Versus Depth for the Morrow Formation

been greater then 200°C (400°F) even with an effective heating time of 300 million years. Pusey (1973) shows that maximum paleotemperatures in the Anadarko basin exceed the current temperatures at comparable depth. We must then evaluate if high temperatures were due to a normal geothermal gradient (increasing temperature with increasing depth), some thermal event (Cardott and Lambert, 1985), or basinal axis shift.

Figure 35 is a geologic reconstruction for the Union of California 1-33 Bruner well, Beckham County, Oklahoma. (Waples, 1980). By reconstruction of the burial history of the Anadarko basin through time an estimate of geothermal gradient may be derived. Erosional removal as the result of the Wichita uplift was estimated at 1700 feet. Erosional removal as a result of regional uplift during the Tertiary was estimated at 1200 feet.

Pusey (1973) and Waples (1980) have shown that the present geothermal gradient for the Anadarko basin is 1.2°F/100feet. Low geothermal gradients for the Anadarko basin are probably caused by the thick sedimentary rock section and the insulating effects of the over-pressured Morrow-Springer sandstones (Harrison et al., 1983).

Present geothermal gradients and paleo-geothermal gradients are non-linear with depth. A change in the present geothermal gradient occurs in the Morrow (Lower Pennsylvanian) from an average of 1.2°F/100feet in older rocks (pre-Pennsylvanian) to an average of 1.0°F/100feet in

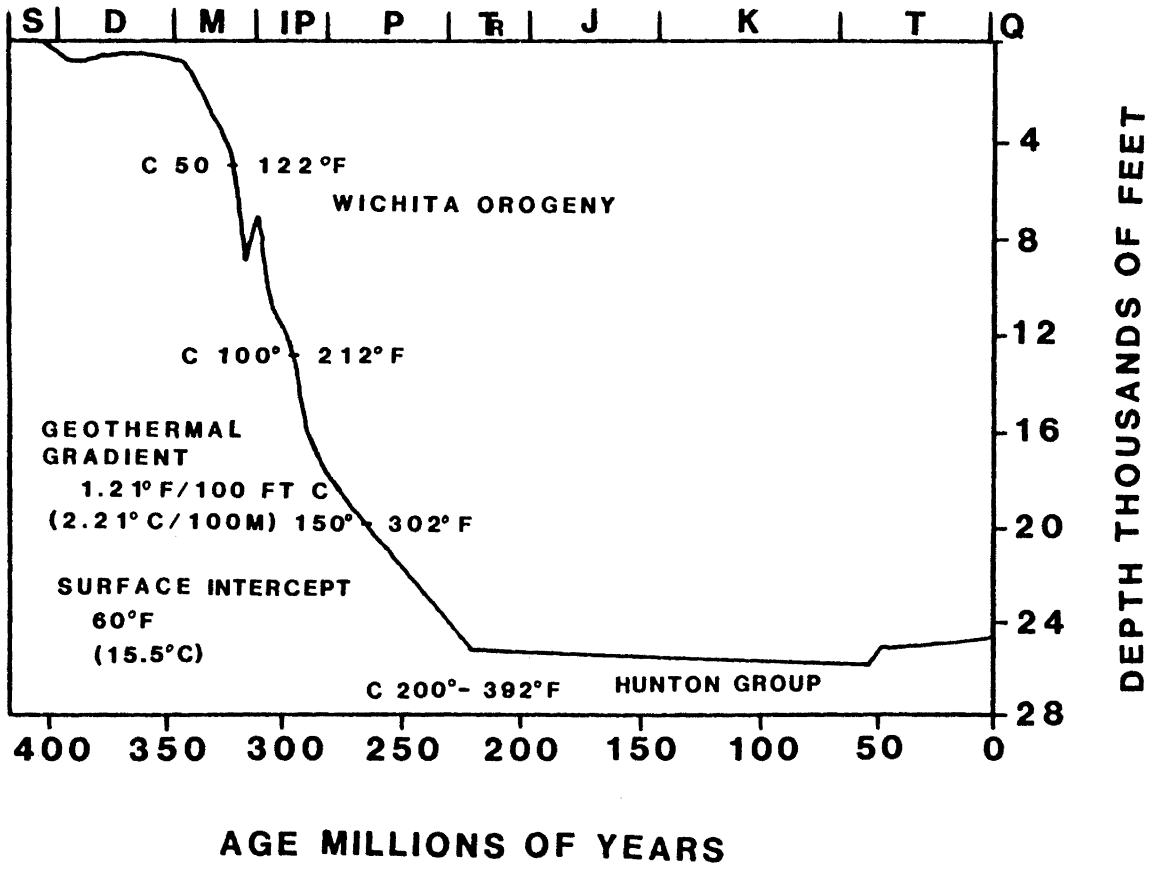

Figure 35. Geologic Reconstruction for Union of California 1-33 Bruner Well, Beckham County, Oklahoma (After Waples, 1982)

younger rocks (post-Lower Pennsylvanian) (Cardott and Lambert, 1985). Pusey (1973) shows a convergence of the paleo- and present- geothermal gradients with depth (Figure 36). He has also predicted paleotemperatures of shallow rocks to be as much as 150 °F higher than present temperatures, but that rocks below about 22,000 feet are now at about their maximum temperatures.

As can be seen in Figure 33, the highest iso-reflectance values for the Morrow Formation do not correspond exactly to the present day structurally deepest part of the basin. Cardott and Lambert (1985) have inferred a thermal anomaly for this zone. They state that if maturity developed from increasing temperature with increasing depth, structural contours and isoreflectance contours should have similar patterns. The mechanism they propose is crustal and lithospheric thinning.

An alternative hypothesis could be related to basinal axis shift through geologic time. If it is true that vitrinite reflectance values record maximum temperatures and are irreversible, then it is possible that the area of high vitrinite reflectance values seen in Figure 33 are recording an older deep basin that was present when "cooking" of the Morrow rocks took place. It can be shown that an episode of tectonic movement took place in the Wichita Mountains after deposition of the Morrow Formation (Donovan, 1985). This tectonic activity could imply that development of the Anadarko basin was ongoing and a shift

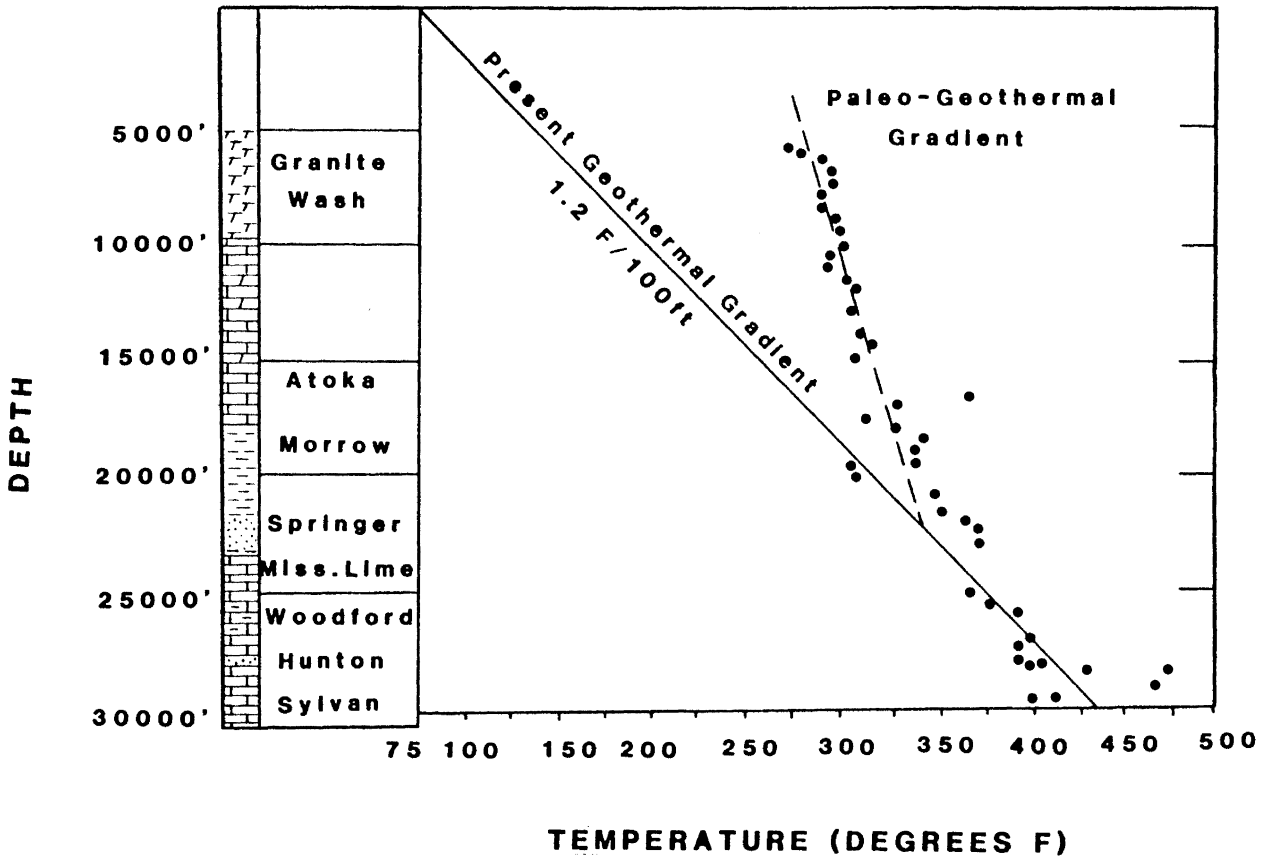

Figure 36. Paleotemperatures from the Lone Star Baden 1, Beckham County, Oklahoma. Note that Paleotemperatures Exceed Present Temperatures, But that They Both Converge at About 22,000 Feet (After Pusey, 1973)

of the deep basin to the south occurred as uplift in the Wichita Mountains continued into the Permian.

Vitrinite Reflectance and Petroleum Generation

Figure 37 shows average vitrinite reflectance values for the Morrow Formation plotted with respect to the petroleum maturation zones and T max. Hood, Gutjahr, and Heacock (1975) combined maximum temperature (T max) with an effective heating time (T eff) to develop a simplified method of predicting vitrinite reflectance values for petroleum occurrence. Several wells within the study area have been plotted on the diagram. This graph does not show a linear relation. At shallow depths, the observed vitrinite reflectance values are significantly greater than those defined by a linear relation of vitrinite reflectance with depth. This non-linearity shows a striking similarity to the graph of paleotemperatures versus depth for the Anadarko basin shown in Figure 36. Hood et al. (1975) suggest that this non-linearity is a result of an increase in activation energy with increasing vitrinite reflectance. The lower activation energies indicate a greater importance of time with respect to temperature. This would result in greater importance of total burial time with lower levels than at higher levels of organic metamorphism.

The stages of petroleum maturation occurring within the Morrow Formation in the Anadarko basin are shown in Figure 38. These stages are defined by the vitrinite reflectance

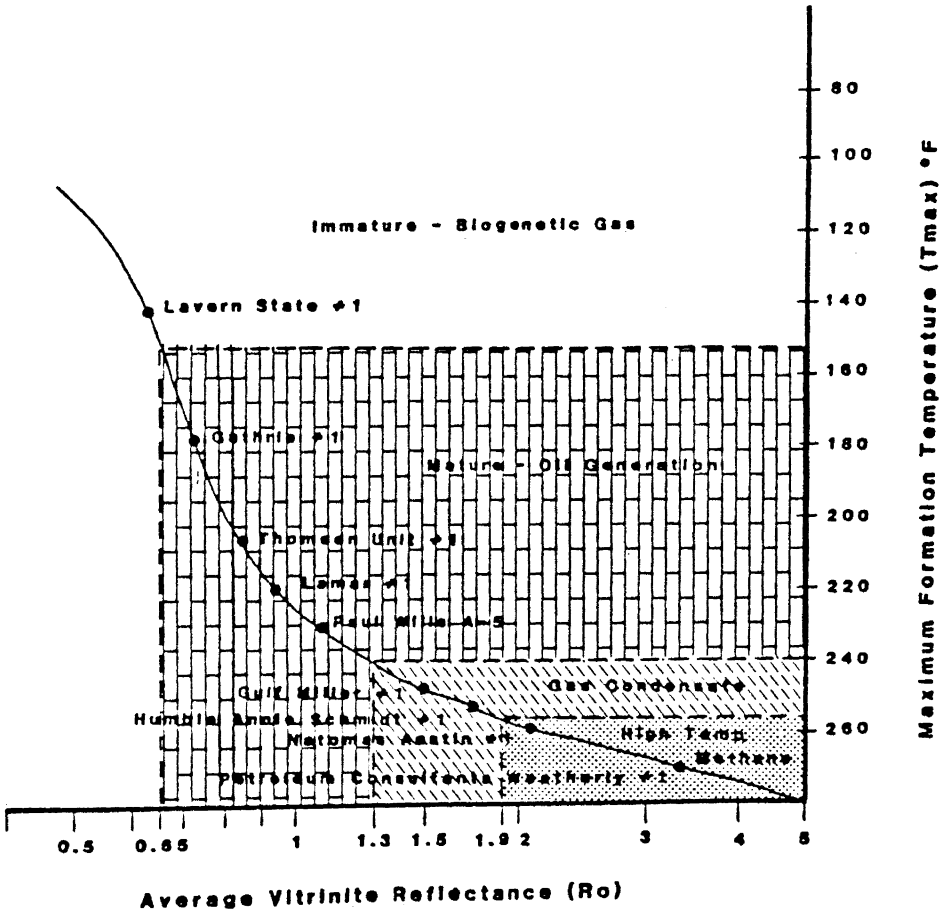

Figure 37. Graph Relating Average Vitrinite Reflectance Against Tmax to Determine Petroleum Generation Zones for the Morrow Formation (Modified After Hood et al., 1975)

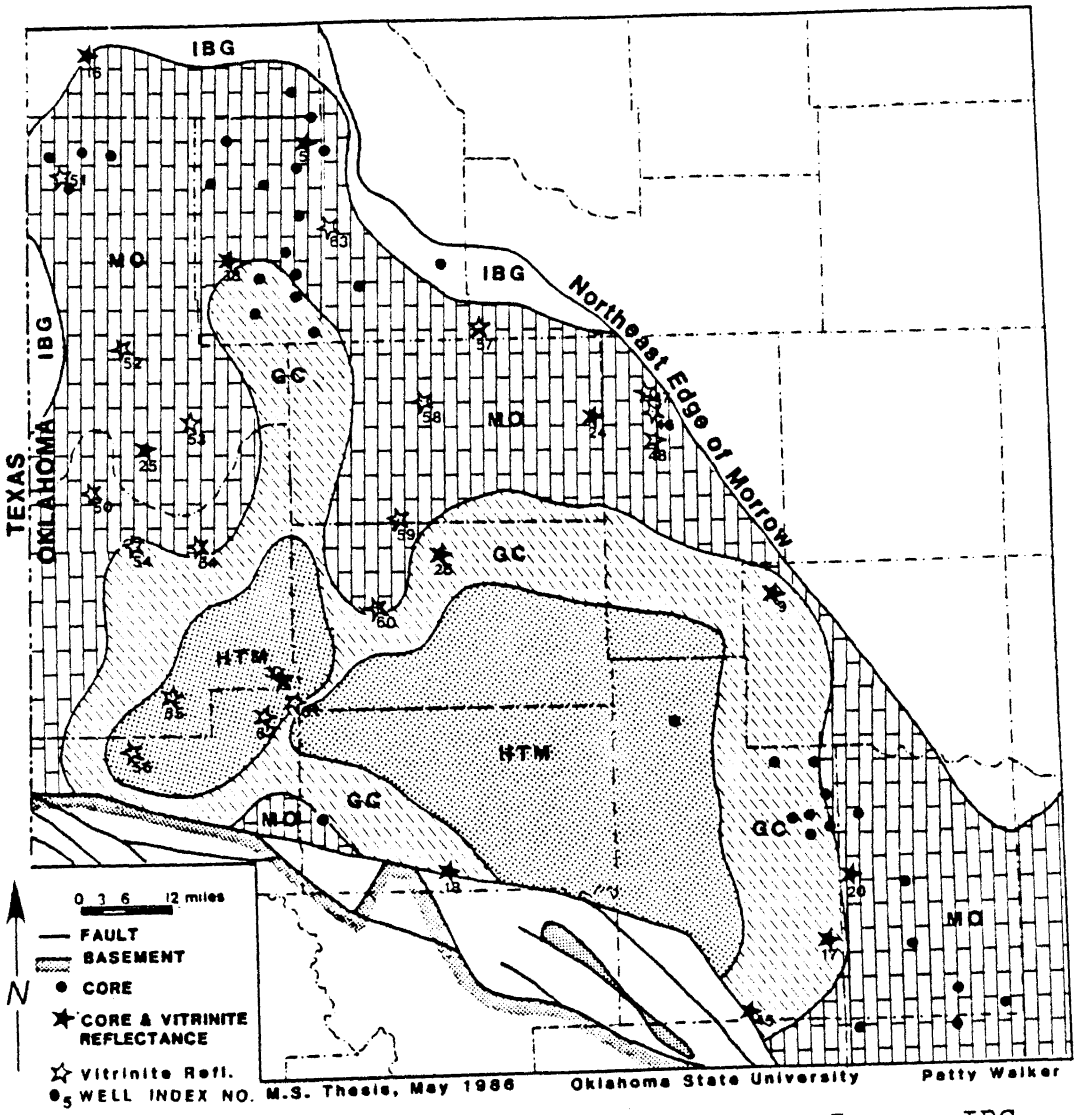

Figure 38. Distribution of Hydrocarbon Zones. IBG, Immature Biogenetic Gas; MO, Mature Oil Generation; GC, Gas Condensate; HTM, High Temperature Methane

values from Figure 37. Although this figure indicates extensive areas of oil generation, gas production in large amounts from the Morrow Formation is seen in the shelf areas as well as the deep basin. Laplante (1974) has shown that gas and gas-condensate accumulations are commonly associated with low-hydrogen kerogens found in sediments (humic shales) derived from mostly terrigenous detritus while oil-like bitumens are found in sediments (sapropelic shales) containing high-hydrogen kerogen associated with well-defined marine and lacustrine sediments.

It is probable that the shales of the Morrow Formation are the source of the petroleum generated in the Morrow sandstones of the Anadarko basin. If this is so, then the gas generated in the Morrow sandstones could be a result of thermal maturation of humic shales. Sapropelic shales could have been the source for the oil in the Morrow producing sandstones. This theory reinforces the importance that depositional environment plays with respect to the type of petroleum generated.

CHAPTER VII

ISOTOPE GEOCHEMISTRY

Basic Concepts

Isotopes are defined as atoms whose nuclei contain the same number of protons but a different number of neutrons. The isotopic composition of elements having low atomic numbers varies due to fractionation, which occurs during chemical and physical processes. This fractionation is proportional to the differences in mass of the isotopes. The most important elements in which natural variations of isotopic composition exist are hydrogen, carbon, nitrogen, oxygen, and sulfur (Faure, 1977).

The separation of isotopes can be expressed in terms of a ratio called the fractionation factor:

$$\alpha = Ra/Rb \qquad 7\text{-}1$$

where Ra is a ratio of the heavy to light isotopic composition of phase `a' and Rb is the same ratio for phase `b' (Krauskopf, 1979).

Generally, isotopic fractionation occurs during several different chemical and physical processes.

1. Physical processes - such as evaporation,

freezing, or condensation.

2. Equilibrium processes - involving the redistribution of an element's isotopes among different molecules containing that element.

3. Kinetic processes - unidirectional reactions in which reaction rates are dependent on isotopic compositions of the reactants and products (Faure, 1977).

Isotopic fractionation in nature is dependent in part on temperature. This relationship can be used to determine the temperature at which mineral precipitation took place. Two of the major uses for stable isotopes are an understanding of origin of cements and use as a paleogeothermometer.

Carbon

Carbon is composed of two major isotopes, C^{12}, and C^{13}. The ratio C^{13}/C^{12} is approximately 1:99 (Fuex, 1977). Carbon occurs in the reduced form in organic compounds. It occurs in the oxidized form primarily as carbon dioxide, carbonate ions in aqueous solutions and as carbonate minerals.

The oxygen and carbon stable isotopic composition of a carbonate is expressed in terms of the delta notation. Delta carbon is defined as follows:

$$d^{13}C‰ = \left[\frac{(^{13}C/^{12}C)spl - (^{13}C/^{12}C)std}{(^{13}C/^{12}C)std}\right] * 10^{3} \qquad 7\text{-}2$$

Relative ratios are obtained by comparison of the sample (spl) ratios to the ratio of the common standard (std), PDB (Belemnites from the Cretaceous, Peedee Formation of South Carolina).

The carbon stable isotopic composition of a carbonate cement can be used to help determine the diagenetic processes responsible for precipitation. Carbon stable isotope values are dependent on the initial composition of the carbonate in the sediment and the type and amount of diagenetic alteration that has taken place. Curtis (1983) has discussed several diagenetic processes for producing $d\ ^{13}C$ depleted CO_2 or HCO_3^- in a subsurface system during burial. Figure 39 shows the redox and acid generating reactions characteristic of individual diagenetic zones. Each of these reactions generates reactive solutes or initiation carbonate reactions. Dependent mineral authigenesis (or dissolution) is a result of interactions of the soluble products of these initiation reactions (Figure 40).

Oxygen

Oxygen is the most abundant element in the Earth's crust and combines with hydrogen to form water. Oxygen has three stable isotopes whose approximate abundances are: ^{16}O = 99.756 percent, ^{17}O = 0.039 percent, ^{18}O = 0.205 percent (Fuex, 1977). The isotopic composition of oxygen is reported in terms of differences in $^{18}O/^{16}O$ relative to a

Diagenetic zone	Reaction (written for complete charge balance)	Comments
ZONE I Oxidation zone Molecular oxygen and 'suboxic' oxidants as documented by Froelich et al. (1979)	$CH_2O + O_2 \rightarrow CO_2 + H_2O$ $= HCO_3^- + H^+$ $CH_2O + 2MnO_2 + H_2O$ $\rightarrow 2Mn^{2+} + HCO_3^- + 3OH^-$ $CH_2O + 2Fe_2O_3 + 3H_2O$ $\rightarrow 4Fe^{2+} + HCO_3^- + 7OH^-$ $5CH_2O + 4NO_3(+4Na^+)$ $\rightarrow 2N_2(+4Na^+) + 5HCO_3^- + H^+ + 2H_2O$	increased acidity and HCO_3^- activity: carbonate dissolution rise in pH, HCO_3^- and cation activity: carbonate precipitation as above, but more so marginal activity increase: rise in HCO_3^- activity
ZONE II Microbial sulphate reduction:	$2CH_2O + SO_4^{2-} (+ 2Na^+)$ $\rightarrow S^{2-} (+ 2Na^+) + 2HCO_3^- + 2H^+$ $7CH_2O + 4SO_4^{2-} (+ 8Na^+)$ $\rightarrow 2S_2^{2-} (+ 8Na^+)$ $+ 2H_2O + 7HCO_3^- + 3H^+$ continuing reduction of available Mn and Fe	increased acidity and HCO_3^- activity: carbonate dissolution S^{2-} usually precipitated quantitatively as iron monosulphide, subsequently converted to pyrite
ZONE III Fermentation (microbial)	$2CH_2O + H_2O \rightarrow CH_4 + HCO_3^- + H^+$ continuing reduction of available Mn^{IV} and Fe^{III}	increased acidity and HCO_3^- activity: carbonate dissolution
ZONE IV Decarboxylation (thermal)	$RCO_2H + H_2O \rightarrow RH + H^+ + HCO_3^-$ (R = kerogen macromolecular substrate) continuing reduction of any residual Fe^{III}	as above also short chain aliphatic acids-especially CH_3COOH
ZONE V Liquid hydrocarbon generation	probably minor CO_2 generation: little likelihood of Fe^{3} reduction	minor acidification?

Figure 39. Redox and Acid Generating Reactions Characteristic of Individual Depth Zones. Each of These Reactions Generates Reactive Solutes--Initiation Reactions (After Curtis, 1983)

Diagenetic zone	Reaction	Comments
ZONE I		
	In basins with moderate to rapid sedimentation rate this zone is very thin (mm to cm) and would be even thinner without the water circulation activities of burrowing organisms. High levels of supersaturation are unlikely to be maintained due to diffusion and mixing of pore waters with overlying depositional waters. All reactions, however, destroy organic matter.	
ZONE II		
	$15CH_2O + 2Fe_2O_3 + 8SO_4^{2-} \rightarrow 4FeS_2 + H_2O + 15HCO_3^- + OH^-$	Iron monosulphide or pyrite rapidly precipitate as dependent reactions. Consequential carbonate supersaturation favors iron-poor carbonate minerals.
	$9CH_2O + 2Fe_2O_3 + 4SO_4^{2-} \rightarrow 4FeS + 4H_2O + 9HCO_3^- + H^+$	
Balanced combination of sulphate and iron reduction (S and Fe)		
ZONE III		
	$7CH_2O + 2Fe_2O_3 + 6H_2O \quad 3CH_4 + 4FeCO_3 + 4H_2O$	MASSIVE carbonate supersaturation quantitative precipitation (dependant reaction) of iron-rich carbonate minerals
Balanced combination of fermentation and iron reduction		
ZONE IV		
(a) excess iron reduction	$RCO_2H + CH_2O + 2Fe_2O_3 + H_2O \rightarrow RH + 2FeCO_3 + 2Fe^{2+} + 4OH^-$	Excess iron leads to dependent carbonate precipitation followed by dependent authigenic silicates
(b) balance	$3RCO_2H + CH_2O + 2Fe_2O_3 \rightarrow 3RH + 4FeCO_3 + H_2O$	——depth trend towards——— Excess acid eventually causing dissolution of carbonates then silicates
(c) excess decarboxylation	$5RCO_2H + CH_2O + 2Fe_2O_3 + H_2O \rightarrow 5RH + 4FeCO_3 + 2HCO_3^- + 2H^+$	
ZONE V		
	Minor CO_2 addition from organic matter possible further addition from the reaction kaolinite + dolomite → chlorite + calcite + CO_2	Pore waters (residual) probably maintained at acid pH

Figure 40. Dependent Mineral Authigenesis (or Dissolution) Consequent Upon Interactions Between the Soluble Products of Initiation Reactions (From Figure 39) (After Curtis, 1983)

standard called SMOW (Standard Mean Ocean Water) or PDB (Peedee Belemnites). Equation 7-2 is also used for the delta values of oxygen.

The oxygen stable isotopic composition of a carbonate cement is dependent on temperature and on the $d^{18}O$ composition of the fluids from which it precipitated (Epstein et al., 1953). These values can be useful in determining temperatures of formation of carbonate cements.

Results

Approximately 105 carbonate samples from the Morrow sandstones were analyzed for carbon and oxygen stable isotopic composition. The results of these analyses are presented in this section. A complete list of the carbon and oxygen stable isotopic data are presented in Table III in Appendix C. All values are reported relative to PDB standard.

Carbon stable isotopic data from the carbonate components in the Morrow Formation range from +3.0‰ to -10.3‰ with a mean $d^{13}C$ value of -3.8‰ (Figure 41). The $d^{13}C$ range for calcite is +0.6‰ to -10.3‰ with a mean value of -3.8‰. Values for $d^{13}C$ of dolomite range from -0.9‰ to -5.9‰ with a mean of -3.3‰. Values for $d^{13}C$ of siderite range from 3.0‰ to -7.2‰ with a mean of -4.08‰.

Depleted (or more negative) $d^{13}C$ values of the Morrow are associated with the deep areas of the basin to the southeast (Figure 42). These negative values are

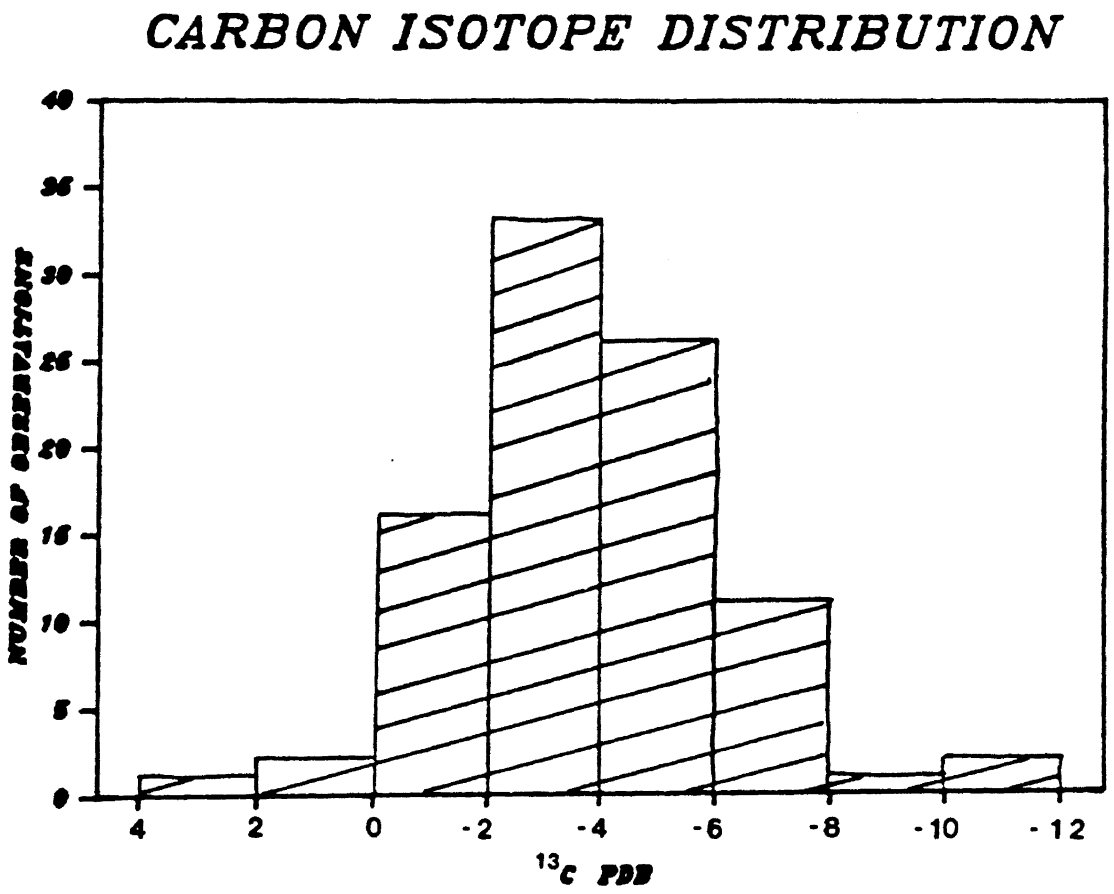

Figure 41. Frequency Distribution of C^{13} Isotopes for the Morrow Sandstones

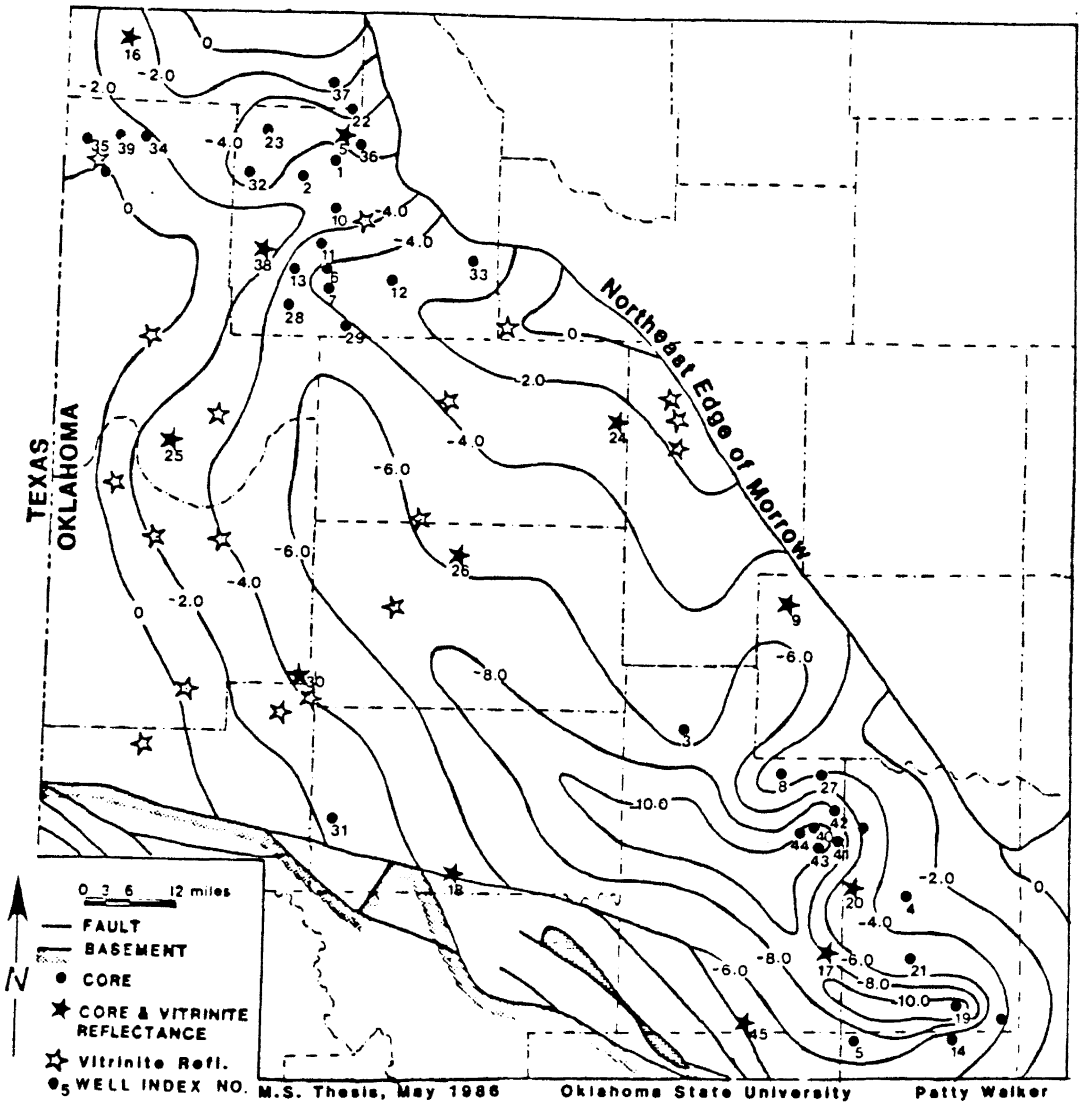

Figure 42. Distribution of C^{13} Isotope Values (Contour Interval is Equal to 2.0‰)

believed to represent an organic contribution during burial. An area of slightly depleted $\delta^{13}C$ values is observed in the northern shelf area of the basin. These values could be due to the oxidation of organic material associated with deltaic deposition.

Oxygen stable isotopic data from the carbonate components in the Morrow Formation range from +0.1‰ to -13.7‰ with a mean $\delta^{18}O$ value of -6.6‰ (Figure 43). The $\delta^{18}O$ range of calcite is -2.1‰ to -13.7‰ with a mean value of -7.1‰. Values for $\delta^{18}O$ of dolomite range from -2.3‰ to -11.2‰ with a mean of -7.3‰. Values for $\delta^{18}O$ of siderite range from +0.1‰ to -9‰ with a mean of -3.3‰.

Figure 44 shows the distribution of $\delta^{18}O$ values within the Anadarko basin for carbonate components of the Morrow Formation. There are two possible explanations for the large area of depleted values (greater than -10.0‰): 1) an influx of meteoric water; 2) the upward migration of high temperature waters through diagenetically formed pathways.

A covariation of the $\delta^{18}O$ and $\delta^{13}C$ compositions of the carbonates is apparent from Figure 45. Negative $\delta^{13}C$ values are accompanied by more negative $\delta^{18}O$ values. This trend suggests that the diagenetic environments in which these sands were cemented were under a significant organic influence during burial. This influence is indicated by the shift of $\delta^{13}C$ values from normal marine carbonate ranges of +0.0‰ to +3.0‰ and fresh water ranges of -1.0‰ to

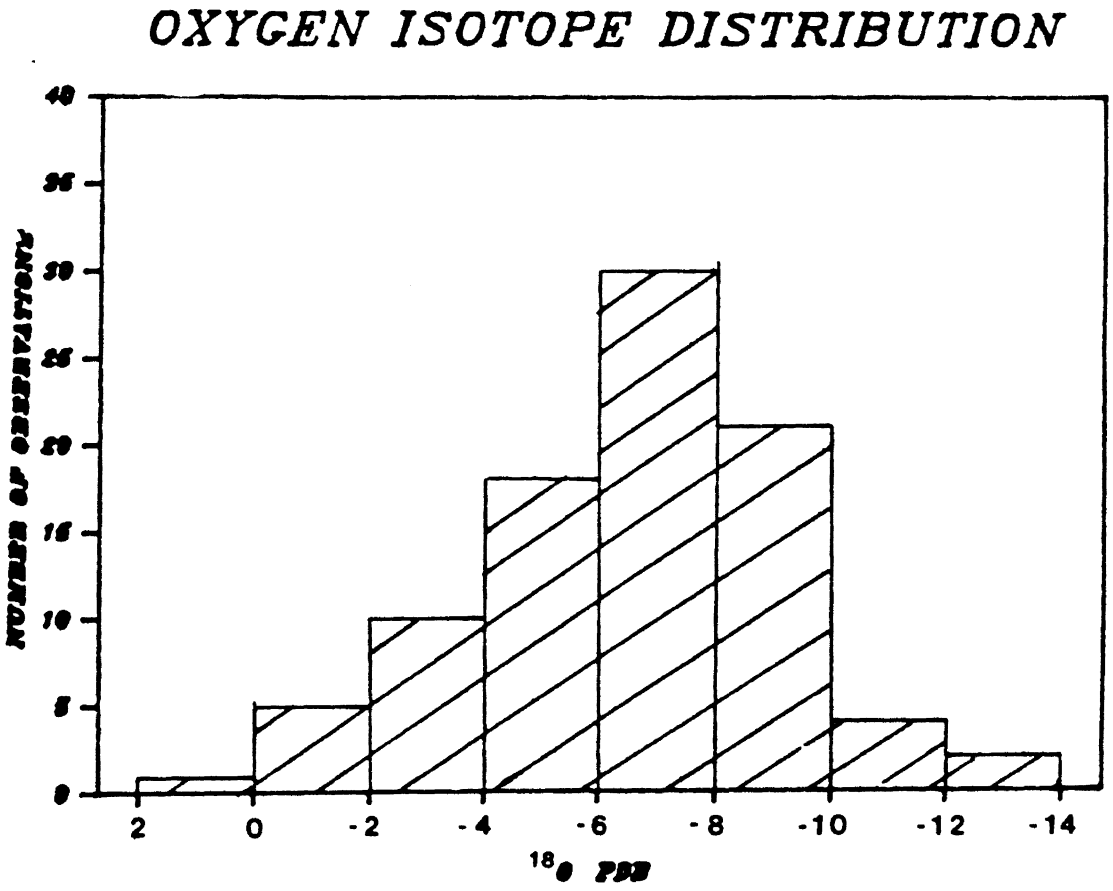

Figure 43. Frequency Distribution of O^{18} Isotope Values

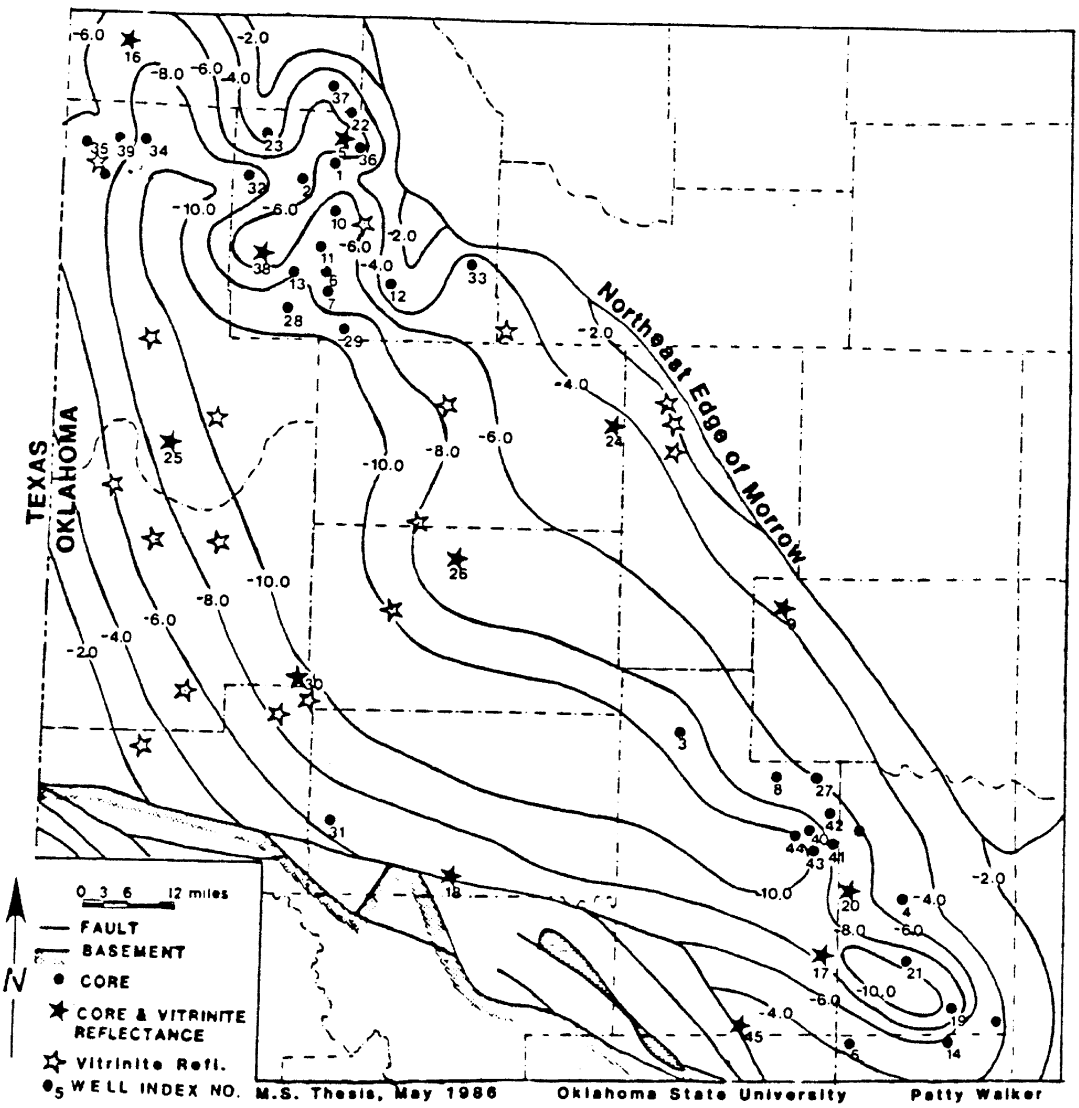

Figure 44. Distribution of O^{18} Isotope Values (Contour Interval is Equal to 2.0‰)

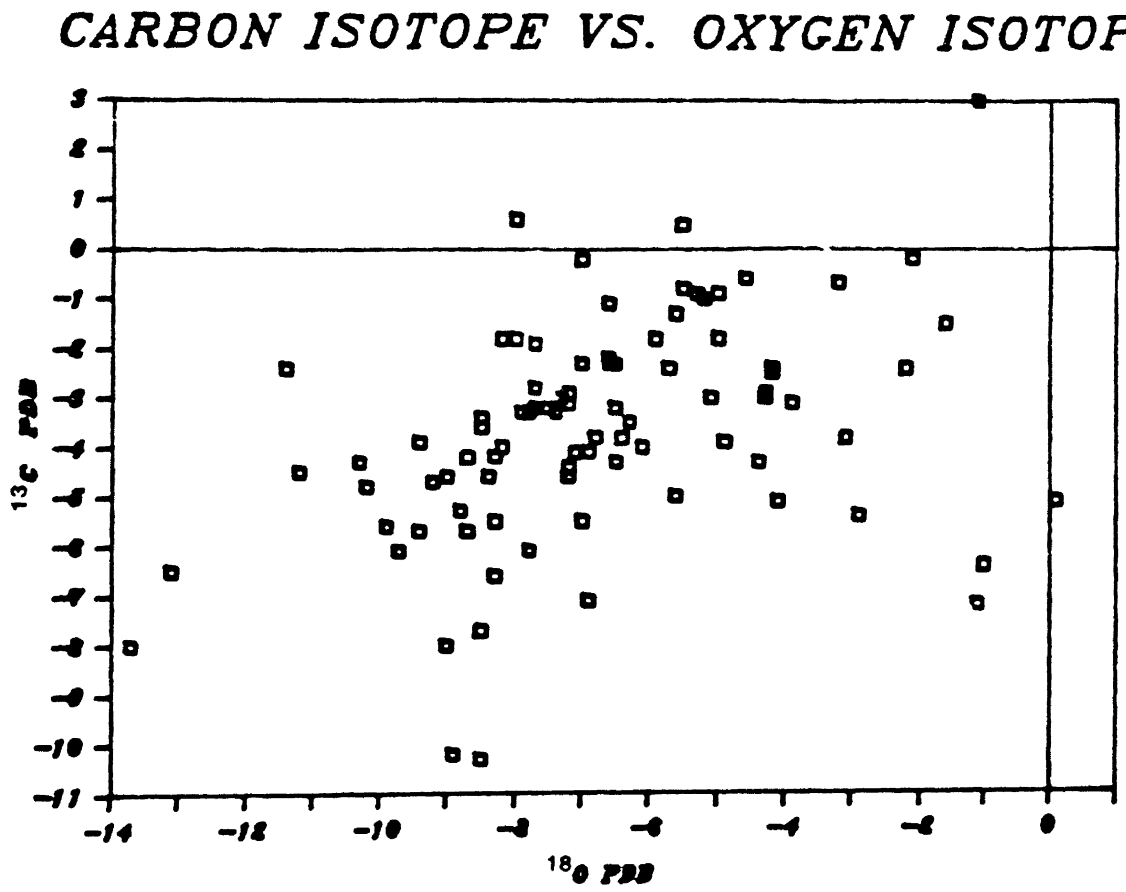

Figure 45. Results of Isotopic Analyses of $d^{13}C$ and $d^{18}O$ of Carbonate Cements of the Morrow Sandstones

-5.0‰ (PDB) (Larese et al., 1984).

Oxygen and Carbon Isotope Interpretations

Larese et al., (1984) have shown evidence in the Jurassic sandstones of the North Sea of an input of $d^{13}C$ depleted carbon derived from thermal alteration of organic material during burial. They also show that $d^{18}O$ depletion trends are controlled by increasing temperatures of precipitation. This interpretation is applicable to the carbonate cements in the sandstones of the Morrow Formation.

Franks and Forester (1984) have also proposed an organic source for depleted $d^{13}C$ observed in Texas Gulf Coast sediments. They apply a two-end member model for sources of carbonate available for cementation: early (shallow) marine carbonate (including recycled shell material) and late (deep) carbonate from organic reactions. Carbonate species from organically derived carbon would be considerably more depleted than those values derived from marine carbonate. This two-end member model for source of carbonate can also be applied to the carbonate cements in the sandstones of the Morrow Formation. Franks' and Forester's (1984) data shows a trend of increasingly negative $d^{13}C$ with an increasingly negative $d^{18}O$. They state that $d^{18}O$ trends are controlled by temperature while $d^{13}C$ values show an organic carbon influence. These trends are also observed in carbonate cements in the Morrow

Formation.

Oxygen

Epstein et al. (1953) has shown that the $d^{18}O$ composition of a carbonate is influenced by the $d^{18}O$ composition of the fluid and the temperature at which it is precipitated. Thus, a negative shift in the $d^{18}O$ values from the marine carbonate composition range of 0‰ to -2.5‰ (PDB) could be the result of either the influx of $d^{18}O$ depleted meteoric water and/or an increase in temperatures of cementation. Meteoric water associated with deltaic and shallow marine sediments would have a depleted $d^{18}O$ composition relative to Pennsylvanian marine waters (-1.5 ‰ SMOW) (Brand, 1982). If we assume a value for fluvial water of approximately -5‰, based on the analogy to the present day $d^{18}O$ composition of Mississippi River water, a calcite precipitated at surface conditions from such waters would have a $d^{18}O$ composition of approximately -5‰ to -7‰ (SMOW). Clearly, a large portion of the oxygen stable isotopic values are more depleted than this. Meteoric influx cannot entirely account for the negative shift of $d^{18}O$ values for carbonate cements of the Morrow sandstones as seen in Figure 45. Therefore, a more plausible explanation for the depleted $d^{18}O$ composition seen in the carbonate cements would be increasing temperature of precipitation during burial. Figures 46 and 47 show calculated temperatures of formation for calcite and

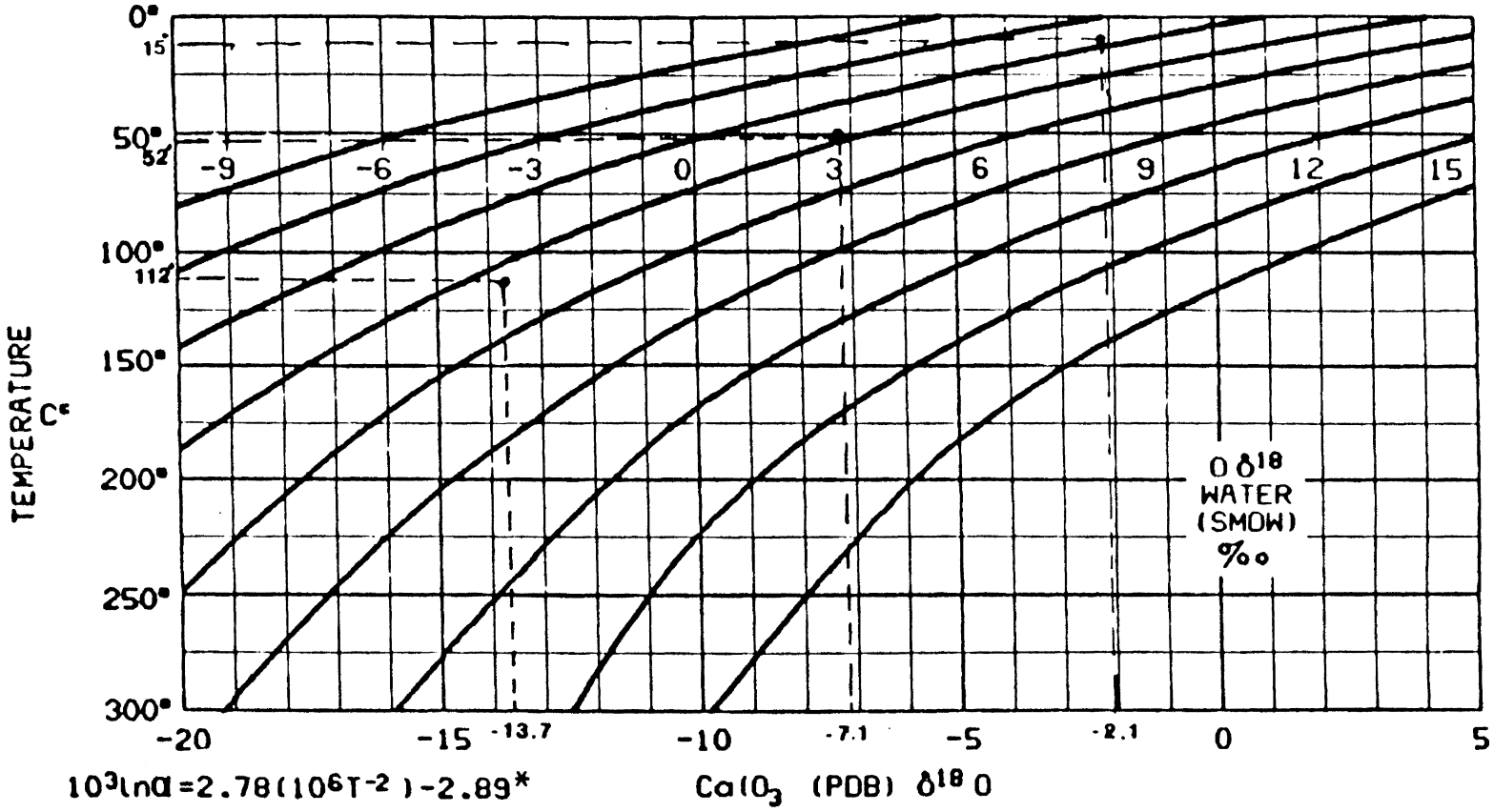

Figure 46. Temperature Versus d^{18} O Calcite (PDB) for Various d^{18} O Waters (SMOW) (Graph Courtesy of D. Prezbindowski) (* O'Neal, Clayton, and Mayeda, 1969)

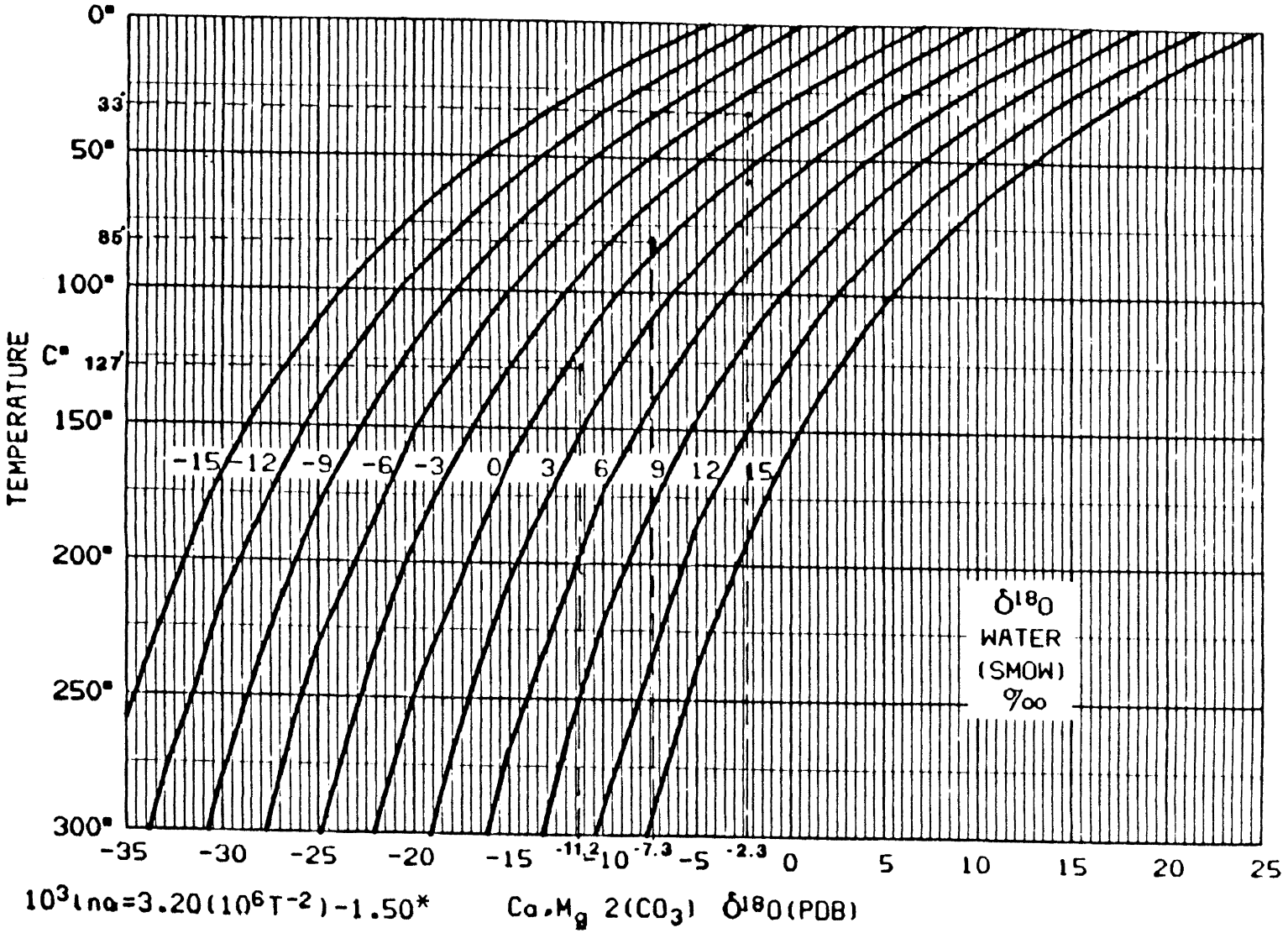

Figure 47. Temperature Versus d^{18}O Dolomite (PDB) for Various d^{18}O Waters (SMOW) (Graph Courtesy of D. Prezbindowski) (* Northrop and Clayton, 1966)

dolomite. These calculations are based on a $d^{18}O$ value of -1.5± 2.0‰ (SMOW) for Pennsylvanian sea water (Brand, 1982). Estimated temperatures for $d^{18}O$ composition of calcite range from 15°C to 112°C with an average temperature of 52°C (Figure 46). Based on a geothermal gradient of 22°C/km for the Anadarko basin, this average temperature would correspond to a depth of approximately 7,750 ft. Estimated temperatures for $d^{18}O$ composition of dolomite range from 35°C to 127°C with an average temperature of 85°C (Figure 47). This average temperature would correspond to a depth of approximately 12,670 ft.

When comparing carbonate species one should keep in mind that siderite and dolomite fractionation factors differ from calcite by 3‰ to 5‰ (PDB) (Land, 1983). A well defined diagenetic sequence (Figure 48) is apparent after adjusting the three carbonate types (siderite, calcite, ferroan dolomite) to a equilibrium isotopic scale referenced to calcite. Siderite and calcite which have more enriched isotopic values would have formed early in the diagenetic sequence, at relatively shallow depths, followed later in time, and at greater depths, by ferroan dolomite, as discussed earlier under diagenesis and shown in Figure 23.

Carbon

The $d^{13}C$ composition of precipitated marine carbonate material is controlled by the carbon isotopic composition

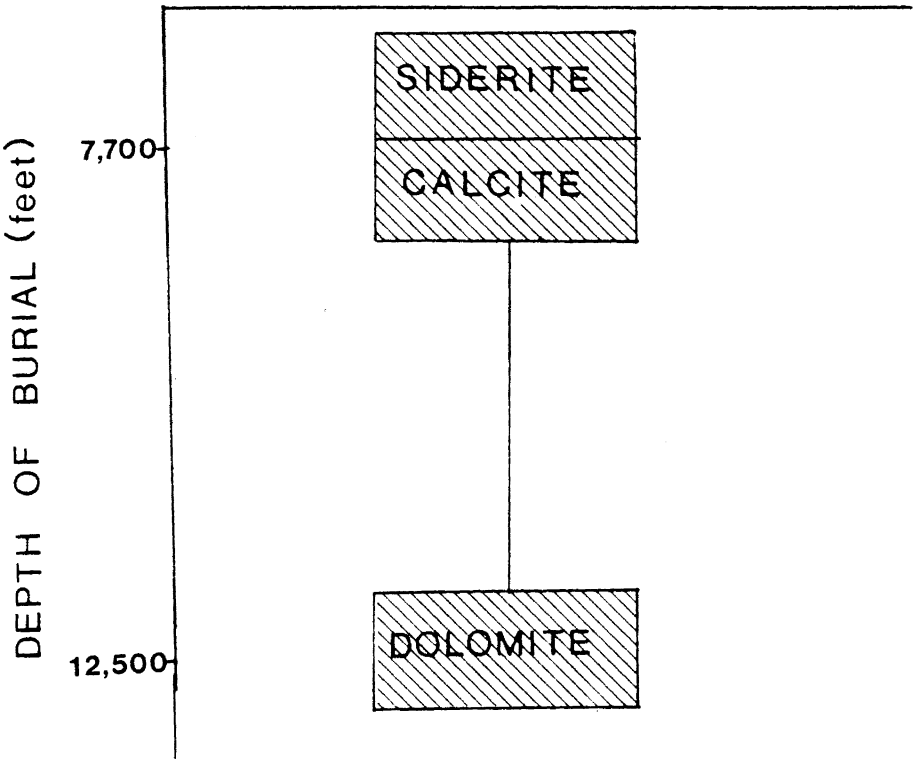

Figure 48. Diagrammatic Sequence of Carbonate Mineral Diagenetic Stages Versus Burial Depth

of the dissolved bicarbonate in the oceans. Normally, this $\delta^{13}C$ composition would fall within the range of +3.0 to +0.0‰ (PDB) (Larese et al., 1984). In order to change this composition, a new source of CO_2 or HCO_3^- must be introduced into the system. $\delta^{13}C$ depleted CO_2 can be generated in place or transported into the diagenetic system. These mechanisms for generation have been discussed by Curtis (1983) (Figures 39 and 40).

A covariation of $\delta^{18}O$ and $\delta^{13}C$ composition for calcite and dolomite cements within the Morrow sandstones is shown in Figures 49 and 50. Scatter within the calcite plot is attributed to early diagenetic microbial oxidation of organic material (associated with deltaic facies) which contributed $\delta^{13}C$ depleted CO_2 to the total carbon reservoir. Another influence on calcite cements is the addition of depleted $\delta^{13}C$ from thermal alteration of organic material during catagenesis. The approximate boundary between these two fields, shown in Figure 49, corresponds to a temperature of approximately 52 °C. This temperature is thought to be the upper limit at which significant microbial oxidation can occur (Andreev et al., 1968). The dolomite plot (Figure 50) along with calculated temperatures indicates a primary influence of $\delta^{13}C$ depleted CO_2 by thermal alteration of organic material. Laplante (1974) has shown that a much as 25% of the kerogen present in a sediment at the time of deposition can be converted into $\delta^{13}C$ depleted CO_2 during burial. Larese et al. (1984)

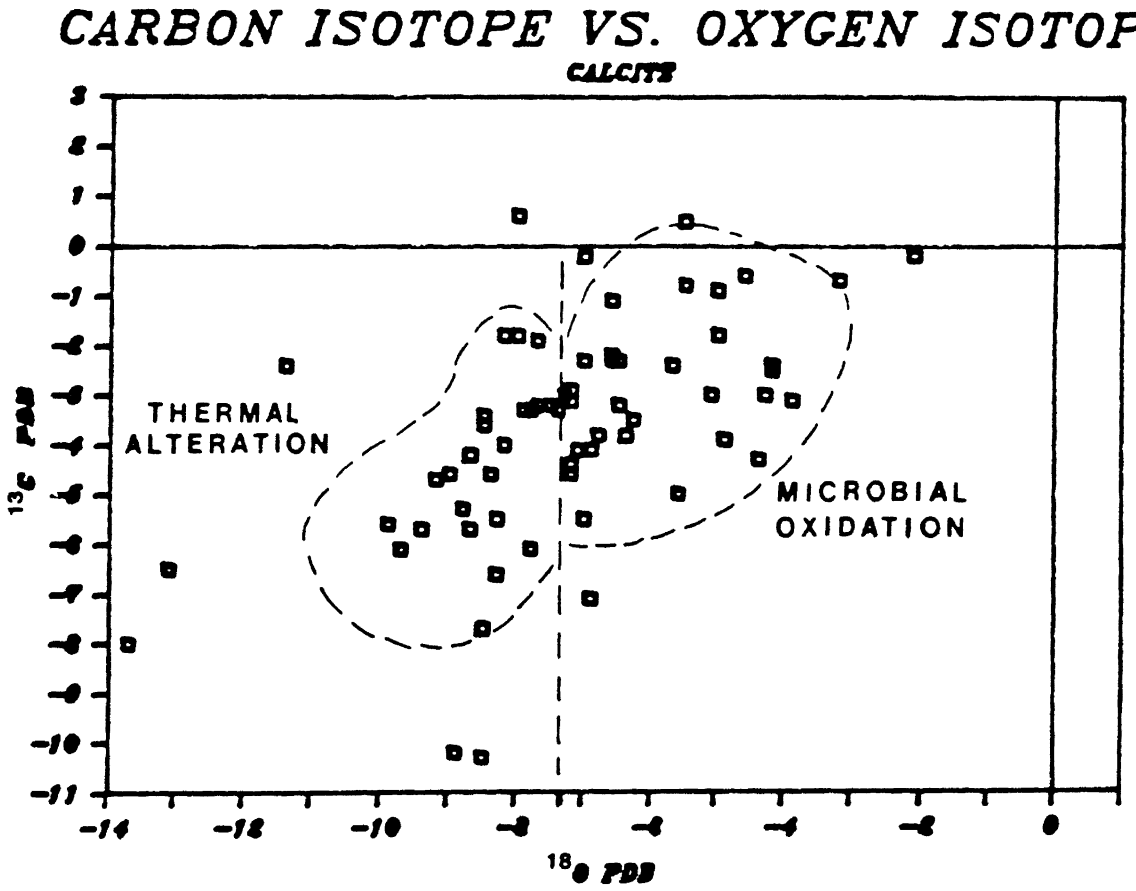

Figure 49. Results of Isotopic Analyses of $\delta^{13}C$ and $\delta^{18}O$ for Calcite Cements of the Morrow Sandstones

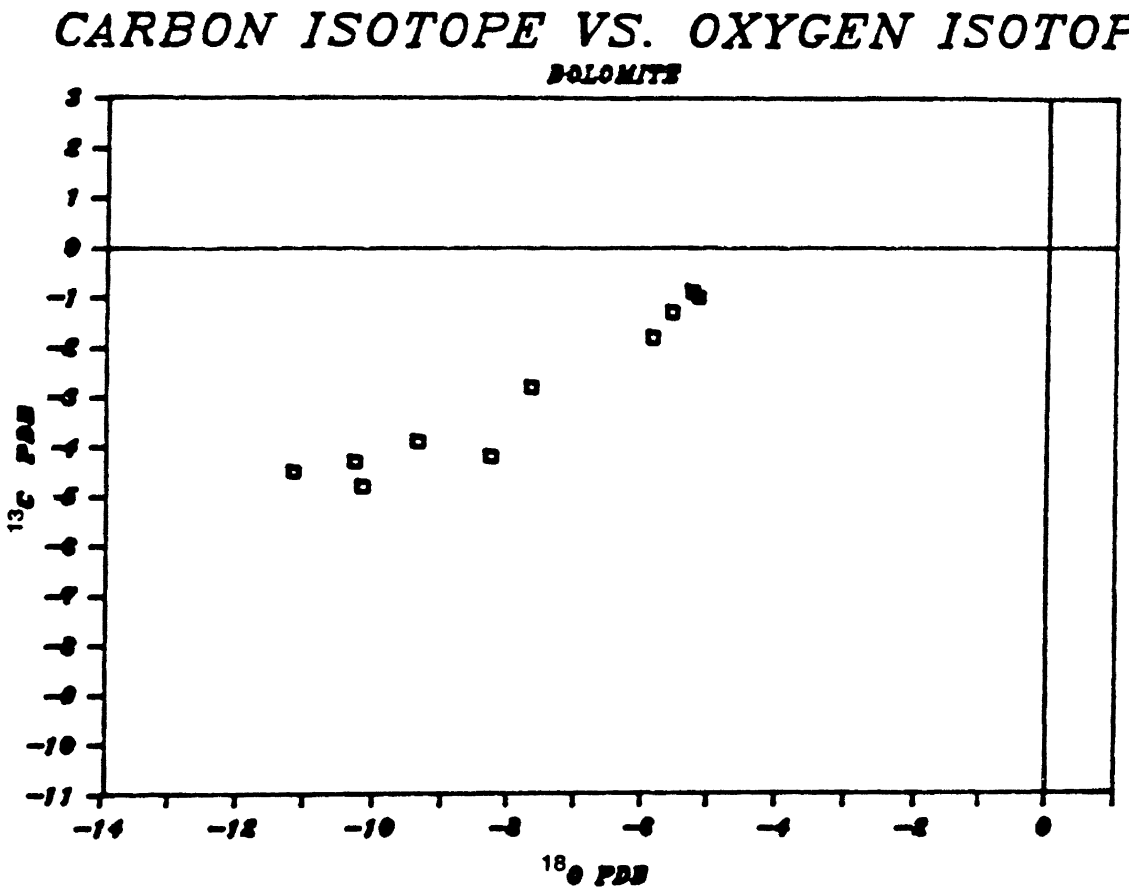

Figure 50. Results of Isotopic Analyses of $d^{13}C$ and $d^{18}O$ for Dolomite Cements of the Morrow Sandstones

showed that carbonate having 100% of its carbon derived from the thermal alteration of organic material during burial would have a $\delta^{13}C$ composition range of -18‰ to -21‰ (PDB). Table IV (Appendix C) contains calculations of percent organic carbon contribution to the $\delta^{13}C$ composition of carbonate cements of the Morrow sandstones. These calculations are based on a model proposed by Al-Shaieb (1986) to represent the contributions of a two end member system. This system consists of a marine member and an organic member. The value range was determined by making the following assumptions: 1) $\delta^{13}C$ composition of derived CO_2 during thermal alteration of organic material would have a value of -21‰ (PDB) (Irwin et al., 1977). 2) Pennsylvanian marine sea water had a $\delta^{13}C$ composition of +2.8‰ (PDB) (Brand, 1982). Values were calculated by the following formula:

$$(-21.0 * x) + (+2.8 * (1-x)) = z \qquad 7\text{-}3$$

where x represents the fraction of organic contribution and z represents the measured $\delta^{13}C$ value.

Figure 51 shows the distribution of percent organic carbon within the Anadarko basin for carbonate cements of the Morrow Formation. The area of greater than 50% organic carbon corresponds well with the area of depleted $\delta^{18}O$ seen in Figure 44, and the areas of depleted $\delta^{13}C$ seen in Figure 42. It is thought that these areas are due primarily to a thermal effect. The area of greater than 30% organic

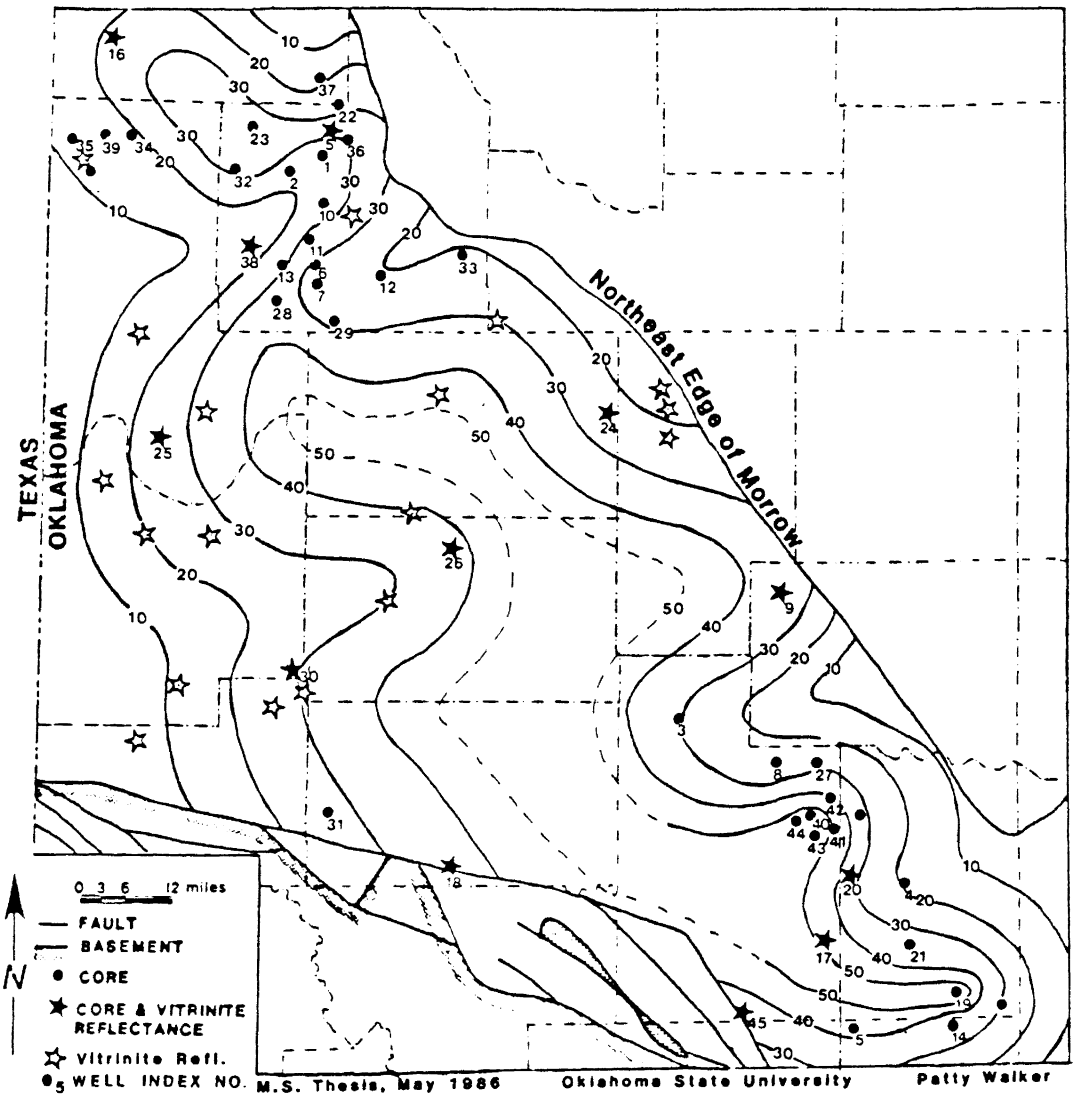

Figure 51. Distribution of % Organic Carbon.
(Contour Interval is Equal to 10%)

carbon in the northern area of Figure 51 may indicate the minor effects of microbial oxidation of organic material associated with deltaic facies.

To summarize, it is important to note that no values greater than approximately 55% organic carbon contribution were calculated for carbonate cements of the Morrow sandstones. The general $d^{13}C$ depletion reflects the interaction between the original marine and fresh water carbon reservoir, including skeletal material, carbonate clasts, etc., and the $d^{13}C$ depleted carbon reservoir derived from the alteration of organic material. The corresponding $d^{18}O$ depletion trend in the carbonate cements suggests that increasing burial is followed by the incorporation of increasing amount of $d^{13}C$ depleted carbon into the precipitating carbonate cements. The rate of $d^{18}O$ depletion is largely controlled by increases in precipitation temperature.

CHAPTER VIII

CONCLUSIONS

Several conclusions can be made from data obtained in this study. They are as follows:

1. Development of secondary porosity in the Pennsylvanian Morrow sandstones is related directly to:

a. Source of H^+ ions in the leaching fluids. The sources are organic acids, carbonic acid, and dissolved H_2S.

b. Composition and texture of the various sandstone lithologies. Compositional variations reflect the two major facies investigated. These are deltaic and shallow marine facies.

2. Observed secondary porosity in the sandstones is due mainly to partial or complete dissolution of detrital matrix, glauconite, fossil fragments, and to a lesser extent silica and pyrite.

3. A multiple stage model is proposed for the development of secondary porosity in the Morrow sandstones. Stage I is dominated by organic acids and carbonic acid; Stage II is composed mainly of carbonic acid; Stage III is composed of carbonic acid and dissolved H_2S in formation water.

4. The complex diagenetic history of the Morrow Formation is a function of inorganic and organic reactions during its burial in the subsident Anadarko basin.

5. The CO_2 content of natural gas increases with increasing depth.

6. Kaolinite rich zones within the Morrow Formation appear to coincide with major producing trends.

7. Chlorite is the dominant clay mineral in the Morrow sandstones of the Anadarko basin.

8. Vitrinite reflectance trends of the Morrow Formation in the Anadarko basin range from 0.62-0.95% Ro in the shallower northeastern part of the basin to 3.34% Ro in the deep basin.

9. The present geothermal gradient for the Anadarko basin is 1.2 ^{o}F/100ft. The present- and paleo- geothermal gradients are non-linear and tend to converge with depth.

10. The area of high vitrinite reflectance values in the Morrow shales of the Anadarko basin may be recording an older deep basin that was present when "cooking" of Morrow rocks took place.

11. Oil and gas produced from the Morrow sandstones are a function of original Morrow shale character as well as depth of burial and temperature. Original shale character is controlled by depositional environment.

12. Covariations of the $\delta^{18}O$ and $\delta^{13}C$ compositions show negative $\delta^{13}C$ values are accompanied by more negative $\delta^{18}O$ values. This trend indicates that the

diagenetic environments that Morrow sandstones were cemented in underwent significant organic influence during burial. These organic influences include minor microbial oxidation of organic material associated with deltaic facies and the thermal alteration of organic material.

13. The $\delta^{18}O$ depletion trend observed in carbonate cements of the Morrow Formation is controlled to a large extent by increasing temperatures of precipitation (burial).

14. Average estimated temperature of formation for calcite is approximately 52 ^{o}C. Average estimated temperature of formation for dolomite is approximately 85 ^{o}C.

15. The $\delta^{18}O$ values for siderite, calcite, and ferroan dolomite establish a well defined diagenetic sequence of carbonate precipitation within the Morrow sandstones. Siderite and calcite form early in the diagenetic sequence at shallow depths followed at a later time and greater depth by ferroan dolomite.

16. The general $\delta^{13}C$ depletion observed in the Morrow reflects the interaction between the original marine and fresh water carbon reservoir and $\delta^{13}C$ depleted carbon reservoir derived from the alteration of organic material. The corresponding $\delta^{18}O$ depletion trend in the carbonate cements suggest that burial is followed by incorporation of increasing amounts of $\delta^{13}C$ depleted carbon into the precipitated carbonate cements. The rate of $\delta^{18}O$ depletion

is largely controlled by an increase in precipitation temperature.

REFERENCES CITED

Abels, T. A., 1959, A Subsurface Lithofacies Study of the Morrow Series in the Northern Anadarko Basin: Shale Shaker, pp. 93-108.

Adams, W. L., 1964, Diagenetic Aspects of Lower Morrowan Pennsylvanian Sandstones, Northwestern Oklahoma: Am. Assoc. Petro. Geol. Bull., Vol. 48, No. 9, pp. 1568-1580.

Adler, F. J.,and Capland, W. M., et al., 1971, Future Petroleum Provinces of the Mid-Continent, Region 7: Am. Assoc. Petro. Geol. Mem. 15, Vol. 2.

Al-Shaieb, Z. and Shelton, J. W., 1977, Evaluation of uranium potential in selected Pennsylvanian and Permian units and igneous rocks in southwestern and southern Oklahoma: U.S. Department of Energy, Open-File Report GJBX-35(78), 248p.

Al-Shaieb, Z. and Shelton, J. W., 1981, Migration of Hydrocarbons and Secondary Porosity in Sandstones: Am. Assoc. Petro. Geol. Bull., Vol. 65, No. 11, pp. 2433-2436.

Al-Shaieb, Z., 1986, Personal Communication, Oklahoma State University, Stillwater, Oklahoma.

Andreev, P. F., Bogomolow, A. I., Dobryanskii, A. F., Kartsev, A. A., 1968, Transformation of Petroleum in Nature: London, Pergamon Press Inc., 466 p.

Arbenz, J. K., 1956, Tectonic map of Oklahoma: Oklahoma Geological Survey Map GM-3.

Arro E., 1965, Morrowan Sandstones in the Subsurface of the Hough Area, Texas County, Oklahoma: Shale Shaker, Vol. 15-17, pp. 16-30.

Barby, B. G., 1960, Subsurface Geology of Pennsylvanian and Upper Mississippian rocks of Beaver County, Oklahoma: Unpublished M.S. thesis, University of Oklahoma, Shale Shaker, Vol. 6, No. 10, pp. 9-32.

Barrett, L. W., 1965, Subsurface Study of Morrowan Rocks in Central and Southern Beaver County, Oklahoma: Shale Shaker, Vol. 4, pp. 425-433.

Benton, J. W., 1972, Subsurface Stratigraphic Analysis, Morrow Formation (Pennsylvanian), North Central Texas County, Oklahoma: Shale Shaker, Vol. 23, No. 1, pp. 4-19.

Bjorlykke, K., 1979, Cementation of Sandstones: Journ. of Sed. Pet., Vol. 49, pp. 1358-1359.

Bloustine, D. A., 1975, Producing Characteristics of Lower Morrow Sandstone in Southern Ellis County, Oklahoma: AAPG Mid-Continent Section Meeting, Wichita, Kansas, Am. Assoc. Petro. Geol. Bull., Vol. 50, No. 3, pp. 318.

Boles, J. R., and Franks, S. T., 1979, Clay Diagenesis in Wilcox Sandstones of Southwest Texas: Implications of Smectite Diagenesis on Sandstone Cementation: Journ. of Sed. Pet., Vol. 21, Nos. 8-9, pp. 172-193.

Brand, U., 1982, The oxygen and carbon isotope composition of Carboniferous fossil components: sea-water effects: Sedimentology, Vol. 29, pp. 139-147.

Breeze, A. F., 1971, Abnormal-Subnormal Pressure Relationships in the Morrow Sands of Northwestern Oklahoma: Shale Shaker, Vol. 21, Nos. 8-9, pp. 172-193.

Burke, K, and Dewey, J. F., 1973, Plume-generated Triple Junctions Key Indicators in Applying Plate Tectonics to Old Rocks: Journ. of Geology., Vol. 81, pp. 406-433.

Busch, Daniel A., 1959, Prospecting for Stratigraphic Traps: Am. Assoc. Petro. Geol. Bull., Vol. 43, pp. 2829-2843.

Cardott, B. J., and Lambert, M., 1985, Thermal maturation of the Woodford Shale, Anadarko Basin, Oklahoma: Am. Assoc. Petro. Geol. Bull., Vol., pp. 1982-1998.

Carothers, W. W., and Kharaka, Y. K., 1978, Alphatic Acid Anions in Oil-field Waters-Implications for Origin of Natural Gas: Am. Assoc. Petro. Geol. Bull., Vol. 62, pp. 2441-2453.

Chenoweth, P. A., 1968, Early Paleozoic (Arbuckle) overlap, Southern Mid-Continent, U.S.: Am. Assoc. Petro. Geol. Bull., Vol. 52, pp. 1670-1688.

Cullins, H. L., 1959, A subsurface study of Morrowan Sandstones (Pennsylvanian), Ellis County, Oklahoma: Unpublished M.S. thesis, University of Oklahoma, 68p.

Curtis, B. F., and Ostergard, D., 1980, Subsurface Stratigraphy of the Morrow Formation in Southeastern Texas County, Oklahoma: Shale Shaker, Vol. 30, No. 5, pp. 112-142.

Curtis, C. D., 1983, Geochemistry of porosity enhancement and reduction in clastic sediments in Petroleum Geochemistry and Exploration of Europe, Spec. Publ. Geol. Soc. London, pp. 113-125.

Davis, H. G., 1971, The Morrow-Springer Trend, Anadarko Basin, Target for the 70's: Shale Shaker, Vol. 22, No. 3, pp. 64-72.

Davis, H. G., 1974, High Pressure Morrow-Springer Gas Trend, Blaine and Canadian Counties, Oklahoma: Shale Shaker, Vol. 24, No. 6, pp. 104-115.

Donovan, R. N., Beachamp, W., Ferraro, T., Lajek, C., McConnell, D., Munsil, M., Ragland, D., Sweet, B., and Taylor, D., 1983, Subsidence Rates in Oklahoma During the Paleozoic: Shale Shaker, Vol. 33, No. 8, pp. 86-88.

Donovan, R. N., 1986, Personal Communication, Oklahoma State University, Stillwater, Oklahoma.

Epstein, S., Buchsbaum, H. A., Lowenstam, H. A., and Urey, H. C., 1953, Revised carbonate-water isotopic temperature scale: Geol. Soc. Am. Bull., Vol. 64, pp. 1315.

Epstein, S., and Mayeda, T., 1953, Variations of O^{18} content of waters from natural sources: Geochim. Cosmochim. Acta., Vol. 4, pp. 213-224.

Evans, J. L., 1979, Major Structural and Stratigraphic Features of the Anadarko Basin, in Pennsylvanian Sandstones of the Mid-Continent: Tulsa Geol. Soc. Spec. Publ. No. 1, pp. 97-113.

Faure, G, 1977, Principles of Isotope Geology: New York, John Wiley and Sons, 464p.

Forgotson, J. M., Statler, A. T., and David, M., 1966, Influence of Regional Tectonics and Local Structures on Deposition of Morrow Formation in Western Anadarko Basin: Am. Assoc. Petro. Geol. Bull., Vol. 50, No. 3, pp. 528-532.

Forgotson, J. M., 1969, Factors Controlling Occurrence of Morrow Sandstones and Their Relation to Production in the Anadarko Basin: Shale Shaker, Vol. 20, pp. 135-149.

Franks, Stephen and Forester, Richard, 1984, Relationships Among Secondary Porosity, Pore-Fluid Chemistry and Carbon Dioxide, Texas Gulf Coast,in Clastic Diagenesis: Am. Assoc. Petro. Geol. Mem. 37, pp. 63-79.

Fuex, A. N., and Baker, D. R., 1973, Stable Carbon Isotopes in selected granitic, mafic, and ultramafic rocks: Geochim. Cosmochim Acta, 37, pp. 2509-2521.

Galloway, W. E., and Dutton, S. P., 1979, Seismic Stratigraphic Analysis of Intracratonic Basin Sandstone Reservoirs,in Pennsylvanian Sandstones of the Mid-Continent: Tulsa Geol. Soc. Spec. Publ., No. 1, pp. 65-81.

Gibbons, Kenneth, 1965, Pennsylvanian of the North Flank of the Anadarko Basin: Shale Shaker, Vol. 28, No. 10, pp. 219-227.

Godard, S. T., 1981, Depositional Environments and Sandstone Trends of the Pennsylvanian Morrowan Series, Southern Major and Woodward Counties, Oklahoma: Unpublished M.S. thesis, Oklahoma State University, 78p.

Harrison, W. E., Luza, K. V., Prater, M. L., and Cheung, P. K., 1983, Geothermal resource assessment in Oklahoma: Oklahoma Geological Survey Special Publication 83-1, 42p.

Hill, G. W.,and Clark, R. H., 1980, The Anadarko Basin-A Regional Petroleum Accumulation. A Model for Future Exploration and Development: Shale Shaker, Vol. 31, pp. 36-48.

Hood, A., Gutjahr, C. C. M., and Heacock, R. L., 1975, Organic metamorphism and the generation of petroleum: Am. Assoc. Petro. Geol. Bull., Vol. 59, pp. 986-996.

Hower, J., Eslinger, E., Hower, M. E., and Perry, E. A., 1976, Mechanism of Burial Metamorphism of Argillaceous Sediments: 1.Mineralogical and Chemical Evidence: Geol. Soc. Amer. Bull., Vol. 87, pp. 725-737.

Huffman, G. G., 1959, Pre-Desmoinesian Isopachous and Paleogeologic Studies in the Central and Mid-Continent Region: Am. Assoc. Petro. Geol. Bull., No. 11, pp.

2541-2574.

Hunt, J. M., 1979, Petroleum Geochemistry and Geology: San Francisco, W. H. Freeman, 617p.

Irwin, H., Curtis, C., and Coleman, M., 1977, Isotopic evidence for source of diagenetic carbonates formed during burial of organic-rich sediments: Nature, London, Vol. 269, pp. 209-213.

Jobe, T. H., 1984, A Diagenetic Study of Morrowan Distributary Channel Deposits in Western Texas County, Oklahoma: Unpublished report, Oklahoma State University, 46p.

Kasino, R. E. and Davies, D. K., 1979, Environments and Diagenesis, Morrow Sands, Cimmaron County (Oklahoma), and Significance to Regional Exploration and Well Completion Practice, in Pennsylvanian Sandstones of the Mid-Continent: Tulsa Geol. Soc. Special Pub. No. 1, pp. 115-168.

Khaiwka, M. H., 1968, Geometry and Depositional Environment of Morrow Reservoir Sandstones, Northwestern Oklahoma: Unpublished Ph.D. dissertation, University of Oklahoma, 100p.

Krauskopf, K. B., 1979, Introduction to Geochemistry: San Francisco, McGraw-Hill Book Company, 200p.

Land, L. S., 1983, The application of stable isotopes to studies of the origin of dolomite and to problems of diagenesis of clastic sediments, in Stable Isotopes in Sedimentary Geology: SEPM Short Course No. 10, pp. 4-1 - 4-22.

Laplante, R. E., 1974, Hydrocarbon Generation in Gulf Coast Tertiary Sediments: Am. Assoc. Petro. Geol. Bull., Vol. 58, No. 7, pp. 1281-1289.

Larese, R. E., Haskel, N. L., Prezbindowski, D. R., and Beju, D., 1984, Sedimentologic and Diagenetic Controls on Porosity Development in Selected Jurrasic Sandstone Specimens from the Norwegian and North Seas, Norway-An Overview: Proceedings of the North European Margin Symposium, Trondhiem, Norway, pp. 81-95.

Loucks, R. G., Dodge, M. M., and Galloway, W. E., 1984, Regional Controls on Diagenesis and Reservoir Quality in Lower Tertiary Sandstones along the Texas Gulf Coast, in Clastic Diagenesis: Am. Assoc. Petro. Geol. Mem. 37, pp. 15-45.

McKinney, C. R., McCrea, J. M., Allen, H. A., and Urey, H. C., 1950, Improvements in mass spectrometers for the measurements of small differences in isotope abundance ratios: Rev. Sci. Inst., Vol. 21, pp. 724-730.

Markert, J. C. and Al-Shaieb, Z., 1984, Diagenesis and Evolution of Secondary Porosity in Upper Minnelusa Sandstones, Powder River Basin, Wyoming, in Clastic Diagenesis: Am. Assoc. Petro. Geol. Mem. 37, pp. 367-389.

Moore, B. J., 1980, Analysis of Natural Gases, 1917-80: Bureau of Mines Information Circular 8870/1982, pp. 365-529.

Moore, G. E., 1979, Pennsylvanian Paleography of the Southern Mid-Continent, in Pennsylvanian Sandstones of the Mid-Continent: Tulsa Geol. Soc. Spec. Publ. No. 1, pp. 2-12.

Pate, J. D., 1959, Stratigraphic traps along the north shelf of the Anadarko basin: Am. Assoc. Petro. Geol. Bull., Vol. 43, No. 1, pp. 39-59.

Prezbindowski, D., 1986, Personal Communication: Oklahoma State University, Stillwater, Oklahoma.

Pusey, W. C. III, 1973, How to evaluate potential gas and oil source rocks: World Oil, Vol. 176, No. 5, pp. 71-75.

Schmidt, V. and McDonald, D. A., 1979, The Role of Secondary Porosity Development in the Course of Sandstone Diagenesis,in Aspects of Diagenesis: SEPM Special Publication 26, pp. 175-208.

Shatski, N. S., 1946, The Great Donets Basin and Wichita System. Comparative Tectonics of Ancient Platforms, USSR: Akad. Nauk, Izv. Geol. Serial, No. 1, pp. 5-62.

Shelby, J. M., 1980, Geologic and Economic Significance of the Upper Morrow Chert Conglomerate Reservoir of the Anadarko Basin: Journ. of Petro. Tech., March 1980, pp. 489-495.

Simon, D. E., Kaul, F. W., and Culbertson, J. N., 1979, Anadarko Basin Morrow Springer Sandstone Stimulation Study: Journ. of Petro. Tech., June 1979, pp. 683-689.

South, M. V., 1983, Stratigraphy, Depositional Environment, Petrology and Diagenetic Character of the Morrow Reservoir Sands, Southwest Canton Field, Blaine and

Dewey Counties, Oklahoma: Unpublished M.S. thesis, Oklahoma State University, 179p.

Staplin, F. L., 1969, Sedimentary organic matter, organic metamorphism, and oil and gas occurrence: Canadian Petro. Geol. Bull., Vol. 17, pp. 47-66.

Surdam, R. C., Boese, S. W., Crossey, L. J., 1984, The Chemistry of Secondary Porosity, in Clastic Diagenesis: Am. Assoc. Petro. Geol. Mem. 37, pp. 127-149.

Swanson, D. C., 1979, Deltaic Deposits in the Pennsylvanian Upper Morrow Formation of the Anadarko Basin, in Pennsylvanian Sandstones of the Mid-Continent: Tulsa Geol. Soc. Special Publication No.1, pp. 115-168.

Takenouchi, S. and Kennedy, G. C., 1965, The Solubility of Carbon Dioxide in NaCl Solutions at High Temperatures and Pressures: Amer. Journ. Science, Vol. 263, pp. 445-454.

Tissot, B. P., and Welte, D. H., 1984, Petroleum formation and occurrence: New York, Springer-Verlag, 699p.

Tsiris, V., 1983, Organic Geochemistry and Thermal History of the Uppermost Morrow Shale (Lower Pennsylvanian) in the Anadarko Basin, Oklahoma: Unpublished M.S. thesis, 122p.

Waples, D. W., 1980, Time and temperature in petroleum formation: application of Lopatin's method to petroleum exploration: Am. Assoc. Petro. Geol. Bull., Vol. 64, pp. 916-926.

Waples, D. W., 1982, Time and temperature in petroleum formation: application of Lopatin's method to petroleum exploration: reply: Am. Assoc. Petro. Geol. Bull., Vol. 66, pp. 1152.

Wickham, J. W., 1978, The Southern Oklahoma Aulacogen, in Field Guide to the structure and stratigraphy of the Ouachita Mountains and the Arkoma Basin: Annual Meeting of Am. Assoc. Petr. Geol., Oklahoma City, 111 p.

APPENDIXES

APPENDIX A

TERNARY DIAGRAM PLOT & DATA SHEET, AND WELL NAME ABBREVIATIONS

TABLE I

LIST OF WELL NAME ABBREVIATIONS AND INDEX NUMBERS

Index	Well Name	Location	Abbrev.
1	Apache Atwell #1		AA
2	Apache Baker	24-23N-21W	AB
3	Apexco Buell A-1	10-11N-12W	AB-A
4	Apexco Penick #1	5-7N-7W	AP
5	Arkla Expl. Carter #1	5-4N-8W	AEC
6	Eason Baird #1	14-21N-21W	EB
7	Eason Bergner-Baird #1	22-21N-21W	EBB
8	Eason Cook-Dodson #1	4-10N-10W	ECD
9	E.L. Cox Miller #1	26-14N-10W	ECML
10	E.L. Cox Meyers #1	27-22N-21W	ECMY
11	Eason Kehl #1	1-21N-21W	EK
12	Eason Mary Griffith #1	35-21N-19W	EMG
13	Eason Parkhurst #1	9-21N-21W	EP
14	Gulf Ida #1	4-4N-6W	GI
15	Gulf Vina Eike #1	15-24N-20W	GVE
16	Gulf Laverne State #1	13-26N-25W	GLS
17	Gulf Miller #1	14-6N-9W	GM
18	Humble Annie Schmidt #1	20-8N-17W	HMAS
19	Humble Patterson #1	23-5N-6W	HP
20	Hump.-Parker Venable-Verden	31-8N-8W	HPVV
21	Humble Richardson #1	10-6N-7W	HR
22	King Stevenson Anderson #1	26-25N-20W	KSA
23	King Stevenson Cooper #1	36-24N-22W	KSC

TABLE I (Continued)

Index	Well Number	Location	Abbrev.
24	Ladd Armstrong #2	36-18N-14W	LA
25	McCulloch Berryman #1-12	12-17N-24W	MCB
26	Michigan-Wisconsin Raab #1	35-15N-17W	MWR
27	Michigan-Wisconsin Smith #1	6-10N-9W	MWS
28	Odessa Natl. Gas Austin #1	8-20N-21W	OA
29	Odessa Natl. Gas Milstead	33-20N-21W	OM
30	Petrol. Consl. Weatherly	3-12N-21W	PCW
31	Phillips Celsor #1	28-9N-20W	PC
32	Shell Blasdel #1	21-23N-22W	SB
33	Shell Coulter #1-19	19-21N-17W	SC
34	Shell O'Hern 1-35	35-24N-25W	SO
35	Shell State of Okla. #1-36	36-24N-26W	SOK
36	Sampson Res. Lamar #1	24N-20W	SRL
37	Shell Smith #1	19-25N-20W	SS1
38	Shell Unit Test State #1-36	36-22N-22W	SUTS
39	Shell White #1	31-24N-25W	SW
40	Tenneco Marie Rumley #1-15	15-9N-9W	TMR
41	Tenneco Willie Lefthand #1-23	23-9N-9W	TWL
42	Tenneco Mollett #1-11	11-9N-9W	TM
43	Tenneco Grant Rumley #1-22	22-9N-9W	TGR
44	Tenneco Shadid #2-16	16-9N-9W	TS
45	Texaco Carr #1	36-5N-11W	TC
46	Humble Kephart #1	20-18N-12W	HKP

TABLE I (Continued)

Index	Well Name	Location	Abbrev.
47	Hall Jones DeMoss A-1	7-18N-12W	HDM
48	Pan-American Winters #1	4-17N-12W	PAW
49	Ladd Paul Willis A-5	25-18N-14W	LPW
50	Cities Service #D-1 McClung	15-16N-25W	CSM
51	Pan Am Fox #C-1	16-23N-25W	PF
52	Harper Burt #1	30-20N-24W	HB
53	Texas Pacific Shrewder #1	23-18N-23W	TPS
54	Inexco Kendall #1	14-15N-24W	IK
55	Dyco Baker #1-20	20-12N-23W	DB
56	Natomas Austin #1	27-11N-24W	NA
57	Continental C.H. Case #1	19-20N-16W	CC
58	Amerada Thomsen #1	24-18N-18W	AT
59	Longhorn Cline #1	34-16N-18W	LC
60	An-Son Fransen #1-26	26-14N-19W	ASF
61	Apache Deal #1-14	14-12N-21W	AD
62	G.H.K.-Apache Russell #1-15	5-11N-21W	GR
63	Harper D.C. Gurthie #1	2-22N-20W	HG
64	Clark Canadian Viersen #1	8-15N-22W	CV

TABLE II

DATA FOR PLOTTING TERNARY DIAGRAM

Well Name	Qtz. %	Clay %	Sk.Gr. %	Qtz. %	Sk.Gr. %	Rk.Frg. %
OA	65	31	4	90	6	4
AB	77	14	9	84	9	7
TC	87	12	1	97	1	2
MCB	91	8	1	97	1	2
SOK	59	32	9	81	13	6
HR	89	10	1	99	1	0
GM	81	10	9	87	10	3
AP	90	2	8	89	8	3
ECD	58	24	18	70	22	8
HPV	86	4	10	89	10	1
EK	83	14	3	93	4	3
EB	74	21	5	92	6	2
MWS	56	14	30	59	31	10
EP	57	36	7	82	9	9
SS1	57	13	30	62	33	5
SC	46	2	52	44	49	7
ECMY	73	17	10	81	11	8
EBB	73	23	4	85	4	11
EMG	78	5	17	81	17	2
SW	52	5	43	51	42	7
SOH	66	34	0	97	0	3
TM	84	9	7	91	8	1
TGR	72	21	7	86	9	5
MDL	90	5	5	94	5	1
TMR	83	11	6	90	6	4
OM	59	32	9	84	12	4
PCW	95	5	0	100	0	0
GLS	75	22	3	95	4	1
SRL	90	8	2	91	2	7
MWR	91	1	8	88	8	4
GI	80	16	4	91	5	1
TS	87	9	4	92	4	4
PC	71	29	0	100	0	0
TWL	71	27	2	96	3	1
HMAS	83	17	0	99	0	1
ECML	97	1	2	96	2	2
AA	93	4	3	93	3	4
GVE	69	24	7	90	9	1
SUTS	77	16	7	86	7	7
KSC	89	6	5	90	5	5
KSA	83	11	6	86	7	7
HP	93	2	5	94	5	1
SB	83	12	5	88	6	6
AB-A	92	2	6	89	6	5

TABLE II (Continued)

Well Name	Qtz. %	Clay %	Sk.Gr. %	Qtz. %	Sk.Gr. %	Rk.Frg. %
AEC	84	5	11	72	10	18
LA	72	28	0	75	0	25

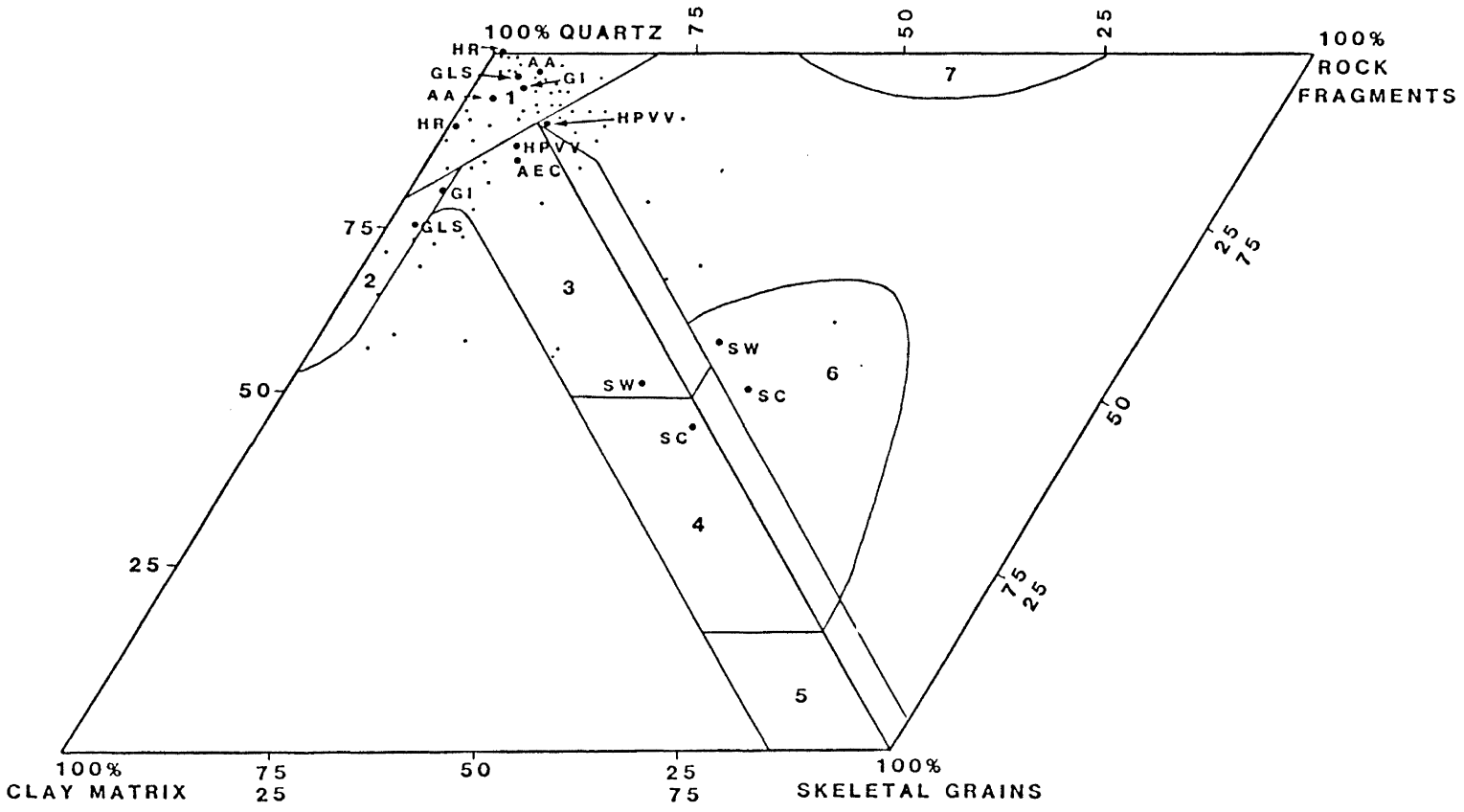
100% QUARTZ
75
50
25
100%
ROCK
FRAGMENTS
HR
AA
GLS
GI
AA
1
HR
HPVV
HPVV
AEC
GI
GLS
75
2
3
7
25
75
SW
6
50
SW
SC
SC
50
4
25
75
25
5
100%
CLAY MATRIX
75
25
50
25
75
100%
SKELETAL GRAINS

APPENDIX B

PETROLOG OF SAMPSON RESOURCES LAMAR #1

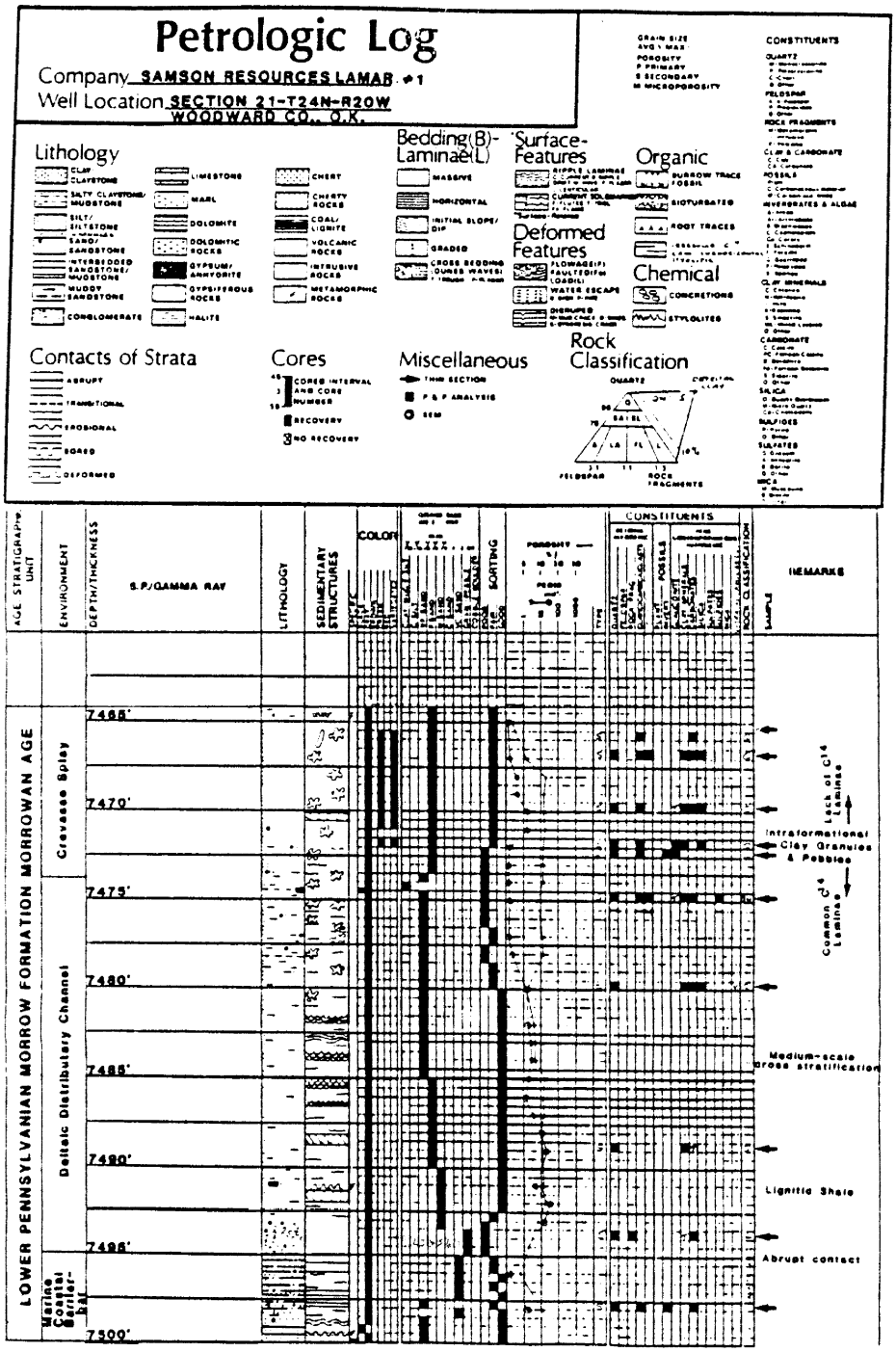
Petrologic Log
Company SAMSON RESOURCES LAMAR #1
Well Location SECTION 21-T24N-R20W
WOODWARD CO., O.K.
Lithology
Bedding(B)-Laminae(L)
Surface-Features
Organic
Deformed Features
Chemical
Contacts of Strata
Cores
Miscellaneous
Rock Classification
CONSTITUENTS
AGE STRATIGRAPHIC UNIT
ENVIRONMENT
DEPTH/THICKNESS
S.P./GAMMA RAY
LITHOLOGY
SEDIMENTARY STRUCTURES
COLOR
SORTING
POROSITY
REMARKS
LOWER PENNSYLVANIAN MORROW FORMATION MORROWAN AGE
Crevasse Splay
Deltaic Distributary Channel
Marine Coastal Barrier-Bar
7465'
7470'
7475'
7480'
7485'
7490'
7495'
7500'
Intraformational Clay Granules & Pebbles
Common Ci4 Lenses
Medium-scale cross stratification
Lignitic Shale
Abrupt contact

APPENDIX C

DATA TABLES

TABLE III

ISOTOPE DATA

Well Name	Depth	Mineral	Carbon ‰	Oxygen ‰	Dep.Env.
AA	7808	Siderite	-2.4	-2.2	Deltaic
AA	7808	Calcite	-3.3	-7.4	Deltaic
AB	7830	Calcite	-2.9	-7.2	SM-D
AB-A	14056	Dolomite	-4.2	-8.3	SM-D
AB-A	14056	Calcite	-3.8	-6.8	SM-D
AB-A/F	13852	Calcite	-3.2	-6.5	SM-D
AB-A/F	13852	Calcite	-5.7	-8.7	SM-D
AB-A/F	13852	Dolomite	-4.8	-10.2	SM-D
AEC	15013	Calcite	-9.4	-4.0	SM-D
AEC	14968	Calcite	-6.1	-7.8	SM-D
AEC	15013	Siderite	-6.4	-1.0	SM-D
EBB	9241	Dolomite	-2.8	-7.7	Sh.Mar.
ECD	12950	Calcite	-3.0	-7.3	Sh.Mar.
ECD	12950	Calcite	-3.1	-7.2	Sh.Mar.
ECML	10160	Calcite	-4.1	-6.9	Deltaic
ECML	10180	Siderite	-7.2	-1.1	Deltaic
ECMY	8761	Calcite	-3.2	-7.5	Sh.Mar.
ECMY	8756	Calcite	-3.6	-8.5	Sh.Mar.
ECMY	8763	Calcite	-3.3	-7.9	Sh.Mar.
ECMY	8773	Calcite	-0.7	-3.2	Sh.Mar.
ECMY	8754	Calcite	-0.6	-4.6	Sh.Mar.
ECMY	8811	Calcite	-4.7	-9.2	Sh.Mar.
ECMY	8766	Calcite	-3.3	-7.8	Sh.Mar.
ECMY	8752	Calcite	-4.0	-8.2	Sh.Mar.
ECMY/F	8735	Calcite	-2.4	-4.2	Sh.Mar.
EK	8810	Calcite	-5.5	-7.0	Sh.Mar.
EMG	8666	Siderite	-1.5	-1.6	Sh.Mar.
EMG	8666	Calcite	-3.0	-5.1	Sh.Mar.
GI	10911	Calcite	-3.1	-3.9	Deltaic
GI	10904	Calcite	-6.6	-8.3	Deltaic
GI/F	11275	Calcite	-7.7	-5.1	Deltaic
GLS	6981	Calcite	-3.2	-7.7	Sh.Mar.
GLS	7011	Calcite	-2.3	-6.5	Sh.Mar.
GLS	6990	Dolomite	-1.8	-5.9	Sh.Mar.
HMAS	17236	Calcite	-3.8	-6.4	Deltaic
HMAS	16727	Calcite	-7.7	-8.5	Deltaic
HP/F	12020	Calcite	-10.2	-8.9	SM-D
HPVV/F	14746	Calcite	-4.6	-7.2	Sh.Mar.
HPVV/F	14746	Calcite	-4.4	-7.2	Sh.Mar.
HR	14141	Calcite	-5.6	-9.9	Sh.Mar.
KSA	7071	Dolomite	-1.3	-5.6	SM-D
KSA	7203	Siderite	-5.4	-2.9	SM-D
KSA	7092	Siderite	-3.8	-3.1	SM-D
KSA	7071	Dolomite	-1.0	-5.2	SM-D
KSA	7080	Calcite	-4.3	-4.4	SM-D

TABLE III (Continued)

Well Name	Depth	Mineral	Carbon ‰	Oxygen ‰	Dep.Env.
KSA	7069	Dolomite	-4.2	-6.0	SM-D
KSA/F	7222	Dolomite	-5.9	-2.3	SM-D
KSA/F	7222	Calcite	-3.9	-4.9	SM-D
KSA/F	7116	Calcite	-5.0	-5.6	SM-D
KSC	7856	Siderite	-5.1	0.1	SM-D
KSC	7871	Calcite	-5.5	-8.3	SM-D
KSC	7868	Siderite	-4.3	-6.5	SM-D
KSC	7861	Siderite	-8.0	-9.0	SM-D
KSC/F	7898	Calcite	-3.5	-6.3	SM-D
LA	9186	Siderite	-2.9	-4.3	SM-D
LA	9186	Calcite	-3.0	-4.3	SM-D
MCB	13186	Calcite	-3.4	-8.5	Sh.Mar.
MWR	12899	Calcite	-4.1	-7.1	Deltaic
MWR/F	12771	Calcite	-7.1	-6.9	Deltaic
OA	9905	Calcite	-5.3	-8.8	Sh.Mar.
OM	10373	Calcite	-4.2	-8.7	Sh.Mar.
PCW	18962	Dolomite	-3.9	-9.4	Sh.Mar.
PCW	19001	Dolomite	-4.3	-10.3	Sh.Mar.
SB	8193	Calcite	-8.0	-13.7	SM-D
SB	8193	Dolomite	-4.5	-11.2	SM-D
SB	8197	Calcite	-4.6	-9.0	SM-D
SB	8174	Calcite	-2.2	-6.6	SM-D
SB	8189	Calcite	-6.1	-9.7	SM-D
SB	8197	Calcite	-4.6	-8.4	SM-D
SB	8236	Calcite	-6.5	-13.1	SM-D
SB	8174	Calcite	-2.3	-6.6	SM-D
SB/F	8243	Calcite	-1.8	-5.0	SM-D
SC/F	7901	Calcite	-2.5	-4.2	Sh.Mar.
SO	8163	Calcite	-1.8	-8.2	Sh.Mar.
SOK	8220	Calcite	0.6	-8.0	Sh.Mar.
SOK	8215	Calcite	-1.1	-6.6	Sh.Mar.
SOK	8217	Calcite	-2.4	-11.4	Sh.Mar.
SOK	8212	Calcite	-0.8	-5.5	Sh.Mar.
SOK	8258	Calcite	-1.9	-7.7	Sh.Mar.
SOK	8254	Calcite	-1.8	-8.0	Sh.Mar.
SOK/F	8234	Calcite	0.5	-5.5	Sh.Mar.
SRL	7466	Calcite	-2.4	-5.7	Deltaic
SRL/F	7466	Calcite	-5.7	-9.4	Deltaic
SRL/F	7466	Siderite	-5.1	-4.1	Deltaic
SS/F	6985	Calcite	-0.9	-5.0	Sh.Mar.
SUTS	9133	Calcite	-0.2	-2.1	Deltaic
SUTS	9253	Siderite	-4.0	-6.1	Deltaic
SUTS	9246	Siderite	3.0	-1.1	Deltaic
SUTS	9246	Calcite	-2.3	-7.0	Deltaic
SW/F	8128	Dolomite	-0.9	-5.3	Sh.Mar.
SW/F	8128	Calcite	-0.2	-7.0	Sh.Mar.

TABLE III (Continued)

Well Name	Depth	Mineral	Carbon ‰	Oxygen ‰	Dep.Env.
TMR	13357	Calcite	-10.3	-8.5	Sh.Mar.

* /F denotes samples containing > 5% fossils

TABLE IV

ORGANIC AND MARINE CARBON PERCENTAGES

Well Name	Depth	Carbon ‰	Oxygen ‰	%Org.Car.	%Mar.Car.
AA	7808	-2.4	-2.2	21.85	78.15
AA	7808	-3.3	-7.4	25.63	74.37
AB	7830	-2.9	-7.2	23.95	76.05
AB-A	14056	-4.2	-8.3	29.41	70.59
AB-A	14056	-3.8	-6.8	27.73	72.27
AB-A/F	13852	-3.2	-6.5	25.21	74.79
AB-A/F	13852	-5.7	-8.7	35.71	64.29
AB-A/F	13852	-4.8	-10.2	31.93	68.07
AEC	15013	-9.4	-4.0	51.26	48.74
AEC	14968	-6.1	-7.8	37.39	62.61
AEC	15013	-6.4	-1.0	38.66	61.34
EBB	9241	-2.8	-7.7	23.53	76.47
ECD	12950	-3.0	-7.3	24.37	75.63
ECD	12950	-3.1	-7.2	24.79	75.21
ECML	10160	-4.1	-6.9	28.99	71.01
ECML	10180	-7.2	-1.1	42.02	57.98
ECMY	8761	-3.2	-7.5	25.21	74.79
ECMY	8756	-3.6	-8.5	26.89	73.11
ECMY	8763	-3.3	-7.9	25.63	74.37
ECMY	8773	-0.7	-3.2	14.71	85.29
ECMY	8754	-0.6	-4.6	14.29	85.71
ECMY	8811	-4.7	-9.2	31.51	68.49
ECMY	8766	-3.3	-7.8	25.63	74.37
ECMY	8752	-4.0	-8.2	28.57	71.43
ECMY/F	8735	-2.4	-4.2	21.85	78.15
EK	8810	-5.5	-7.0	34.87	65.13
EMG	8666	-1.5	-1.6	18.07	81.93
EMG	8666	-3.0	-5.1	24.37	75.63
GI	10911	-3.1	-3.9	24.79	75.21
GI	10904	-6.6	-8.3	39.50	60.50
GI/F	11275	-7.7	-5.1	44.12	55.88
GLS	6981	-3.2	-7.7	25.21	74.79
GLS	7011	-2.3	-6.5	21.43	78.57
GLS	6990	-1.8	-5.9	19.33	80.67
HMAS	17236	-3.8	-6.4	27.73	72.27
HMAS	16727	-7.7	-8.5	44.12	55.88
HP/F	12020	-10.2	-8.9	54.62	45.38
HPVV/F	14746	-4.6	-7.2	31.09	68.91
HPVV/F	14746	-4.4	-7.2	30.25	69.75
HR	14141	-5.6	-9.9	35.29	64.71
KSA	7071	-1.3	-5.6	17.23	82.77
KSA	7203	-5.4	-2.9	34.45	65.55
KSA	7092	-3.8	-3.1	27.73	72.27
KSA	7071	-1.0	-5.2	15.97	84.03
KSA	7080	-4.3	-4.4	29.83	70.17

TABLE IV (Continued)

Well Name	Depth	Carbon ‰	Oxygen ‰	%Org.Car.	%Mar.Car.
KSA	7069	-4.2	-6.0	29.41	70.59
KSA/F	7222	-5.9	-2.3	36.55	63.45
KSA/F	7222	-3.9	-4.9	28.15	71.85
KSA/F	7116	-5.0	-5.6	32.77	67.23
KSC	7856	-5.1	0.1	33.19	66.81
KSC	7871	-5.5	-8.3	34.87	65.13
KSC	7868	-4.3	-6.5	29.83	70.17
KSC	7861	-8.0	-9.0	45.38	54.62
KSC/F	7898	-3.5	-6.3	26.47	73.53
LA	9186	-2.9	-4.3	23.95	76.05
LA	9186	-3.0	-4.3	24.37	75.63
MCB	13186	-3.4	-8.5	26.05	73.95
MWR	12899	-4.1	-7.1	28.99	71.01
MWR/F	12771	-7.1	-6.9	41.60	58.40
OA	9905	-5.3	-8.8	34.03	65.97
OM	10373	-4.2	-8.7	29.41	70.59
PCW	18962	-3.9	-9.4	28.15	71.85
PCW	19001	-4.3	-10.3	29.83	70.17
SB	8193	-8.0	-13.7	45.38	54.62
SB	8193	-4.5	-11.2	30.67	69.33
SB	8197	-4.6	-9.0	31.09	68.91
SB	8174	-2.2	-6.6	21.01	78.99
SB	8189	-6.1	-9.7	37.39	62.61
SB	8197	-4.6	-8.4	31.09	68.91
SB	8236	-6.5	-13.1	39.08	60.92
SB	8174	-2.3	-6.6	21.43	78.57
SB/F	8243	-1.8	-5.0	19.33	80.67
SC/F	7901	-2.5	-4.2	22.27	77.73
SO	8163	-1.8	-8.2	19.33	80.67
SOK	8220	0.6	-8.0	9.24	90.76
SOK	8215	-1.1	-6.6	16.39	83.61
SOK	8217	-2.4	-11.4	21.85	78.15
SOK	8212	-0.8	-5.5	15.13	84.87
SOK	8258	-1.9	-7.7	19.75	80.25
SOK	8254	-1.8	-8.0	19.33	80.67
SOK/F	8234	0.5	-5.5	9.66	90.34
SRL	7466	-2.4	-5.7	21.85	78.15
SRL/F	7466	-5.7	-9.4	35.71	64.29
SRL/F	7466	-5.1	-4.1	33.19	66.81
SS/F	6985	-0.9	-5.0	15.55	84.45
SUTS	9133	-0.2	-2.1	12.61	87.39
SUTS	9253	-4.0	-6.1	28.57	71.43
SUTS	9246	3.0	-1.1	0.00	100.00
SUTS	9246	-2.3	-7.0	21.43	78.57
SW/F	8128	-0.9	-5.3	15.55	84.45
SW/F	8128	-0.2	-7.0	12.61	87.39

TABLE IV (Continued)

Well Name	Depth	Carbon ‰	Oxygen ‰	%Org.Car.	%Mar.Car.
TMR	13357	-10.3	-8.5	55.04	44.96

* /F denotes samples containing > 5% fossils

TABLE V

VITRINITE REFLECTANCE VALUES

Well Name	Location	Depth	No.Obs.	%Ro
Texaco Carr	36-5N-11W	17016	20	1.59
Gulf Oil #1 Laverne State	13-26N-25W	6967	20	0.62
Sampson Resources Lamar #1	24N-20W	7463	28	0.91
E. L. Cox Miller #1	26-14N-10W	10157	20	1.46
Michigan-Wisconsin Raab #1	32-15N-17W	12800	40	1.77
Humphrey-Parker Venable-Verden	31-8N-8W	14991	20	1.24
Gulf Oil #1 Lillian Miller	14-6N-9W	16545	20	1.44
Petroleum Consultants Weatherly #1	3-12N-21W	18900	41	3.34
Shell Unit Test State 1-36	36-22N-22W	9300	40	1.24
Humble Annie Schmidt #1	20-8N-17W	16500	40	1.62
Humble Oil Kephart #1	20-18N-12W	8515	22	0.95
Hall Jones Oil DeMoss A-1	7-18N-12W	8454	21	0.87
Pan-American Winters #1	4-17N-12W	8627	20	0.72
Ladd Paul Willis A-5	25-18N-14W	9050	27	1.01
Cities Service #D-1 McClung	15-16N-25W	6815	81	0.84

TABLE V (Continued)

Well Name	Location	Depth	No.Obs.	%Ro
Pan Am Fox #C-1	16-23N-25W	8255	62	0.89
Harper Oil Burt #1	30-20N-24W	10160	48	0.78
Texas Pacific Shrewder #1	23-18N-23W	11150	45	0.98
Inexco Oil Kendall #1	14-15N-24W	13685	42	1.31
Dyco Petr. Baker #1-20	20-12N-23W	17240	117	2.02
Natomas Austin #1	27-11N-24W	18350	52	2.13
Continental C.H. Case #1	19-20N-16W	8180	42	0.66
Amerada Thomsen Unit #1	24-18N-18W	9850	40	0.87
Longhorn Cline #1	34-16N-18W	11375	43	0.96
An-Son Fransen #1-26	26-14N-19W	14020	47	1.26
Apache Deal #1-14	14-12N-21W	16812	55	1.97
G.H.K.-Apache Russell #1-15	5-11N-21W	17735	60	2.06
Harper Oil D.C. Gurthie #1	2-22N-20W	7835	47	0.71
Clark Canadian Viersen #1	8-15N-22W	13365	50	1.26

TABLE VI

VALUES USED IN CLAY AND CARBONATE MAPS

Well Name	Kaolinite %	Illite %	Chlorite %	Carb. %
GLS	0.5	1.6	7.0	6.5
SS	0	0	1.0	10.0
KSA	5.1	0.4	0.1	7.5
SOK	0.8	3.5	1.0	17.0
SW	0	0	0.1	13.0
SOH	0.2	1.7	3.7	4.2
KSC	5.8	0.4	2.2	12.0
GVE	3.3	0.8	1.2	8.2
SRL	3.0	0.3	3.2	3.1
SB	3.7	0.5	2.5	8.6
AB	1.2	0	6.6	11.0
AA	4.6	0.2	2.4	5.0
SUTS	1.1	0.6	3.1	7.4
ECMY	2.4	1.1	1.0	13.0
EK	0.5	0	7	9.0
EP	0	0	3.0	17.0
EB	0	0.5	7.6	10.0
EBB	3.0	0	3.1	8.1
EMG	2.1	0.3	5.9	11.0
SC	0	2.6	0.1	26.0
OA	5.8	1.1	4.4	9.7
OM	1.1	1.8	2.1	11.0
LA	0	3.0	4.0	9.5

TABLE VI (Continued)

Well Name	Kaolinite %	Illite %	Chlorite %	Carb. %
MCB	0.1	0.6	5.6	5.3
MWR	1.4	0.2	3.7	16.0
PCW	0.8	2.1	4.6	5.3
ECML	5.7	0	2.9	6.5
AB-A	0.6	0	6.3	8.1
PC	0	0	3.5	6.0
HMAS	3.2	1.2	6.2	3.6
ECD	0.3	0.5	1.1	27.0
MWS	1.6	0.1	2.4	32.0
TS	4.6	1.5	3.4	9.2
TM	0	0.8	7.8	16.0
TWL	0	2.0	4.6	9.8
TGR	0.8	0	4.8	12.0
TMR	1.0	0.3	4.0	17.0
HPVV	0	0	8.1	6.3
AP	2.2	0	6.3	9.1
HR	1.4	0	11.0	2.8
GM	1.1	0.5	7.1	5.6
TC	1.4	0	5.8	7.8
AEC	1.8	0	4.8	11.0
HP	2.5	0	5.7	3.6
GI	0.5	1.0	4.0	6.0
MDL	5.5	0	3.0	7.0

APPENDIX D

FACTOR ANALYSIS RESULTS AND OTHER WORK

```
1          SAS(R) LOG   OS SAS 5 08          VS2/MVS JOB U10063AA STEP SAS                    12:40 WEDNESDAY, FEBRUARY 5, 1986

NOTE  COPYRIGHT (C) 1984 SAS INSTITUTE INC , CARY, N C   27511, U S A
NOTE  THE JOB U10063AA HAS BEEN RUN UNDER RELEASE 5 08 OF SAS AT OKLAHOMA STATE UNIVERSITY (0135-4001)

NOTE  CPUID    VERSION = 23  SERIAL = 021194  MODEL = 3081
      CPUID    VERSION = 23  SERIAL = 221194  MODEL = 3081

NOTE  SAS OPTIONS SPECIFIED ARE:
       SORT=4

1           DATA WALKER;                                                          00070000
2           INFILE PATTY;                                                         00080000
3           INPUT SAMPLE $ 1-10 SAMPLEL $ 11 QUARTZ 13-15 FELDSPAR 17-18          00090000
4              CALCITE 20-21 FERRODOL 23-24 SIDERITE 26-27 PYRITE 29-30           00100000
5              KAOLINTE 32-33 CHLORITE 35-36 ILLITE 38-39 ILL_SMEC 41-42          00110000
6              DEPTH 44-48 POROSITY 50-51 CARBON_I 53-57 OXYGEN_I 59-63           00120000
7              VITRREFL 65-68 DEP_ENV 70;                                         00130000


NOTE: INFILE PATTY IS:
      DSNAME=U11236A.PWALKER2.DATA,
      UNIT=STORAGE,VOL=SER=OSU000,DISP=SHR,
      DCB=(BLKSIZE=7440,LRECL=80,RECFM=FB)

NOTE: 91 LINES WERE READ FROM INFILE PATTY
NOTE: DATA SET WORK.WALKER HAS 91 OBSERVATIONS AND 18 VARIABLES.  133 OBS/TRK.
NOTE: THE DATA STATEMENT USED 0.10 SECONDS AND 552K.

8           PROC PRINT;                                                           00131003
NOTE: THE PROCEDURE PRINT USED 0.20 SECONDS AND 740K AND PRINTED PAGES 1 TO 2.

9           PROC FACTOR OUTSTAT=FACTORS METHOD=PRIN MINEIGEN=1 ROTATE=VARIMAX      00140001
10             SIMPLE CORR SCREE  SCORE;                                          00150001
NOTE: THE DATA SET WORK.FACTORS HAS 46 OBSERVATIONS AND 18 VARIABLES.  128 OBS/TRK.
NOTE: THE PROCEDURE FACTOR USED 0.26 SECONDS AND 860K AND PRINTED PAGES 3 TO 8.

11          PROC SCORE DATA=WALKER SCORE=FACTORS OUT=SCORES;                       00151004
NOTE: THE DATA SET WORK.SCORES HAS 91 OBSERVATIONS AND 24 VARIABLES.  99 OBS/TRK.
NOTE: THE PROCEDURE SCORE USED 0.14 SECONDS AND 736K

12          PROC PRINT DATA=SCORES; VAR FACTOR1-FACTOR6;                          00152004
13          TITLE 'DATA WERE STANDARDIZED BEFORE SCORING';                        00153004
NOTE: THE PROCEDURE PRINT USED 0.13 SECONDS AND 732K AND PRINTED PAGES 9 TO 10.

14          PROC SCORE DATA=WALKER SCORE=FACTORS OUT=SCOREN;                       00154004
NOTE: THE DATA SET WORK.SCOREN HAS 91 OBSERVATIONS AND 24 VARIABLES.  99 OBS/TRK.
NOTE: THE PROCEDURE SCORE USED 0.14 SECONDS AND 736K.

15          PROC PRINT DATA=SCOREN; VAR FACTOR1-FACTOR6;                          00155004
16          TITLE 'DATA WERE NOT STANDARDIZED BEFORE SCORING';                    00156004
NOTE: THE PROCEDURE PRINT USED 0.14 SECONDS AND 732K AND PRINTED PAGES 11 TO 12.
NOTE: SAS USED 860K MEMORY.

NOTE: SAS INSTITUTE INC.
      SAS CIRCLE
      PO BOX 8000
      CARY, N C.  27511-8000
```

OBS	SAMPLE	SAMPLE	QUARTZ	FELDSPAR	CALCITE	FERROOLITE	SIDERITE	PYRITE	KAOLINITE	CHLORITE	ILLITE	ILLSMEC	DEPTH	POROSITY	CARBON	OXYGEN	VITREFL	DEPENV
1	AA #2	S	89	0.5	5.0	1.0	3.0	0.6	1.0	3.0	0.1	0.1	7808	1	-2.4	-2.2	1.01	1
2	AA #2	C	89	0.5	5.0	1.0	3.0	0.6	1.0	3.0	0.1	0.1	7808	1	-3.3	-7.4	1.01	1
3	AB #1	C	83	0.1	6.0	1.0	3.0	2.0	0.1	7.0	2.0	0.1	7830	6	-2.9	-7.2	1.10	2
4	AB-A	C	98	0.5	0.1	2.0	3.0	0.1	1.0	0.1	0.1	0.1	14056	12	-3.8	-6.8	2.40	2
5	AB-A/F #1	C	89	0.5	3.0	2.0	3.0	0.6	0.1	3.0	0.1	0.1	13852	10	-3.2	-6.5	2.40	1
6	AB-A/F #1	C	89	0.5	3.0	2.0	3.0	0.6	0.1	3.0	0.1	0.1	13852	10	-5.7	-9.7	2.40	1
7	AB-A/F #1	D	89	0.5	3.0	2.0	3.0	0.6	0.1	3.0	0.1	0.1	13852	10	-4.8	-10.2	2.40	1
8	AEC #2	C	74	1.0	5.0	5.0	10.0	2.0	1.0	3.0	0.5	0.1	15013	0	-9.4	-4.0	0.97	1
9	AEC #1	C	83	0.5	16.0	1.0	3.0	0.6	1.0	1.0	0.5	0.1	14968	2	-6.1	-7.8	0.97	2
10	AEC #2	S	74	1.0	5.0	5.0	10.0	2.0	1.0	3.0	0.5	0.1	15013	0	-6.4	-1.0	0.97	1
11	EBB	D	93	0.1	0.1	0.1	0.1	2.0	1.0	4.0	0.1	0.1	9241	2	-2.8	-7.7	1.20	2
12	ECD	C	89	0.5	4.0	1.0	0.1	0.1	1.0	7.0	0.5	0.1	12950	1	-3.0	-7.3	1.40	2
13	ECD	C	89	0.5	4.0	1.0	0.1	0.1	1.0	7.0	0.5	0.1	12950	1	-3.1	-7.2	1.40	2
14	ECMIL	C	92	0.1	1.0	2.0	3.0	0.6	4.0	1.0	0.1	0.1	10160	7	-4.1	-6.9	1.46	1
15	ECML #2	S	65	0.5	7.0	1.0	28.0	0.6	3.0	4.0	0.1	0.1	10180	3	-7.2	-1.1	1.46	1
16	ECMY #4	C	70	1.0	20.0	1.0	3.0	3.0	1.0	6.0	0.1	0.1	8761	12	-3.2	-7.5	1.00	2
17	ECMY #3	C	89	0.1	6.0	1.0	3.0	0.6	1.0	5.0	0.1	0.1	8756	7	-3.6	-8.5	1.00	2
18	ECMY #5	C	95	1.0	1.0	1.0	3.0	0.6	1.0	3.0	0.5	0.1	8763	5	-3.3	-7.9	1.00	2
19	ECMY	C	92	1.0	3.0	1.0	3.0	0.6	0.1	4.0	0.1	0.1	8773	19	-0.7	-3.2	1.00	2
20	ECMY #2	C	82	0.1	2.0	1.0	2.0	4.0	1.0	5.0	3.0	2.0	8754	6	-0.6	-4.6	1.00	2
21	ECMY #8	C	97	0.5	1.0	2.0	3.0	0.1	0.1	0.1	0.5	0.1	8811	5	-4.7	-9.2	1.00	2
22	ECMY #6	C	89	0.1	3.0	1.0	0.1	2.0	1.0	6.0	0.1	0.1	8766	2	-3.3	-7.8	1.00	2
23	ECMY #1	C	79	0.1	10.0	1.0	3.0	2.0	1.0	7.0	2.0	0.1	8752	1	-4.0	-8.2	1.00	2
24	ECMY/F #1	C	53	0.1	4.0	1.0	10.0	0.1	1.0	7.0	18.0	7.0	8735	0	-2.4	-4.2	1.00	2
25	EK #1	C	89	0.1	2.0	1.0	3.0	0.6	1.0	6.0	0.5	0.1	8810	20	-5.5	-7.0	1.00	2
26	EMG #1	S	46	0.1	2.0	1.0	50.0	0.6	1.0	2.0	0.1	0.1	8666	2	-1.5	-1.6	0.60	2
27	EMG #1	C	46	0.1	2.0	1.0	50.0	0.6	1.0	2.0	0.1	0.1	8666	2	-3.0	-5.1	0.60	2
28	GI	C	94	1.0	2.0	0.1	3.0	0.1	1.0	3.0	0.1	0.1	10911	8	-3.1	-3.9	0.60	1
29	GI #2	C	96	2.0	0.1	1.0	3.0	0.6	1.0	2.0	0.5	0.1	10904	3	-6.6	-8.3	0.60	1
30	GI/F #1	C	85	0.5	4.0	4.0	3.0	0.6	1.0	4.0	0.5	0.1	11275	22	-7.7	-5.1	0.60	1
31	GLS #2	C	92	2.0	1.0	1.0	3.0	0.6	1.0	3.0	2.0	0.1	6981	20	-3.2	-7.7	0.62	2
32	GLS #4	C	100	0.5	0.1	0.1	3.0	0.6	0.1	0.1	0.5	0.1	7011	23	-2.3	-6.5	0.62	2
33	GLS #3	D	96	0.5	7.0	1.0	3.0	0.1	1.0	3.0	0.5	0.1	6990	22	-1.8	-5.9	0.62	2
34	HMAS	C	98	0.1	2.0	1.0	3.0	0.1	0.1	0.1	0.5	0.1	17236	3	-3.8	-6.4	1.62	1
35	HMAS	C	100	0.1	0.1	1.0	3.0	0.6	1.0	0.1	0.5	0.1	16727	8	-7.7	-8.5	1.62	1
36	HP/F #1	C	86	0.1	2.0	5.0	3.0	0.6	0.1	7.0	0.1	0.1	12020	12	-10.2	-8.9	0.80	2
37	HPVU/F #1	C	93	0.1	1.0	0.1	2.0	0.6	1.0	4.0	0.5	0.1	14746	10	-4.6	-7.2	1.24	2
38	HPVU/F #1	C	93	0.1	1.0	0.1	2.0	0.6	1.0	4.0	0.5	0.1	14746	10	-4.4	-7.2	1.24	2
39	HR	C	94	0.5	2.0	1.0	3.0	2.0	0.1	2.0	0.1	0.1	14141	7	-5.6	-8.9	0.60	2
40	KSA #2	D	100	0.5	7.0	0.1	3.0	0.6	0.1	0.1	0.1	0.1	7071	9	-1.3	-5.6	0.80	2
41	KSA #7	S	92	0.1	7.0	1.0	4.0	0.6	2.0	2.0	0.1	0.1	7203	17	-5.4	-2.9	0.80	1
42	KSA	S	85	0.1	7.0	1.0	13.0	0.6	1.0	2.0	0.1	0.1	7092	2	-3.8	-3.1	0.80	2
43	KSA #2	D	100	0.5	7.0	0.1	3.0	0.6	0.1	0.1	0.1	0.1	7071	9	-1.0	-5.2	0.80	2
44	KSA	C	91	0.5	7.0	2.0	0.1	0.1	1.0	4.0	2.0	0.1	7080	6	-4.3	-4.4	0.80	2
45	KSA #1	D	91	0.5	7.0	3.0	4.0	0.6	1.0	2.0	0.5	0.1	7069	7	-4.2	-6.0	0.80	2
46	KSA/F #2	D	59	0.5	25.0	3.0	7.0	0.6	3.0	3.0	0.5	0.1	7222	22	-5.9	-2.3	0.80	1
47	KSA/F #2	C	59	0.5	25.0	3.0	7.0	0.6	3.0	3.0	0.5	0.1	7222	22	-3.9	-1.9	0.80	1

OBS	SAMPLE	SAMPLE	QUARTZ	FELDSPAR	CALCITE	FERROOL	SIDERITE	PYRITE	KAOLINITE	CHLORITE	ILLITE	ILL_SMEC	DEPTH	POROSITY	CARBON	OXYGEN	VITRREF	DEP_ENV
48	KSA/F #1	C	86	0.1	2.0	2.0	5.0	0.1	2.0	3.0	0.5	0.1	7116	19	-5.0	-5.6	0.80	2
49	KSC	S	65	0.1	7.0	0.1	30.0	0.6	3.0	2.0	0.1	0.1	7856	7	-5.1	0.1	1.01	1
50	KSC #6	C	79	1.0	7.0	2.0	3.0	3.0	1.0	8.0	0.5	0.1	7871	1	-5.5	-8.3	1.01	2
51	KSC	S	90	0.1	7.0	0.1	2.0	0.1	6.0	2.0	0.1	0.1	7868	25	-4.3	-6.5	1.01	1
52	KSC #4	S	94	0.1	7.0	1.0	0.1	6.0	3.0	3.0	0.5	0.1	7861	7	-8.0	-9.0	1.01	1
53	KSC/F #1	C	57	0.1	3.0	27.0	7.0	4.0	1.0	2.0	0.5	0.1	7898	7	-3.5	-6.3	1.01	2
54	LA #1	S	88	2.0	2.0	1.0	2.0	2.0	1.0	4.0	0.1	0.1	9186	5	-2.9	-4.3	1.01	2
55	LA #1	C	88	2.0	2.0	1.0	2.0	2.0	1.0	4.0	0.1	0.1	9186	5	-3.0	-4.3	1.01	2
56	MCB #2	C	93	0.1	7.0	1.0	3.0	0.6	1.0	0.1	0.5	0.1	13186	2	-3.4	-8.5	0.75	2
57	MWR #1	C	94	0.5	4.0	0.1	3.0	0.6	1.0	2.0	0.5	0.1	12899	1	-4.1	-7.1	1.77	1
58	MWR/F #1	C	92	0.5	1.0	2.0	3.0	0.1	1.0	5.0	0.5	0.1	12771	2	-7.1	-6.9	1.77	1
59	OA #1	C	91	0.1	3.0	1.0	3.0	0.6	1.0	5.0	0.1	0.1	9905	4	-5.3	-8.8	1.50	2
60	OM	C	89	2.0	4.0	1.0	3.0	0.6	0.1	5.0	0.1	0.1	10373	2	-4.2	-8.7	1.00	2
61	PCW #3	D	94	0.5	7.0	2.0	3.0	0.1	1.0	4.0	0.5	0.1	18962	1	-3.9	-9.4	3.34	2
62	PCW #4	D	92	0.5	7.0	2.0	3.0	2.0	1.0	4.0	0.5	0.1	19001	1	-4.3	-10.3	3.34	2
63	SB #3	C	93	0.5	3.0	1.0	3.0	0.6	1.0	4.0	0.5	0.1	8193	3	-8.0	-13.7	1.10	1
64	SB #3	D	93	0.5	3.0	1.0	3.0	0.6	1.0	4.0	0.5	0.1	8193	3	-4.5	-11.2	1.10	1
65	SB #4	C	94	0.5	3.0	1.0	3.0	0.6	1.0	3.0	0.5	0.1	8197	3	-4.6	-9.0	1.10	1
66	SB	C	81	2.0	2.0	4.0	3.0	2.0	1.0	6.0	2.0	0.1	8174	3	-2.2	-6.6	1.10	2
67	SB #2	C	93	0.5	0.1	0.1	3.0	0.6	1.0	7.0	0.5	0.1	8189	4	-6.1	-9.7	1.10	1
68	SB #4	C	94	0.5	3.0	1.0	3.0	0.6	1.0	3.0	0.5	0.1	8197	3	-4.6	-8.4	1.10	1
69	SB #5	C	91	1.0	4.0	1.0	3.0	0.6	1.0	4.0	0.5	0.1	8236	2	-6.5	-13.1	1.10	2
70	SB	C	81	2.0	2.0	4.0	3.0	2.0	1.0	6.0	2.0	0.1	8174	3	-2.3	-6.6	1.10	2
71	SB/F #1	C	35	0.5	54.0	2.0	4.0	2.0	1.0	3.0	0.1	0.1	8243	0	-1.8	-5.0	1.10	2
72	SC/F	C	25	0.5	65.0	2.0	6.0	0.6	1.0	1.0	0.5	0.1	7901	1	-2.5	-4.2	0.30	2
73	SD	C	89	0.1	6.0	1.0	3.0	0.6	1.0	4.0	0.5	0.1	8163	5	-1.8	-8.2	0.90	2
74	SOK #4	C	89	2.0	6.0	0.1	3.0	1.0	1.0	2.0	0.5	0.1	8220	1	0.6	-8.0	0.60	2
75	SOK	C	88	0.1	2.0	1.0	0.1	3.0	1.0	5.0	2.0	0.1	8215	1	-1.1	-6.6	0.60	2
76	SOK #3	C	85	2.0	1.0	1.0	3.0	2.0	0.1	5.0	5.0	0.1	8217	1	-2.4	-11.4	0.60	2
77	SOK #1	C	76	2.0	3.0	1.0	3.0	5.0	1.0	6.0	5.0	3.0	8212	1	-0.8	-5.5	0.60	2
78	SOK #7	C	89	2.0	3.0	0.1	0.1	0.1	1.0	6.0	0.1	0.1	8258	1	1.9	-7.7	0.60	2
79	SOK #6	C	84	2.0	8.0	1.0	1.0	0.6	1.0	5.0	0.5	0.1	8254	1	-1.8	-8.0	0.60	2
80	SOK/F #1	C	15	2.0	75.0	7.0	3.0	0.6	1.0	1.0	0.5	0.1	8234	0	0.5	-5.5	0.60	2
81	SRL	C	82	0.1	8.0	1.0	3.0	0.6	2.0	5.0	0.1	0.1	7466	1	-2.4	-5.7	0.91	1
82	SRL/F	C	82	0.1	8.0	1.0	3.0	0.6	2.0	5.0	0.1	0.1	7466	1	-5.7	-9.4	0.91	1
83	SRL/F	S	82	0.1	8.0	1.0	3.0	0.6	2.0	5.0	0.1	0.1	7466	1	-5.1	-4.1	0.91	1
84	SSI/F #1	C	42	0.5	48.0	1.0	3.0	3.0	0.1	6.0	0.1	0.1	6985	1	-0.9	-5.0	0.70	2
85	SUTS	C	83	0.1	6.0	1.0	3.0	2.0	0.1	6.0	2.0	1.0	9133	1	-0.2	-2.1	1.24	1
86	SUTS #3	S	89	0.5	4.0	1.0	4.0	0.6	0.1	3.0	0.5	0.1	9253	1	-4.0	-6.1	1.24	1
87	SUTS #2	S	88	0.5	2.0	1.0	7.0	0.6	0.1	3.0	0.1	0.1	9246	0	3.0	-1.1	1.24	1
88	SUTS #2	C	88	0.5	2.0	1.0	7.0	0.6	0.1	3.0	0.1	0.1	9246	0	-2.3	-7.0	1.24	1
89	SW/F #1	D	53	2.0	36.0	7.0	3.0	0.6	1.0	2.0	0.5	0.1	8128	0	0.9	-5.3	0.70	2
90	SW/F #1	C	53	2.0	36.0	7.0	3.0	0.6	1.0	2.0	0.5	0.1	8128	0	-0.2	-7.0	0.70	2
91	TMR #1	C	90	1.0	4.0	1.0	3.0	0.6	1.0	5.0	0.5	0.1	13357	0	-10.3	-8.5	1.30	2

MEANS AND STANDARD DEVIATIONS FROM 91 OBSERVATIONS

	QUARTZ	FELDSPAR	CALCITE	FERRODOL	SIDERITE	PYRITE	KAOLINTE	CHLORITE
MEAN	82.8022	0.66044	7.83077	1.80549	4.92088	1.04615	1.06484	3.59121
STD DEV	16.89	0.655045	13.2043	3.04866	8.06743	1.10366	0.90681	1.96207

	ILLITE	ILL_SMEC	DEPTH	POROSITY	CARBON_I	OXYGEN_I	VITRREFL	DEP_ENV
MEAN	0.792308	0.238462	9786.23	5.71429	-3.79341	-6.58571	1.08418	1.62637
STD DEV	2.0248	0.807571	2927.09	6.58498	2.35664	2.59823	0.5317	0.486446

CORRELATIONS

	QUARTZ	FELDSPAR	CALCITE	FERRODOL	SIDERITE	PYRITE	KAOLINTE	CHLORITE
QUARTZ	1.00000	-0.11942	-0.79633	-0.36513	-0.43631	-0.15698	-0.12147	-0.00676
FELDSPAR	-0.11942	1.00000	0.16692	0.08118	-0.17484	0.09446	-0.17689	0.07131
CALCITE	-0.79633	0.16692	1.00000	0.19109	-0.02797	0.04701	0.06617	-0.14683
FERRODOL	-0.36513	0.08118	0.19109	1.00000	0.01081	0.25502	-0.01536	-0.10347
SIDERITE	-0.43631	-0.17484	-0.02797	0.01081	1.00000	-0.09800	0.14090	-0.17868
PYRITE	-0.15698	0.09446	0.04701	0.25502	-0.09800	1.00000	-0.01257	0.27578
KAOLINTE	-0.12147	-0.17689	0.06617	-0.01536	0.14090	-0.01257	1.00000	-0.07892
CHLORITE	-0.00676	0.07131	-0.14683	-0.10347	-0.17868	0.27578	-0.07892	1.00000
ILLITE	-0.16847	0.04174	-0.06790	-0.02233	-0.00103	0.11362	-0.06387	0.29549
ILL_SMEC	-0.18468	-0.03259	-0.05540	-0.04580	0.03786	0.14222	-0.02468	0.24789
DEPTH	0.25300	-0.11699	-0.20273	-0.02380	-0.07225	-0.13237	-0.18877	-0.11630
POROSITY	0.19849	-0.18065	-0.12482	-0.00933	-0.07964	-0.16879	0.29248	-0.19464
CARBON_I	-0.25207	0.24496	0.27257	-0.01467	-0.00682	0.08165	-0.22741	-0.05699
OXYGEN_I	-0.39281	-0.08107	0.18921	0.06567	0.42582	0.00271	0.18234	-0.15030
VITRREFL	0.29034	-0.21853	-0.22242	-0.02647	-0.11631	-0.11000	-0.06906	0.01547
DEP_ENV	-0.15380	0.23903	0.15213	0.08906	-0.04188	0.15665	-0.31727	0.16183

	ILLITE	ILL_SMEC	DEPTH	POROSITY	CARBON_I	OXYGEN_I	VITRREFL	DEP_ENV
QUARTZ	-0.16847	-0.18468	0.25300	0.19849	-0.25207	-0.39281	0.29034	-0.15380
FELDSPAR	0.04174	-0.03259	-0.11699	-0.18065	0.24496	-0.08107	-0.21853	0.23903
CALCITE	-0.06790	-0.05540	-0.20273	-0.12482	0.27257	0.18921	-0.22242	0.15213
FERRODOL	-0.02233	-0.04580	-0.02380	-0.00933	-0.01467	0.06567	-0.02647	0.08906
SIDERITE	-0.00103	0.03786	-0.07225	-0.07964	-0.00682	0.42582	-0.11631	-0.04188
PYRITE	0.11362	0.14222	-0.13237	-0.16879	0.08165	0.00271	-0.11000	0.15665
KAOLINTE	-0.06387	-0.02468	-0.18877	0.29248	-0.22741	0.18234	-0.06906	-0.31727
CHLORITE	0.29549	0.24789	-0.11630	-0.19464	-0.05699	-0.15030	0.01547	0.16183
ILLITE	1.00000	0.92560	-0.09394	-0.12775	0.14592	0.04839	-0.08479	0.16739
ILL_SMEC	0.92560	1.00000	-0.06754	-0.11868	0.16112	0.14520	-0.05187	0.10770
DEPTH	-0.09394	-0.06754	1.00000	-0.13420	-0.36268	-0.19319	0.68425	-0.10149
POROSITY	-0.12775	-0.11868	-0.13420	1.00000	-0.15267	0.10649	-0.08417	-0.05451
CARBON_I	0.14592	0.16112	-0.36268	-0.15267	1.00000	0.29472	-0.18882	0.33656
OXYGEN_I	0.04839	0.14520	-0.19319	0.10649	0.29472	1.00000	-0.24752	-0.14694
VITRREFL	-0.08479	-0.05187	0.68425	-0.08417	-0.18882	-0.24752	1.00000	-0.18979
DEP_ENV	0.16739	0.10770	-0.10149	-0.05451	0.33656	-0.14694	-0.18979	1.00000

INITIAL FACTOR METHOD: PRINCIPAL COMPONENTS

PRIOR COMMUNALITY ESTIMATES: ONE

EIGENVALUES OF THE CORRELATION MATRIX: TOTAL = 16 AVERAGE = 1

	1	2	3	4	5	6	7	8
EIGENVALUE	3.081975	2.308755	1.851556	1.541204	1.301641	1.010066	0.955985	0.824349
DIFFERENCE	0.773219	0.457199	0.310353	0.239563	0.291575	0.054081	0.131636	0.038753
PROPORTION	0.1926	0.1443	0.1157	0.0963	0.0814	0.0631	0.0597	0.0515
CUMULATIVE	0.1926	0.3369	0.4526	0.5490	0.6303	0.6934	0.7532	0.8047

	9	10	11	12	13	14	15	16
EIGENVALUE	0.785596	0.652139	0.577116	0.514074	0.355739	0.166305	0.062629	0.010871
DIFFERENCE	0.133457	0.075023	0.063042	0.158334	0.189434	0.103676	0.051759	
PROPORTION	0.0491	0.0408	0.0361	0.0321	0.0222	0.0104	0.0039	0.0007
CUMULATIVE	0.8538	0.8946	0.9306	0.9628	0.9850	0.9954	0.9993	1.0000

6 FACTORS WILL BE RETAINED BY THE MINEIGEN CRITERION

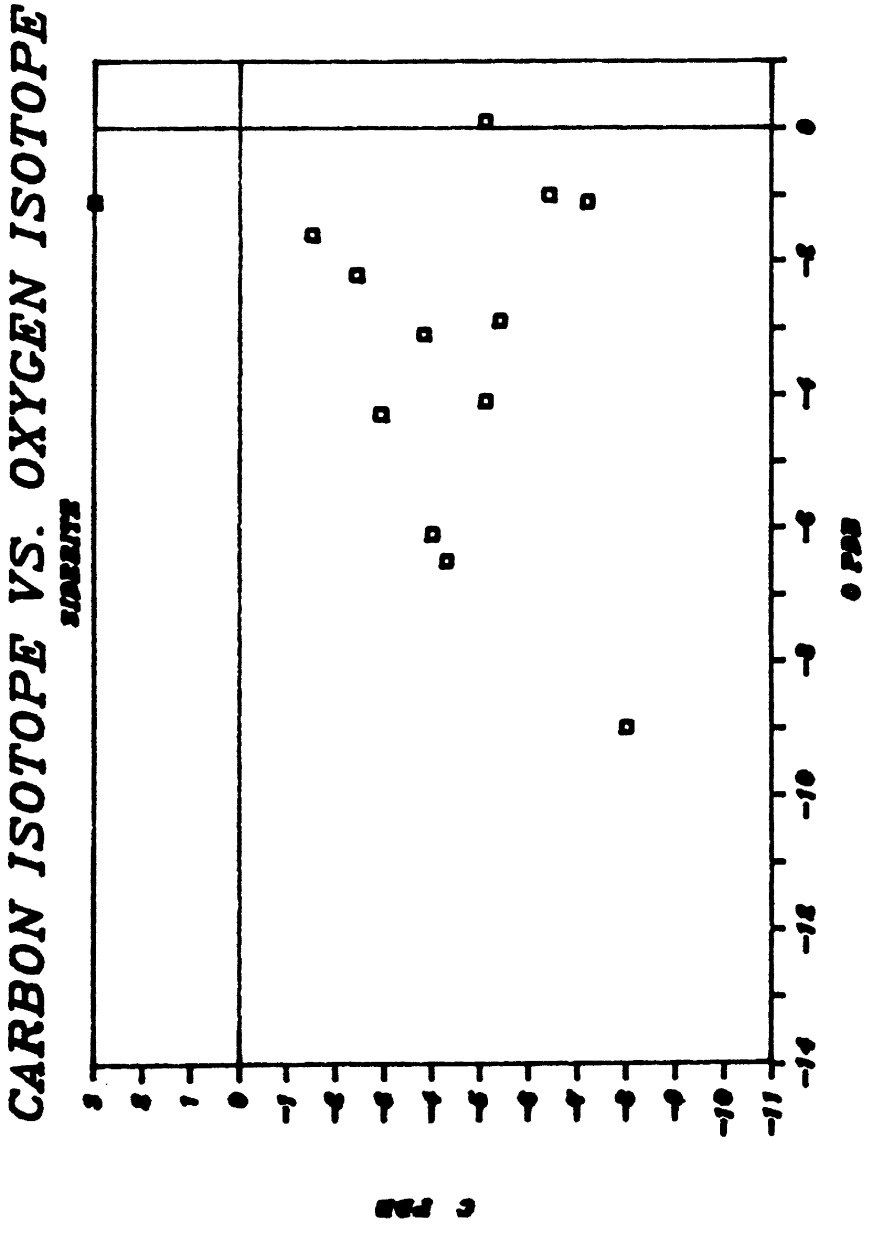
CARBON ISOTOPE VS. OXYGEN ISOTOPE

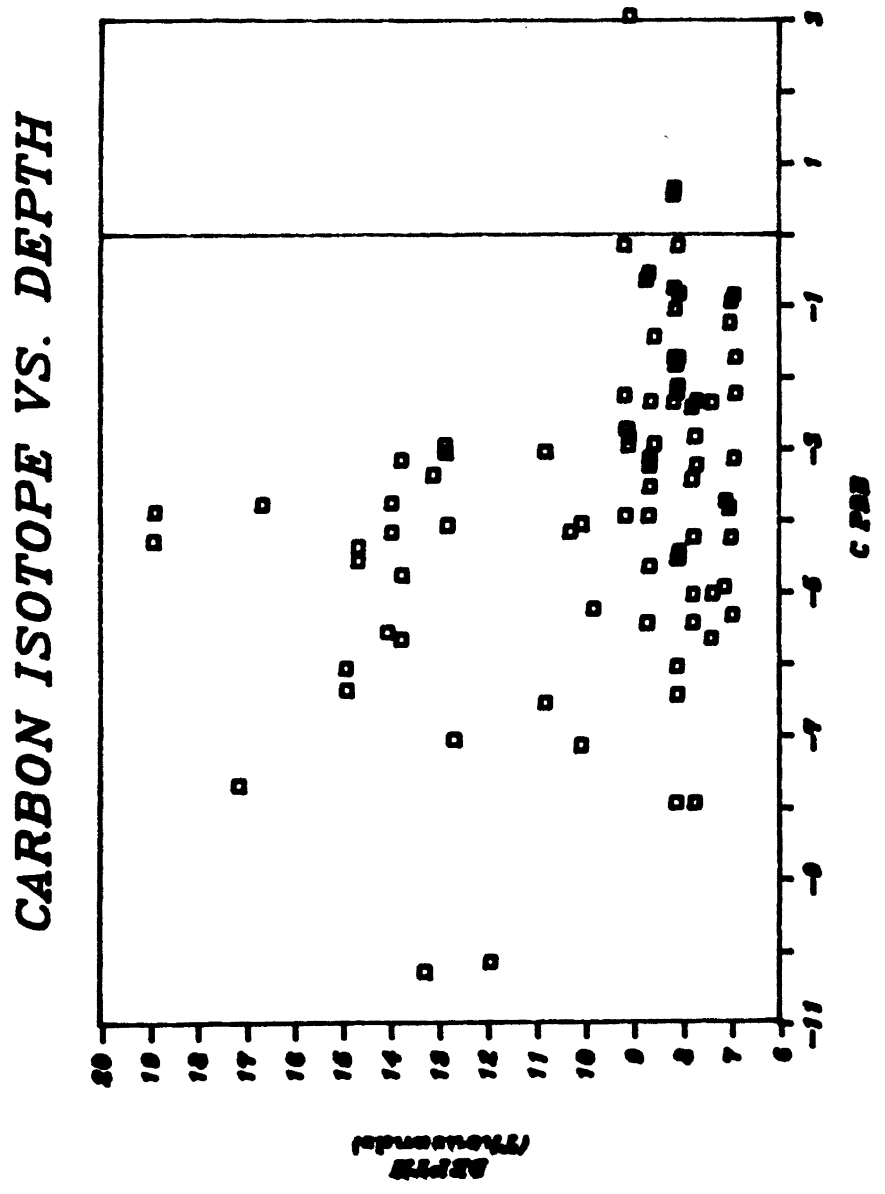
CARBON ISOTOPE VS. DEPTH

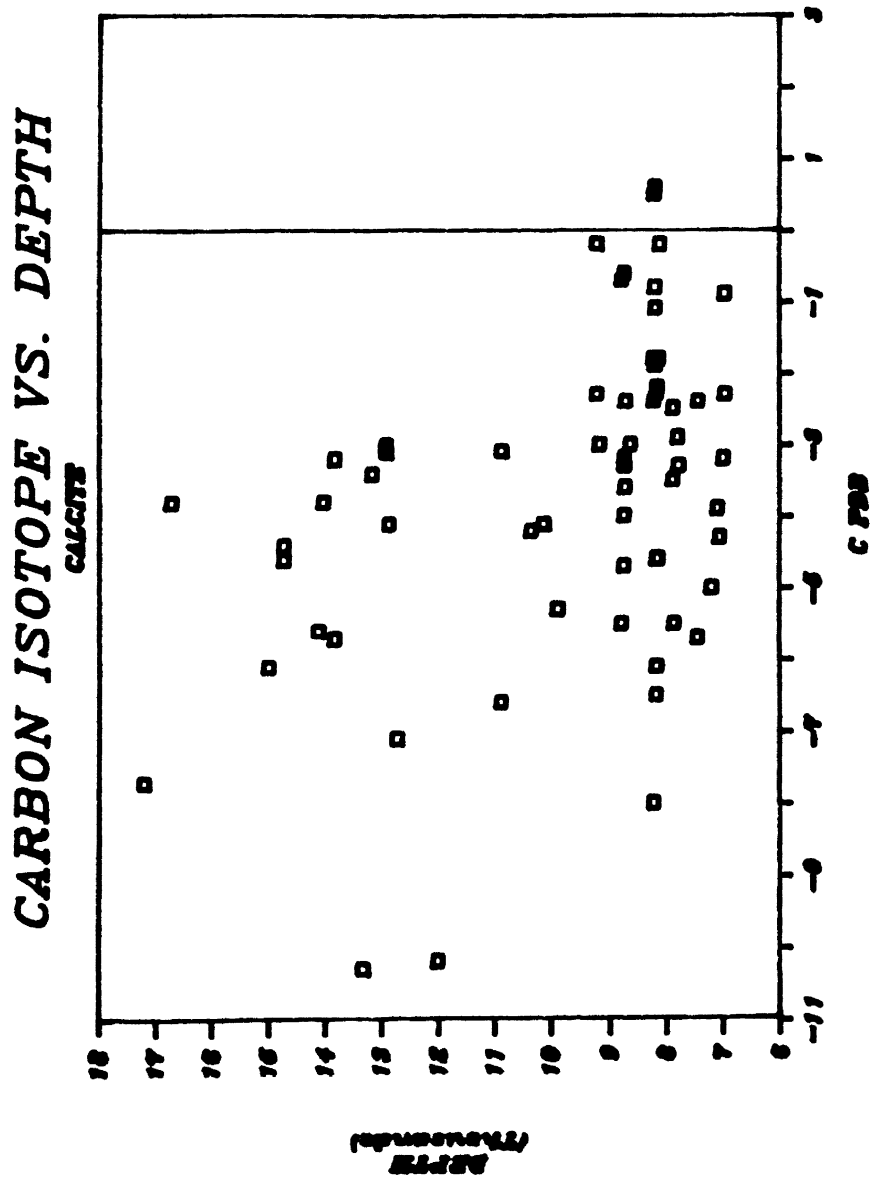
CARBON ISOTOPE VS. DEPTH

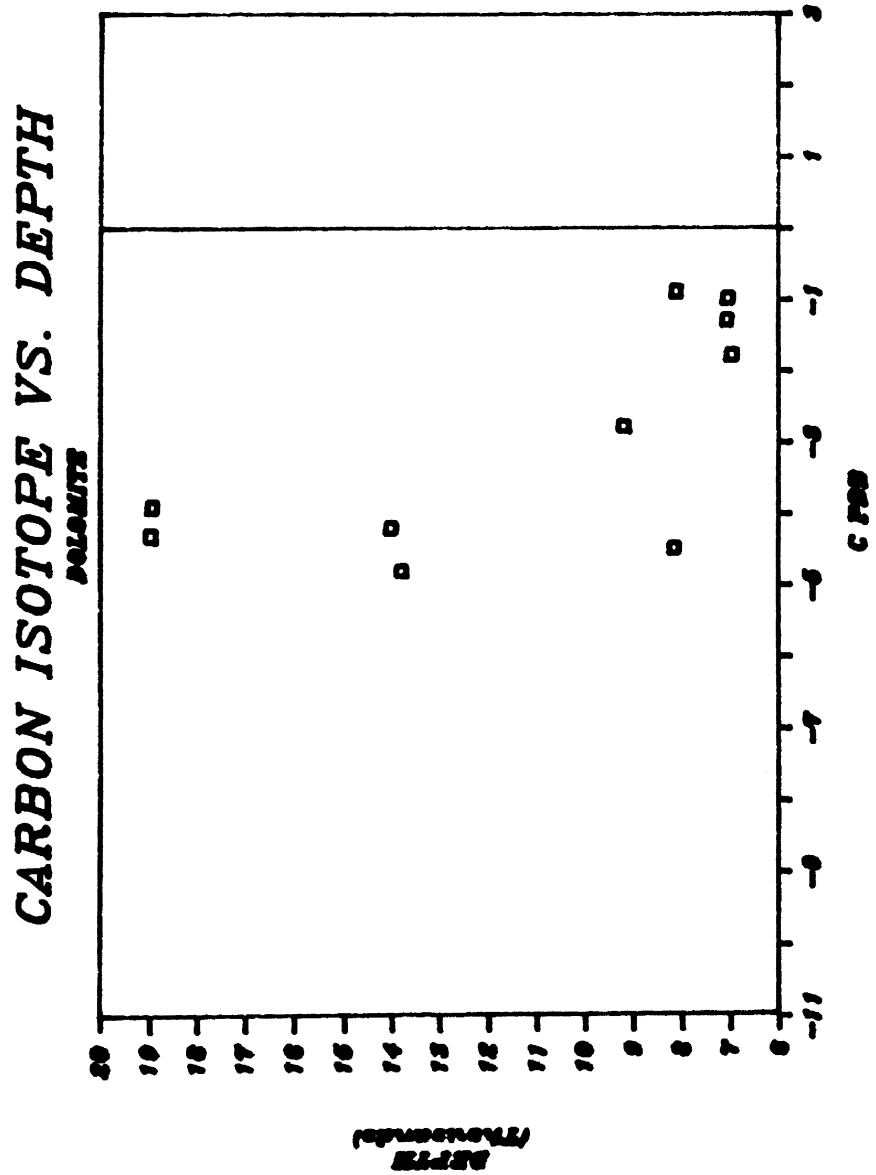
CARBON ISOTOPE VS. DEPTH

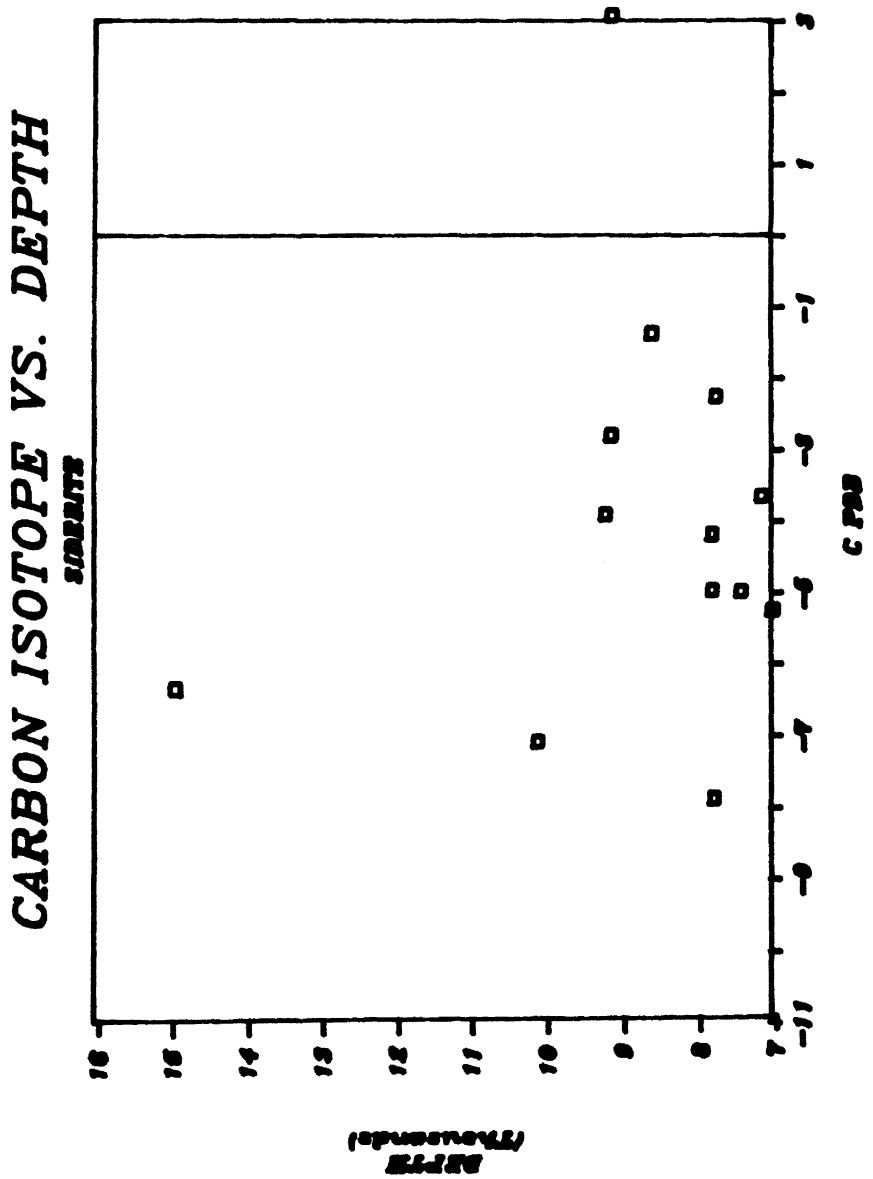
CARBON ISOTOPE VS. DEPTH

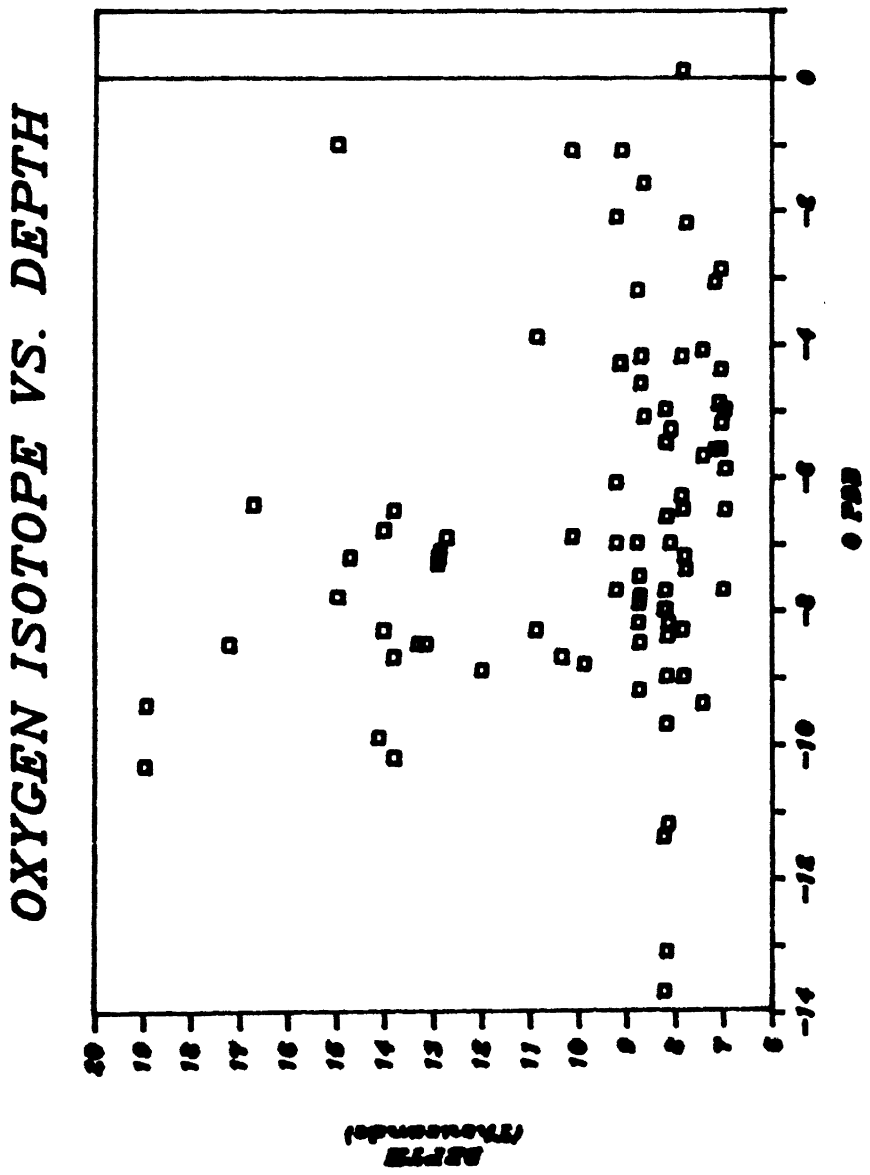
OXYGEN ISOTOPE VS. DEPTH

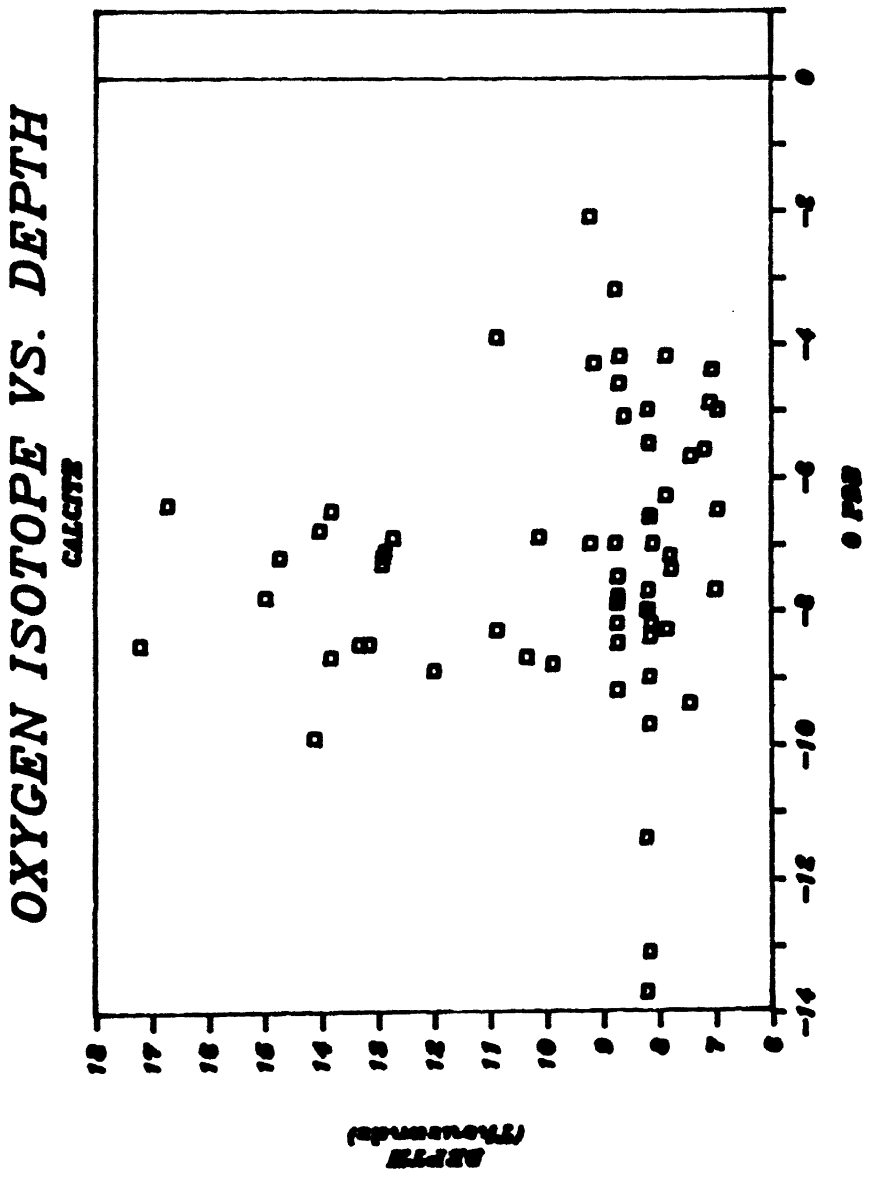
OXYGEN ISOTOPE VS. DEPTH
CALCITE
DEPTH
(Thousands)
0
-4
-8
-12
-16
18
17
16
15
14
13
12
11
10
9
8
7

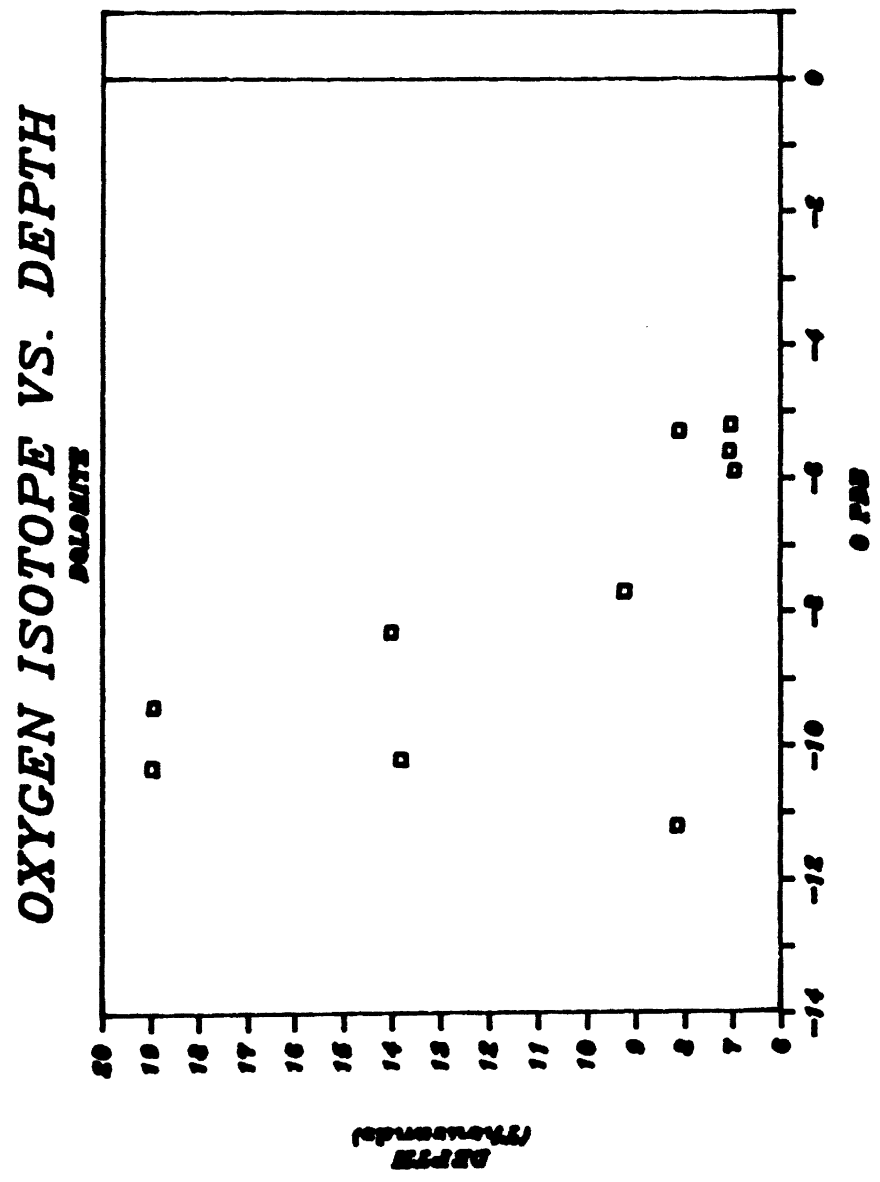
OXYGEN ISOTOPE VS. DEPTH

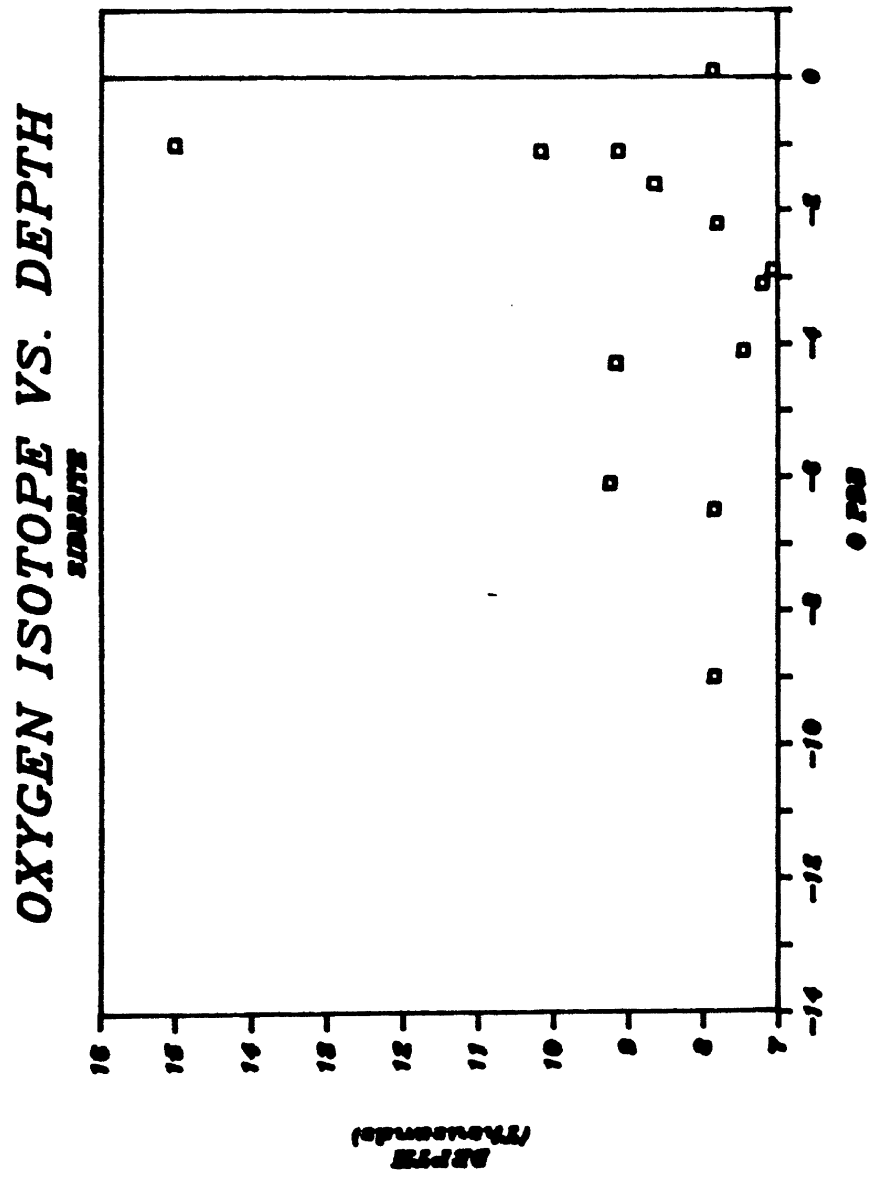
OXYGEN ISOTOPE VS. DEPTH

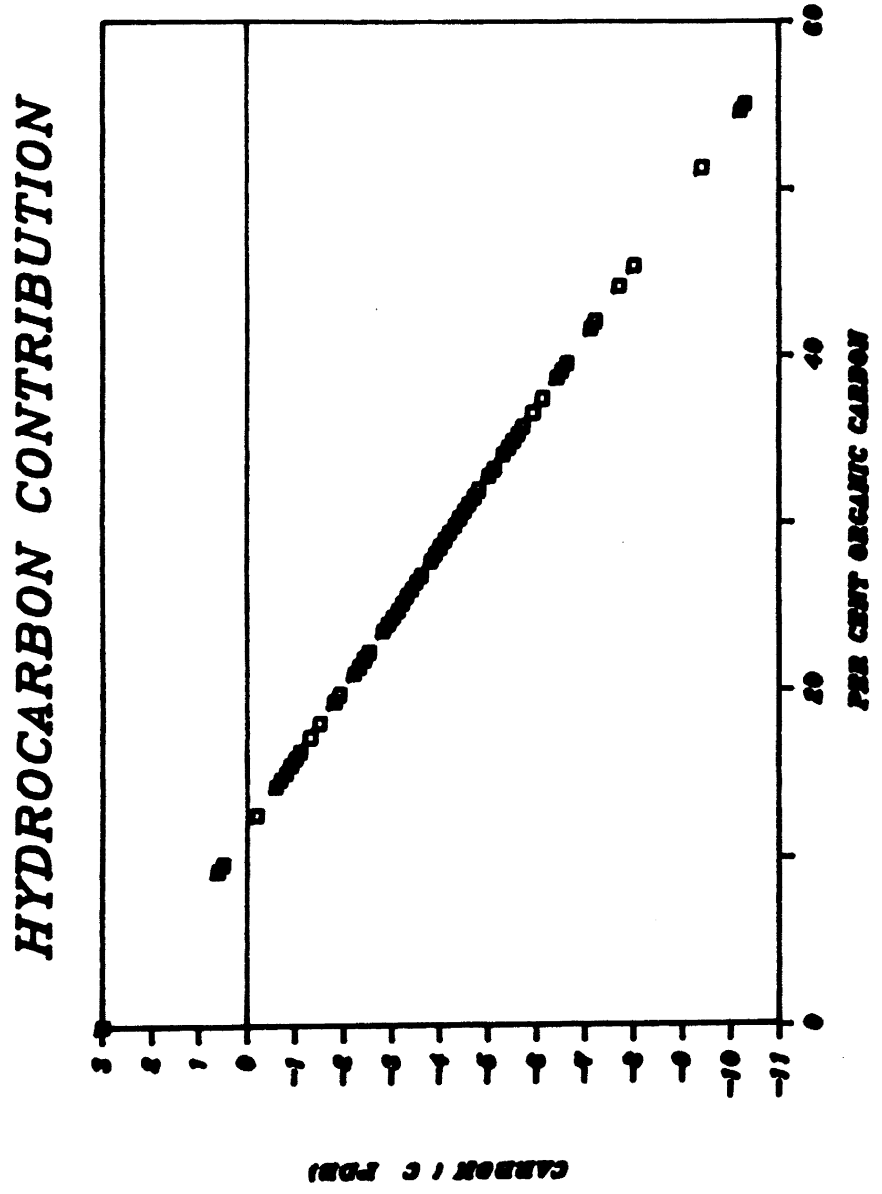
HYDROCARBON CONTRIBUTION
PER CENT ORGANIC CARBON

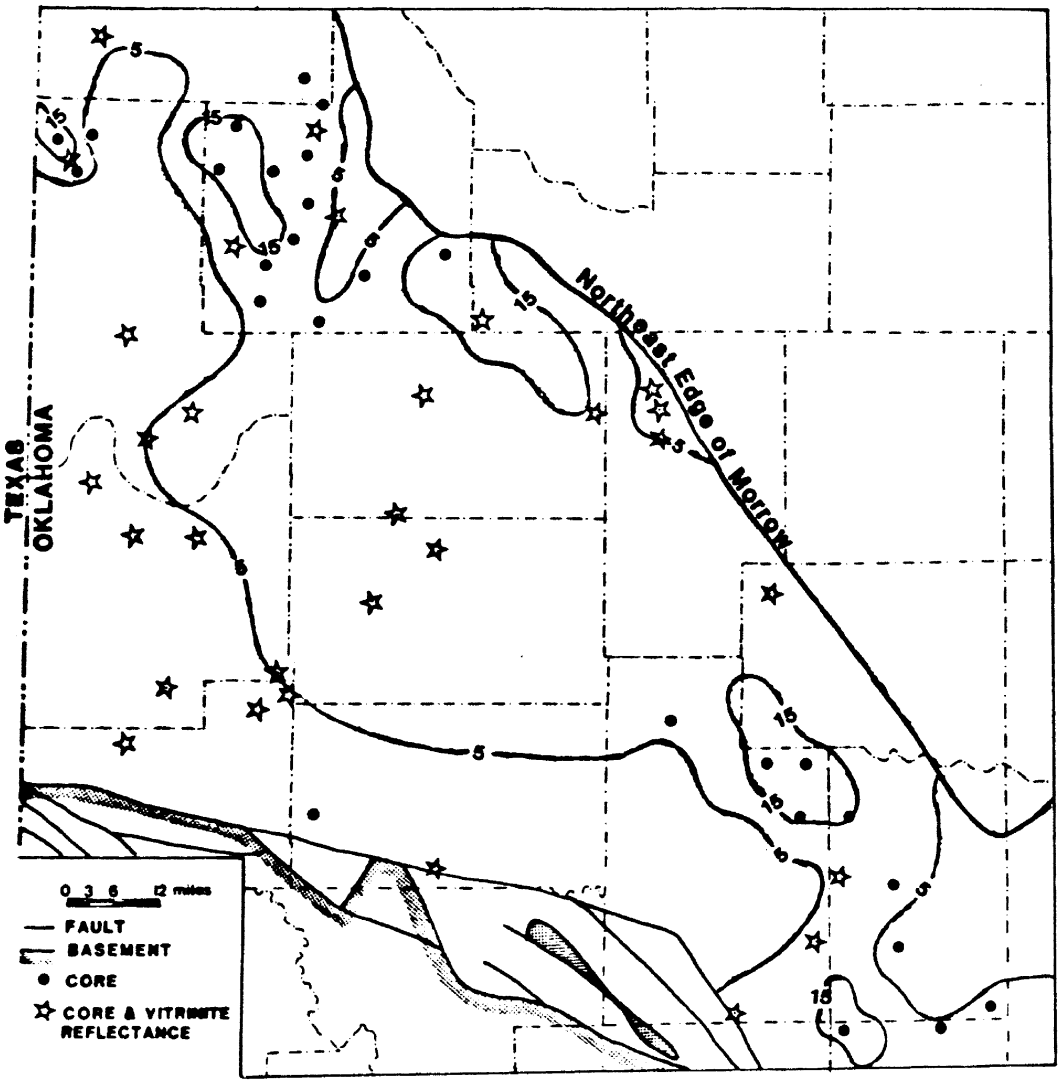

DISTRIBUTION OF CARBONATE CEMENT IN SHALLOW MARINE FACIES

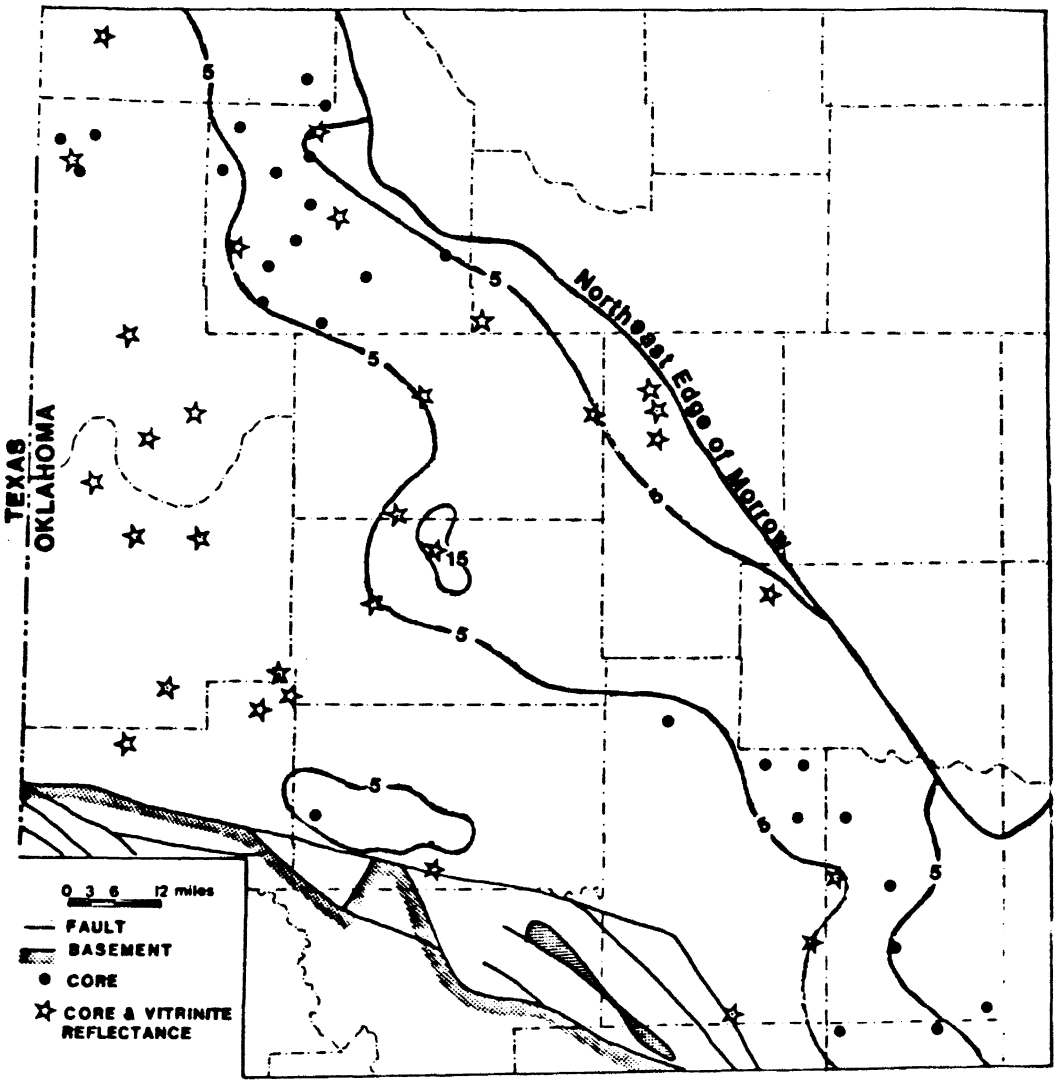

DISTRIBUTION OF CARBONATE CEMENT IN DELTAIC FACIES

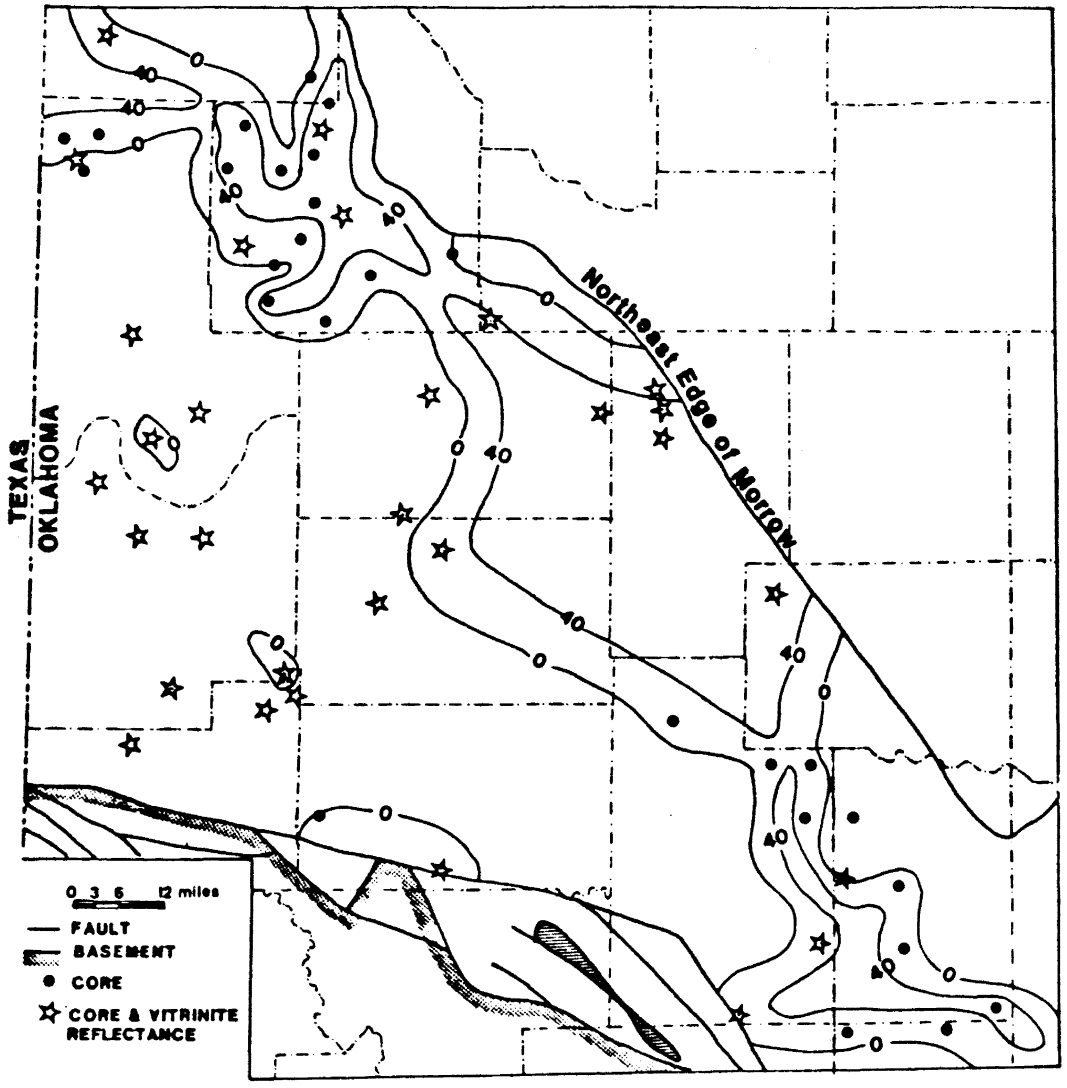

DISTRIBUTION OF % KAOLINITE

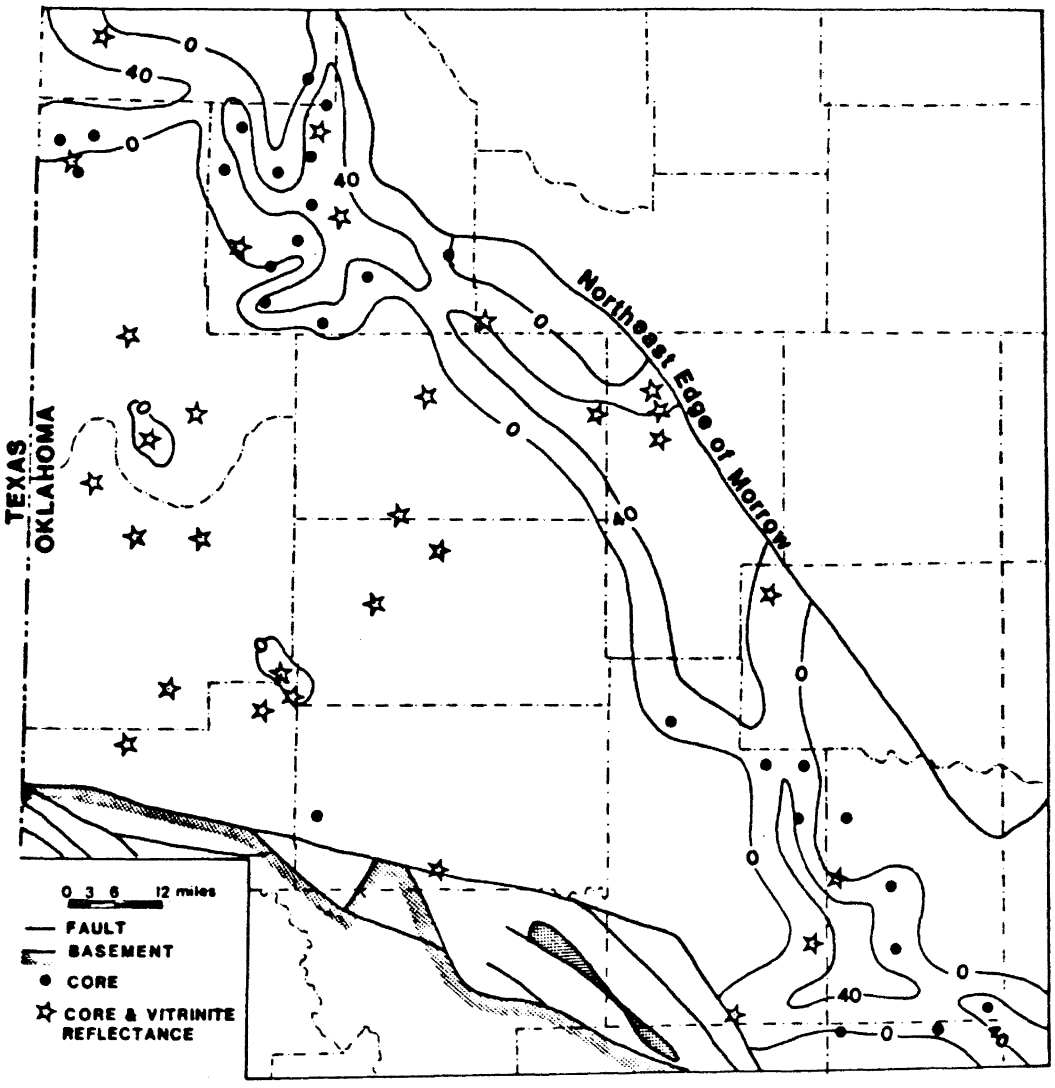

DISTRIBUTION OF % KAOLINITE IN SHALLOW MARINE FACIES

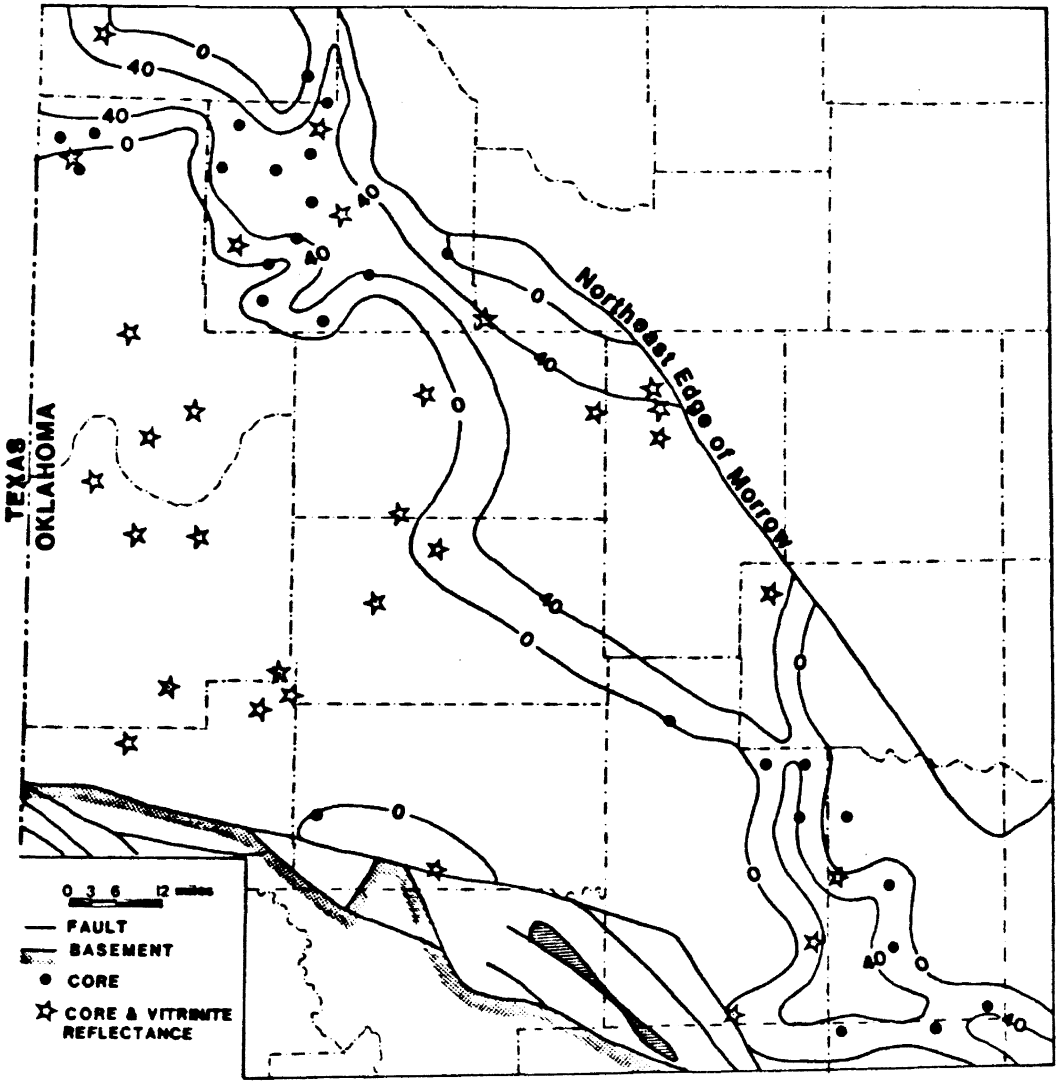

DISTRIBUTION OF % KAOLINITE IN DELTAIC FACIES

VITA

Patricia Ellen Grove Walker

Candidate for the Degree of

Master of Science

Thesis: A REGIONAL STUDY OF THE DIAGENETIC AND GEOCHEMICAL CHARACTER OF THE PENNSYLVANIAN MORROW FORMATION, ANADARKO BASIN, OKLAHOMA

Major Field: Geology

Biographical:

Personal Data: Born in Tulsa, Oklahoma, May 23, 1961, the daughter of W.F. and Clara Grove. Married to Lawrence P. Walker on October 13, 1984.

Education: Graduated from Union High School, Tulsa, Oklahoma, in May, 1979; received Bachelor of Science Degree in Geology from Oklahoma State University in December, 1983; completed requirements for the Master of Science degree at Oklahoma State University in May, 1986.

Professional Experience: Geologic Aide, Cities Service Oil Company, 1981; Summer Geologist, Grace Petroleum Corporation, 1984; Summer Geologist, Exxon Company, USA, 1985; Graduate Research Assistant, Geology Department, Oklahoma State University, 1983-1986.